Aus der Medizinischen Klinik III des Universitätsklinikums Carl Gustav Carus Dresden

Direktor: Prof. Dr. Stefan R. Bornstein

Regulated necrosis in the adrenal glands and the kidney

Dissertationsschrift

zur Erlangung des akademischen Grades

Doktor rerum medicinalium (Dr. rer. medic.)

vorgelegt

der Medizinischen Fakultät Carl Gustav Carus der Technischen Universität Dresden

von

M.Sc., Alexia Belavgeni

aus Patras, Griechenland

Dresden 2022

1. Gutachter: Ben Wielockx

Digitally signed by Ben Wielockx
DN: cn=Ben Wielockx, c=DE, o=TU Dresden, ou=Insitute of Clinical chemistry and Laboratory Medicine, email=ben.wielockx@tu-dresden.de
Date: 2022.07.15 13:31:25 +02'00'

2. Gutachter:

Tag der mündlichen Prüfung:

gez.: _____

Vorsitzender der Promotionskommission

Dedicated to my family, who helped me find the strength in me to fulfil this big chapter of my life.

Σας ευχαριστώ για όλα!

Acknowledgments

My first words of gratitude must go to my mentor Prof. Andreas Linkermann as well as to Prof. Stefan R. Bornstein, without whom the beginning, the progression and the completion of my dissertation would not have been possible. Andreas Linkermann trusted me from the very beginning and supported me to complete not only one, but two projects. His guidance, endless discussions with agreements and disagreements, and patience throughout all those years shaped me personally, and professionally. With high confidence I can say that I developed to a critically thinking scientist who questions everything and most importantly "does not fall in love with the hypothesis"! Prof. Stefan R. Bornstein supported me from my first moments as a PhD student and helped me every time there was obstacle to overcome. His kind and inspiring talks helped me see the "bigger picture" in endocrinology.

Being part of a laboratory means being part of a team and I was blessed to work with some of the most amazing people, who supported me in the best possible way throughout my PhD. The memories that I share with each one of the people of my lab I will forever cherish and keep close to my heart. Cloudy and Anne guided me many times with insightful suggestions for planning and performing experiments. They were always available for me every time I had a new question and ready to help me right away. Francesca has been by my side lifting my spirit whenever that was needed, but also offering a lot of help whenever I had big experiments to perform. Many thanks to Wulf, Markus, and Florian who have been of extraordinary help when it comes to working with mice. Without the hard work of Romy parts of my thesis would have taken me much longer to finish. She made sure that I had help every time it was necessary. I would also like to acknowledge the assistance of Anne, and Celine for their help during my dissertation. Julian did an amazing work on analysing the databases providing fruitful discussion in the dissertation, for which I am extremely grateful. The medical students of our lab, Evelyn, Nadia, and Sophie, had been always by my side offering supportive and funny discussions that kept my spirit up.

At this point, I would like to express my deepest appreciation to my Thesis Advisory Committee members, Prof. Stefan R. Bornstein, Prof. Dr. Ben Wielockx and Dr. Jörg Mansfeld for all their useful and practical suggestions during the annual meetings ensuring that the dissertation moves forward in best possible direction.

My dear friend Katerina, whom I have known since we started studying biology at the University of Patras, has been by my side ever since while supporting all my dreams until now, making me feel like she is literally here with me. My wonderful friend Lydia has spent so much time with me making sure to keep my spirits up and make me smile. I cannot potentially express with words how much their friendship helped me throughout these years.

I would not be the person I am today if it was not for my mom and dad who raised me with values for which I will forever be grateful. Always by my side even though the distance of being in another country

is keeping us apart, giving me all their love. All my steps mark their restless efforts that helped me become a strong but also thoughtful person. My twin brother made my life rich and full of amazing memories, while being one of my biggest supporters. Finally, Marko walked into my life during some difficult moments, but stayed by my side at all costs. He helped me rise to every situation and made sure that I will always smile no matter what was happening. His way of seeing things helped me become a better person and for this I am forever grateful.

Table of contents

Abstract

Regulated cell death (RCD) is indispensable for homeostasis and plays a crucial role in the pathophysiology of numerous diseases. Adrenocortical carcinomas (ACCs) represent a rare and highly malignant type of cancer. Currently, the most common therapeutic options include the complete surgical removal of the adrenal gland and/or the administration of mitotane, a derivative of the pesticide DDT. Yet patient survival remains poor and the mechanism of action of mitotane remains elusive. In this thesis it is demonstrated that the human ACC cell line NCI-H295R is sensitive to mitotane-induced cell death. In the first part, the involvement of three different RCD pathways, namely apoptosis, necroptosis and ferroptosis, in mitotane induced necrosis was investigated. To this end, different inhibitors were used, which were not able to block mitotane-induced cell death. When the medium was supplemented with insulin, transferrin, sodium selenite and linoleic acid (ITS+1) no cell death of the ACC cells was observed. This phenomenon was attributed to the presence of linoleic acid, since ITS supplementation lacking this component was not able to reverse mitotane-induced necrosis.

Identification of new drug targets for alternative options of ACC treatment led to the investigation of key molecules involved in the pathways of necroptosis and ferroptosis. The receptor-interacting protein kinase 1 and 3 (RIPK1 and 3) and the mixed lineage kinase domain-like protein (MLKL) were considered as interesting targets given their crucial role in the execution of necroptosis. A western blot analysis of those molecules revealed the presence only of RIPK1, suggesting that the necroptosis machinery is not present in the NCI-H295R cells. Of interest, evaluation of the expression levels of glutathione peroxidase four (GPX4), one of the main inhibitory molecules of ferroptosis, showed a much higher expression in the ACC cells compared to the standard cell line used for studying ferroptosis, the human fibrosarcoma HT1080 cells. A hypothesis that the NCI-H295R cells are susceptible to ferroptosis induction was formed based on this finding. Compounds representative of all the four classes of ferroptosis inducers (FINs) were tested. Direct inhibition of GPX4 using the small compound RSL3, a type II FIN, led to high necrotic populations. Co-treatment with the ferroptosis inhibitor ferrostatin-1 (Fer-1) completely reversed RSL3-induced ferroptosis. Type IV FIN FINO2, that causes indirect loss of the enzymatic activity of GPX4, lead also to high necrotic populations, while Fer-1 prevented FINO2-induced ferroptosis.

Data from public databases concerning gene methylation or mutation status of ACC tissues and normal human adrenal tissues was used to investigate potential key players of ferroptosis that might be either mutated or silenced in ACCs. Of note, glutathione peroxidases 3 and 5 (GPX3 and 5) were highly methylated, while the enzyme cystathionine gamma-lyase (CSE) involved in the transsulfuration pathway via the break down of cystathionine into cysteine and α-ketobutyrate and ammonia was found to be highly mutated. Collectively, these data point towards a high sensitivity of ACCs to ferroptosis induction. This could provide a new chapter for the therapeutic approaches of ACCs. Additionally, these findings provide

a better understanding of the biology of this type of cancer that highly mutates or silences ferroptosis-related genes.

The second part of this thesis focuses on the involvement of RCD in spontaneous cell death in isolated murine tubules. Existing literature points towards an involvement of necroptosis and ferroptosis pathways in the kidney in models of acute kidney injury (AKI). Acute tubular necrosis (ATN) represents a hallmark of AKI. While the work in the Linkermann lab has shown that isolated tubules perfused with type I FIN erastin undergo cell death in a "wave-of-death" manner, no deeper insights into the propagation of tubular necrotic injury exist. A protocol for isolation of murine kidney tubules was established, providing an *ex-vivo* model for investigation of tubular death. The absence of potentially confounding blood cells as well as immune cells was ensured by extensive washing steps as well as the use of collagenase. Visual observation and staining of isolated tubules with the nucleic acid stain SYTOX green revealed a spontaneous cell death in a "wave-of-death" manner. This wave was running in parallel with a calcium concentration change, indicating its involvement in the spontaneous necrosis. To investigate the potential involvement of mitochondria in this process, electron microscopy images were obtained from parts of the tubules with different levels of damage which revealed highly damaged and ballooned mitochondria. These data provided with a phenotypic characterisation of the spontaneous tubular necrosis.

Aiming to approach this type of death genetically, necroptosis and pyroptosis deficient mice (MLKL/GSDMD^{DKO}) were used. Comparison of the LDH release, used as a measure of necrosis, from isolated kidney tubules of the MLKL/GSDMD^{DKO} mice and wild type (WT) mice showed no difference. This indicated that neither necroptosis nor pyroptosis are involved in the tubular necrosis. Therefore, the next step was to investigate the effects of Fer-1 at the levels of LDH of isolated tubules from WT mice. A significantly lower LDH release was observed in tubules treated with Fer-1 compared to the ones treated with vehicle. However, this reduction in the LDH release was not complete, suggesting that ferroptosis is only partially responsible for the spontaneous death of isolated tubules.

The difference of male and female mice towards AKI sensitivity has been noted in the literature in that female mice are less susceptible compared to the male mice. Therefore, the next step was to investigate whether this protection of females can be observed at the level of isolated tubules. Indeed, the LDH release from tubules isolated from female mice was significantly less compared to the LDH release of tubules isolated from male mice. Based on the data obtained from isolated tubules from WT male mice treated with Fer-1, a similar experiment was performed with tubules isolated from WT female mice. No difference in the LDH release was observed between the Fer-1-treated tubules and the vehicle-treated ones, indicating that another cell death pathway might be involved.

The most obvious difference between male and female organisms is the sex hormones. Whether testosterone or β-estradiol are responsible for the higher susceptibility or protection against cell death has

been a debate over the last years. To test this hypothesis, three different cell lines were utilised. A pre-treatment of 16 h with either testosterone or β-estradiol was performed. Treatment with either type I FIN erastin or type II FIN RSL3 followed, and cells were analysed via flow cytometry. Data revealed protective effects of β-estradiol against ferroptosis induction. Next, the effects of β-estradiol in a simultaneous treatment with RSL3 were investigated. Interestingly the protective effects of the hormone were still observed. Among the metabolites of β-estradiol, 2-hydroxyestradiol (2-OHE2) has been reported to exert antioxidant effects. Therefore, 2-OHE2 was used in a simultaneous treatment with RSL3, and the obtained data showed that it was a much more potent inhibitor of necrotic cell death than β-estradiol even at lower concentrations. Collectively these data indicate that the lower susceptibility of female organisms towards cell death might be explained by the presence of β-estradiol and its more potent antioxidant metabolites. Such findings could change the way the two sexes are approached scientifically, while providing new insights on different therapeutic strategies between male and female organisms.

Zusammenfassung

Der regulierte Zelltod (RCD) ist für die Homöostase unverzichtbar und spielt eine entscheidende Rolle in der Pathophysiologie zahlreicher Krankheiten. Nebennierenrindenkarzinome (ACCs) stellen eine seltene und hochgradig bösartige Krebsart dar. Die derzeit gängigsten Therapieoptionen sind die vollständige chirurgische Entfernung der Nebenniere und/oder die Verabreichung von Mitotane, einem Derivat des Pestizids DDT. Die Überlebenschancen der Patienten sind jedoch nach wie vor schlecht, und der Wirkmechanismus von Mitotane ist nach wie vor nicht klar. In dieser Arbeit wird gezeigt, dass die menschliche ACC-Zelllinie NCI-H295R empfindlich gegenüber dem durch Mitotane ausgelösten Zelltod ist. Im ersten Teil wurde die Beteiligung von drei verschiedenen RCD-Wegen, nämlich Apoptose, Nekroptose und Ferroptose, an der Mitotane-induzierten Nekrose untersucht. Zu diesem Zweck wurden verschiedene Inhibitoren eingesetzt, die den Mitotane-induzierten Zelltod nicht blockieren konnten. Wurde das Medium mit Insulin, Transferrin, Natriumselenit und Linolsäure (ITS+1) ergänzt, wurde kein Zelltod der ACC-Zellen beobachtet. Dieses Phänomen wurde auf das Vorhandensein von Linolsäure zurückgeführt, da eine ITS-Ergänzung ohne diese Komponente die Mitotane-induzierte Nekrose nicht umkehren konnte.

Die Identifizierung neuer Zielmoleküle für alternative Behandlungsmöglichkeiten von ACC führte zur Untersuchung von Schlüsselmolekülen, die an den Wegen der Nekroptose und Ferroptose beteiligt sind. Die rezeptorinteragierende Proteinkinase 1 und 3 (RIPK1 und 3) und das Mixed-Lineage-Kinase-Domain-ähnliche Protein (MLKL) wurden als interessante Zielmoleküle betrachtet, da sie eine entscheidende Rolle bei der Durchführung der Nekroptose spielen. Eine Western-Blot-Analyse dieser Moleküle ergab nur das Vorhandensein von RIPK1, was darauf hindeutet, dass die Nekroptose-Maschinerie in den NCI-H295R-Zellen nicht vorhanden ist. Interessanterweise zeigte die Auswertung der Expression von Glutathionperoxidase 4 (GPX4), einem der wichtigsten hemmenden Moleküle der Ferroptose, eine viel höhere Expression in den ACC-Zellen im Vergleich zu der Standard-Zelllinie, die für die Untersuchung der Ferroptose verwendet wird, den menschlichen Fibrosarkomzellen HT1080. Auf der Grundlage dieses Ergebnisses wurde die Hypothese aufgestellt, dass die NCI-H295R-Zellen für die Ferroptose-Induktion empfänglich sind. Es wurden Verbindungen getestet, die für alle vier Klassen von Ferroptose-Induktoren (FINs) repräsentativ sind. Die direkte Hemmung von GPX4 mit dem kleinen Wirkstoff RSL3, einem FIN des Typs II, führte zu hohen nekrotischen Populationen. Die gleichzeitige Behandlung mit dem Ferroptose-Inhibitor Ferrostatin-1 (Fer-1) kehrte die RSL3-induzierte Ferroptose vollständig um. FINO2 vom Typ IV, das einen indirekten Verlust der enzymatischen Aktivität von GPX4 bewirkt, führte ebenfalls zu hohen nekrotischen Populationen, während Fer-1 die FINO2-induzierte Ferroptose verhinderte.

Daten aus öffentlichen Datenbanken über den Methylierungs- oder Mutationsstatus von ACC-Gewebe und normalem menschlichen Nebennierengewebe wurden verwendet, um potenzielle

Schlüsselfiguren der Ferroptose zu untersuchen, die in ACC entweder mutiert oder stillgelegt sein könnten. Bemerkenswert ist, dass die Glutathionperoxidasen 3 und 5 (GPX3 und 5) stark methyliert waren, während das Enzym Cystathionin-Gamma-Lyase (CSE), das am Transsulfurierungsweg über die Aufspaltung von Cystathionin in Cystein, α-Ketobutyrat und Ammoniak beteiligt ist, stark mutiert war. Insgesamt deuten diese Daten auf eine hohe Empfindlichkeit von ACCs gegenüber der Ferroptose-Induktion hin. Dies könnte ein neues Kapitel für die therapeutischen Ansätze bei ACCs darstellen. Darüber hinaus ermöglichen diese Ergebnisse ein besseres Verständnis der Biologie dieser Krebsart, bei der Ferroptose-regulierende Gene stark mutiert oder stillgelegt sind.

Der zweite Teil dieser Arbeit befasst sich mit der Beteiligung der RCD am spontanen Zelltod in isolierten murinen Tubuli. Die vorhandene Literatur deutet darauf hin, dass Nekroptose- und Ferroptosewege in der Niere bei Modellen der akuten Nierenschädigung (AKI) eine Rolle spielen. Die akute tubuläre Nekrose (ATN) ist ein charakteristisches Merkmal der AKI. Während die Arbeit im Linkermann-Labor gezeigt hat, dass isolierte Tubuli, die mit Typ I FIN Erastin perfundiert wurden, einen Zelltod in Form einer "Welle des Todes" erfahren, gibt es keine tieferen Einblicke in die Ausbreitung der tubulären nekrotischen Schädigung. Es wurde ein Protokoll für die Isolierung von Nierentubuli der Maus entwickelt, das ein Ex-vivo-Modell für die Untersuchung des Tubulustods bietet. Die Abwesenheit von potenziell störenden Blutzellen und Immunzellen wurde durch umfangreiche Waschschritte und die Verwendung von Kollagenase sichergestellt. Die visuelle Beobachtung und die Anfärbung isolierter Tubuli mit dem Nukleinsäure-Farbstoff SYTOX grün zeigten einen spontanen Zelltod in Form einer "Welle des Todes". Diese Welle verlief parallel zu einer Veränderung der Kalziumkonzentration, was auf deren Beteiligung an der spontanen Nekrose hindeutet. Um die mögliche Beteiligung von Mitochondrien an diesem Prozess zu untersuchen, wurden elektronenmikroskopische Aufnahmen von Teilen der Tubuli mit unterschiedlichem Schädigungsgrad gemacht, die stark geschädigte und aufgeblähte Mitochondrien zeigten. Diese Daten ermöglichten eine phänotypische Charakterisierung der spontanen tubulären Nekrose.

Um diese Art des Todes genetisch zu erfassen, wurden Nekroptose- und Pyroptose-defiziente Mäuse (MLKL/GSDMD^{DKO}) verwendet. Der Vergleich der LDH-Freisetzung, die als Maß für die Nekrose verwendet wird, aus isolierten Nierentubuli der MLKL/GSDMD^{DKO}-Mäuse und der Wildtyp-Mäuse (WT) ergab keinen Unterschied. Dies deutet darauf hin, dass weder Nekroptose noch Pyroptose an der tubulären Nekrose beteiligt sind. In einem nächsten Schritt wurden daher die Auswirkungen von Fer-1 auf die LDH-Konzentration in isolierten Tubuli von WT-Mäusen untersucht. In den mit Fer-1 behandelten Tubuli wurde eine signifikant geringere LDH-Freisetzung beobachte*t al*s in den mit dem Vehikel behandelten Tubuli. Diese Verringerung der LDH-Freisetzung war jedoch nicht vollständig, was darauf hindeutet, dass die Ferroptose nur teilweise für den spontanen Tod der isolierten Tubuli verantwortlich ist.

Der Unterschied zwischen männlichen und weiblichen Mäusen in Bezug auf AKI wurde in der Literatur dahingehend beschrieben, dass weibliche Mäuse im Vergleich zu männlichen Mäusen weniger empfindlich sind. Daher wurde in einem nächsten Schritt untersucht, ob dieser Schutz der weiblichen Tiere auch auf der Ebene der isolierten Tubuli beobachtet werden kann. In der Tat war die LDH-Freisetzung aus den isolierten Tubuli weiblicher Mäuse deutlich geringer als die LDH-Freisetzung aus den isolierten Tubuli männlicher Mäuse. Auf der Grundlage der Daten, die aus isolierten Tubuli von mit Fer-1 behandelten männlichen WT-Mäusen gewonnen wurden, wurde ein ähnliches Experiment mit Tubuli durchgeführt, die aus weiblichen WT-Mäusen isoliert wurden. Es wurde kein Unterschied in der LDH-Freisetzung zwischen den mit Fer-1 behandelten Tubuli und den mit dem Vehikel behandelten Tubuli festgestellt, was darauf hindeutet, dass ein anderer Zelltodweg beteiligt sein könnte.

Der offensichtlichste Unterschied zwischen männlichen und weiblichen Organismen sind die Geschlechtshormone. Ob Testosteron oder β-Östradiol für die höhere Anfälligkeit oder den Schutz vor dem Zelltod verantwortlich sind, wurde in den letzten Jahren diskutiert. Um diese Hypothese zu testen, wurden drei verschiedene Zelllinien verwendet. Es wurde eine Vorbehandlung von 16 Stunden mit Testosteron oder β-Estradiol durchgeführt. Anschließend wurden die Zellen entweder mit Typ-I-FIN-Erastin oder Typ-II-FIN-RSL3 behandelt und mittels Durchflusszytometrie analysiert. Die Daten zeigten eine schützende Wirkung von β-Östradiol gegen die Ferroptose-Induktion. Als nächstes wurde die Wirkung von β-Östradiol bei gleichzeitiger Behandlung mit RSL3 untersucht. Interessanterweise wurden die schützenden Wirkungen des Hormons weiterhin beobachtet. Von den Metaboliten des β-Estradiols wurde berichtet, dass 2-Hydroxyestradiol (2-OHE2) eine antioxidative Wirkung hat. Daher wurde 2-OHE2 in einer gleichzeitigen Behandlung mit RSL3 verwendet, und die erhaltenen Daten zeigten, dass es ein viel stärkerer Inhibitor des nekrotischen Zelltods war als β-Östradiol, selbst bei niedrigeren Konzentrationen. Insgesamt deuten diese Daten darauf hin, dass die geringere Anfälligkeit weiblicher Organismen für den Zelltod durch das Vorhandensein von β-Östradiol und seinen stärkeren antioxidativen Metaboliten erklärt werden könnte. Diese Erkenntnisse könnten die Art und Weise, wie die beiden Geschlechter wissenschaftlich betrachtet werden, verändern und gleichzeitig neue Erkenntnisse über unterschiedliche therapeutische Strategien für männliche und weibliche Organismen liefern.

List of abbreviations

ACCs	adrenicortical carcinomas
ACSL4	acyl-CoA synthetase long chain family member 4
ACTH	adrenocorticotropic hormone
ADPKD	autosomal dominant polycystic kidney disease
AKI	acute kidney injury
ATN	acute tubular necrosis
cFLIP	cellular FLICE-inhibitory protein
cIAP1	cellular inhibior of apoptosis protein 1
cIAP2	cellular inhibior of apoptosis protein 2
CNS	central nervous system
CKD	chronic kidney disease
CoQ10	coenzyme Q10
CRH	corticotropin-releasing hormone
DAMPs	damage associated molecular patterns
DD	death domain
DED	death effector domain
DHEA	dehydroepiandrosterone
DHEAS	dehydroepiandrosterone sulfate
DIRE	damage-induced release of endocrine factors
DUBs	deubiquitinases
ENSAT	European network for the Study of Adrenal Tumours
ER	endoplasmic reticulum
ESCRT-III	endosomal sorting complexes required for transport III
FA	fatty acid
FACS	fluorescence-activated cell sorting
FADD	Fas-associated protein with death domain
Fer-1	ferrostatin-1
FINs	ferroptosis inducers
FSP1	ferroptosis-supressing protein 1
GCL	glutamate-cysteine ligase
GPX4	glutathione peroxidase 4
GSDMA	gasdermin A
GSDMD	gasdermin D

GSH	glutathione
GSS	glutathione synthetase
H_2O_2	hydrogen peroxide
HPA axis	hypothalamus-pituitary-adrenal axis
IL-18	interleukin 18
IL-1β	interleukin 1β
LPS	lipopolysaccharide
MLKL	mixed lineage kinase domain-like protein
MOMP	mitochondrial outer membrane permeabilization
MVBs	multivesicular bodies
Nec-1	necrostatin-1
Nec-1f	necrostatin-1f
Nec-1s	necrostatin-1s
PL-OH	phospholipid alcohol
PL-OOH	phospholipid hydroperoxide
pMLKL	phosphorylated MLKL
PUFAs	polyunsaturated fatty acids
RCD	regulated cell death
RIPK1	receptor-interacting protein kinase 1
RIPK3	receptor-interacting protein kinase 3
RHIM	RIP homotypic interaction motif
RN	regulated necrosis
ROS	reactive oxygen species
RTA	radical trapping antioxidant
SCN	suprachiasmatic nucleus
TNF	tumor necrosis factor
TNFR	tumor necrosis factor receptor family
TRADD	TNFR1-associated death domain protein
TRIF	TIR domain-containing adapter-inducing interferon-β
TUNEL	TdT-mediated dUTP-biotin nick end-labelling
WHO	World Health Organization
ZBP1	Z-DNA-binding protein 1

List of tables

List of Figures

Introduction

1. Introduction

1.1. Regulated cell death

Regulated necrosis (RN) of a cell is defined by the loss of the integrity of its plasma membrane, caused in a traumatic manner or via regulated signalling pathways (RCD). It is essential during homeostasis and in some cases the capacity of adaptation to stress stimuli (Tonnus *et al*., 2021a). Physiological or pathophysiological conditions *in vivo* that result in necrosis, can lead to the dysfunction of the tissue but also cause the release of molecules, termed as damage associated molecular patterns (DAMPs) (Sarhan *et al*., 2018b). The release of DAMPs can modulate the immune system and can cause an immune response referred to as necroinflammation, a process which is becoming increasingly more relevant (Maremonti *et al*., 2022).

Many pathways related to RCD have been described aiming to unravel the biology of cells under physiological conditions as well as the contribution of RCD in a wide variety of diseases. Until around 2006 apoptosis was tightly linked with the term regulated cell death. However, the increased knowledge on cell death has expanded dramatically the way necrosis is viewed (Galluzzi *et al*., 2018). Since then, new details concerning different pathways, such as necroptosis, pyroptosis, ferroptosis and others have emerged. The first two mentioned pathways are tightly interconnected via a caspase-controlled system (Tonnus *et al*., 2018), which will be further explained in sections 1.1.2, 1.1.3 and 1.1.4. On the other hand, ferroptosis is a peroxidation/autooxidation-mediated process, leading to a very distinct cell death which can lead to a synchronized cell death pattern across the tissue (Tonnus *et al*., 2018). More details on this matter are given in the section 1.1.5. Necroptosis, pyroptosis and ferroptosis, in contrast to apoptosis, result in plasma membrane integrity loss. Schematic illustrations of the regulated cell death pathways are shown in **Figure 1**.

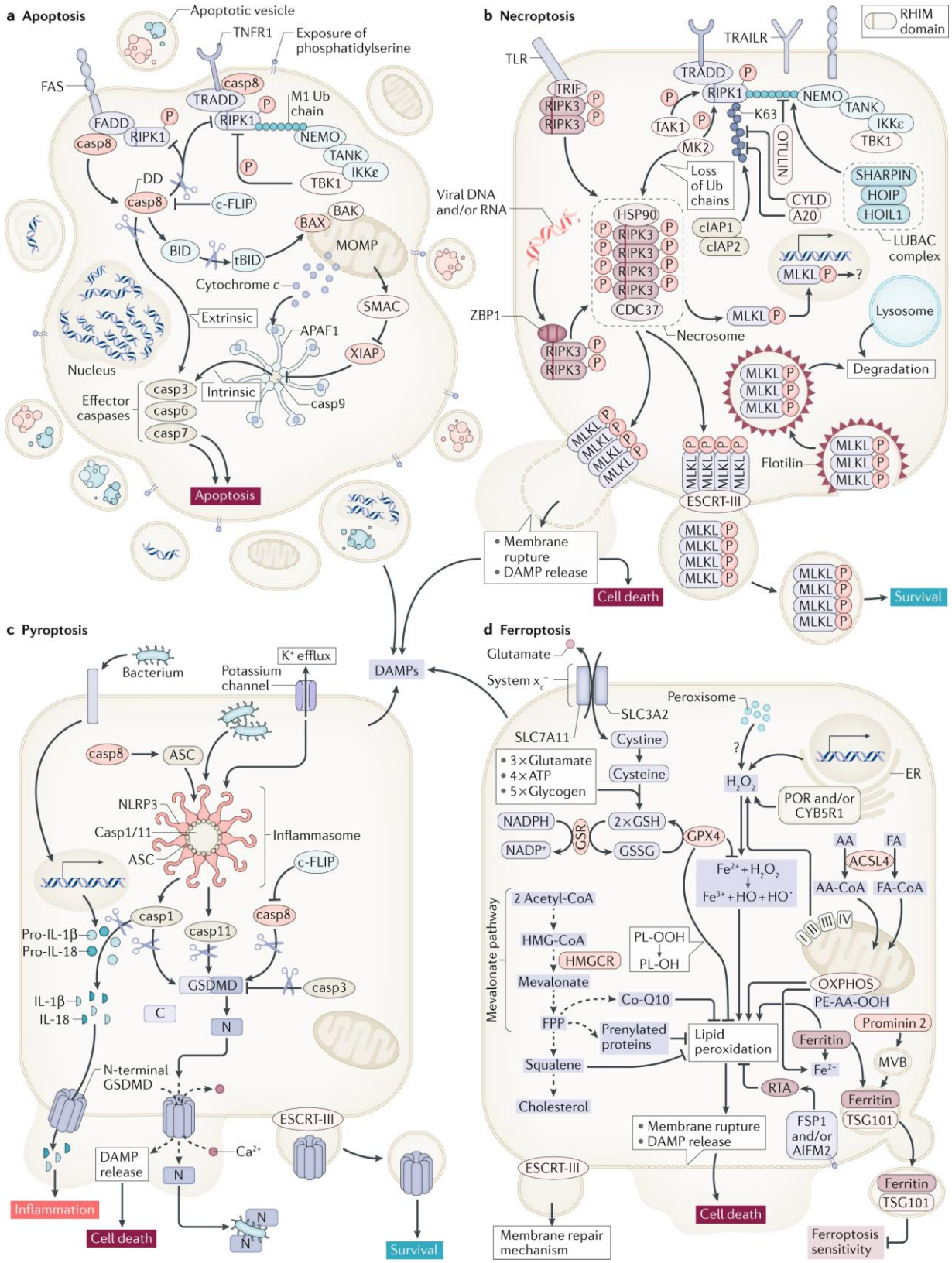

Figure 1. The regulated cell death pathways. A. Apoptosis represents a caspase-mediated and non-inflammatory pathway. The intrinsic and extrinsic apoptosis pathways have been characterized as two distinct signalling pathways which can be triggered by death receptors, such as the tumour necrosis factor

receptor family 1 (TNFR1). A cascade of proteolytic cleavages of caspases lead to the activation of the initiator caspase 8 (casp8) and the concomitant activation of the effector caspases (casp3, 6 and 7). During the intrinsic pathway mitochondrial outer membrane permeabilization (MOMP) is observed. **B.** Necroptosis, a kinase-mediated pathway, depends on RIPK1 and RIPK3, which participate in the formation of the necrosome. RIPK3 phosphorylates the pseudokinase MLKL, which triggers the rupture of the plasma membrane. This process can be counteracted by the membrane repair ESCRT-III complex. **C.** Pyroptosis, in contrast to apoptosis, involves inflammasomes which will activate the caspases 1, 4 and 11. This step results in the cleavage of pro-IL-1β, pro-IL-18 and gasdermin D (GSDMD). The N-terminus of GSDMD will form pores in the plasma membrane leading to the release of pro-inflammatory cytokines. **D.** Ferroptosis, an iron-dependent form of regulated cell death, is characterised by the lipid peroxidation of the plasma membrane, which will lead to membrane rupture. Lipid peroxidation is prevented by the glutathione peroxidase 4 (GPX4), in a GSH-dependent manner. Other molecules, such as the oxidoreductase FSP1 (also known as AIFM2) prevents the lipid peroxidation upon myristoylation-dependent recruitment to the plasma membrane in a GSH-independent manner. casp; caspase, DAMP; damage-associated molecular pattern, DD; death domain, DED; death effector domain, ER; endoplasmic reticulum, FA; fatty acid, MLKL; mixed lineage kinase domain-like protein, PL-OH; phospholipid alcohol, PL-OOH; phospholipid hydroperoxide, RIPK1; receptor-interacting protein kinase 1, RIPK3; receptor-interacting protein kinase 3, RTA; radical trapping antioxidant. (Image obtained from Tonnus *et al*., 2021).

1.1.1. Apoptosis

More than 10 billion cells die by apoptosis each day, representing the default pathway of regulated cell death (RCD) in tissue development. As a consequence of apoptosis, the cell shrinks, the nucleus condenses, the DNA is fragmented and the exposure of phosphatidylserine, normally constrained to the inner part of the plasma membrane, acts as the "eat me" signal to macrophages. Membrane blebbing is another characteristic of apoptosis. However, the plasma membrane remains intact, therefore preventing the release of intracellular contents to the extracellular space. Therefore, apoptosis is considered as immunologically silent.

There are two distinct identified pathways of apoptosis; the extrinsic and the intrinsic. The extrinsic pathway is mediated by death receptors, such as the tumour necrosis factor receptor family (TNFR) and the Fas receptor (also known as CD95). The binding of the tumour necrosis factor (TNF) to the TNFR leads to the activation of initiator caspases (caspase-8 and caspase-10) through the recruitment of Fas-associated death domain protein (FADD) at the intracellular region of the death receptor. The bound procaspase-8 recruits additional procaspase-8 molecules, which will be activated by dimerization. Active capsase-8 cleaves and concomitantly activates the executioner capsase-3, caspase-6 and caspase-7. Caspase-8 cleaves and thereby activates BID, a BH3-only protein, resulting in tBID. The cleaved product, tBID antagonizes the anti-apoptotic Bcl-2 proteins, activates BAX and BAK therefore causing mitochondrial outer membrane permeabilization (MOMP). The activation of caspase-8 does not only occur upon ligation to death receptors. The kinase RIPK1 can bind to FADD to promote caspase-8 activation and ultimately apoptosis (Green, 2019; Tonnus *et al*., 2019).

In the intrinsic pathway, also referred to as the mitochondrial pathway of apoptosis, caspase-8 cleaves and activates the BH3 protein, Bid, which antagonizes the anti-apoptotic Bcl-2 proteins. As a result, BAX and BAK are being activated, recruited to the outer mitochondrial membrane leading to mitochondrial outer membrane permeabilization (MOMP). Among the mitochondrial content that is being released into the cytosol, cytochrome c assembles with the cytosolic proteins APAF1 and caspase-9. This complex is referred to as the apoptosome, a large heteroheptameric structure that will eventually activate the executioner caspases (**Figure 1A**). Caspase-3, 7 and 9 are bound and inhibited by the X-linked inhibitor of apoptosis (XIAP). Smac and Omi are also released upon MOMP, which antagonise XIAP, disabling this mode of caspase inhibition and thereby aiding their function (Sarhan *et al*., 2018b; Green, 2019; Tonnus *et al*., 2019; Tonnus *et al*., 2021a).

1.1.2. Necroptosis

Necroptosis, another type of RN (**Figure *1*B**), is evolutionarily conserved as a pathway to defend the cell against viral infection. Some pathogens are capable of inhibiting caspase-8 in order to prevent apoptosis. As a cellular backup mechanism this inhibition would also lead to the activation of RIPK1 and RIPK3, the key kinases in the necroptotic pathway (Mocarski *et al*., 2011). Both RIPK1 and RIPK3 contain a RIP homotypic interaction motif (RHIM), which is typical of the necroptosis pathway (Kaiser *et al*., 2013). The deubiquitination of RIPK1 no longer intercalates its RHIM domains between the RIPK3 RHIM domains. Concomitantly RIPK1 mediates the phosphorylation of RIKP3 and therefore activates it. RIPK3 can then oligomerize through its RHIM domain, forming a large amyloid-like platform, referred to as the necrosome (Kaiser *et al*., 2008; Kaiser *et al*., 2013). Two chaperone proteins, HSP90 and CDC37, stabilize the necrosome rendering it fully active (Li *et al*., 2015; Li *et al*., 2016).

Other than RIPK1 and RIPK3, two more proteins are known to contain a RHIM domain. The Z-DNA-binding protein 1 (ZBP1, also referred to as DAI) can recognize intracellular oligonucleotides. As a result, another detection of viral infection is being merged to the necroptosis machinery pathway (Kaiser *et al*., 2008; Rebsamen *et al*., 2009; Upton *et al*., 2012; Lin *et al*., 2016). The other RHIM-containing protein, the TIR domain-containing adapter-inducting interferon-β (TRIF) links necroptosis to host recognition of bacteria.

Necroptosis is not only activated in response to viral or bacterial invasion, but also as a result of the activation of the TNF receptor 1 (TNFR1), the toll-like receptors (TLRs) and the tumor necrosis factor related apoptosis inducing ligand receptor (TRAILR). The default behaviour of TNFR1 receptor is the recruitment of a complex comprised of TNFR1-associated death domain (TRADD) and RIPK1. RIPK1 is post-translationally modified by K63 (linear, also known as M1) linkages or K48 linked polyubiquitination by E3-ligase complexes, such as the cellular inhibitor of apoptosis protein 1 (cIAP1) and cellular inhibitor

of apoptosis protein 2 (cIAP2) (Feoktistova *et al*., 2011; Vanlangenakker *et al*., 2011). In a similar manner, the linear ubiquitin chain assembly complex (LUBAC), consisting of the SHARPIN, HOIP and HOIL1 proteins, generate linear polyubiquitin chains (Haas *et al*., 2009; Ikeda *et al*., 2011; Peltzer *et al*., 2018). In this state, the receptor activation triggers the downstream NF-κB signalling (Wong *et al*., 2010; Dondelinger *et al*., 2015). Concomitantly, the cellular FLICE-inhibitory protein (cFLIP) will be expressed, rendering the cell resistant to cell death (Krammer *et al*., 2007). With prolonged receptor activation, deubiquitinases (DUBs), such as A20 (Wartz *et al*., 2004; Onizawa *et al*., 2015) and CYLD (Moquin *et al*., 2013; Hrdinka *et al*., 2016; Newton *et al*., 2019a), remove K63 polyubiquitin chains from RIPK1 molecules. Linear chains are being removed by OTULIN (Keusekotten *et al*., 2013; Damgaard *et al*., 2016; Heger *et al*., 2018). Deubiquitination of RIPK1 then leads to the recruitment of pro-caspase-8 via its death domain (DD) that binds FADD. This complex results in a functional caspase-8 homodimer capable of cleaving the effector caspases (caspase-3, 6 and 7) that will mediate and execute apoptosis (Krammer *et al*., 2007). Caspase-8 also forms heterodimers with the long version of cFLIP, and by mechanisms which include RIPK1, RIPK3 and CYLD, inactivates RIPK3. Hereby, the necroptosis pathway is inhibited. This inhibitory effect of cFLIP/caspase-8 explains the embryonic lethality of caspase-8 deficient mice, a phenotype reversed on a RIPK3-deficient background in mice (Kaiser *et al*., 2011; Oberst *et al*., 2011). Hence, the loss of cFLIP or viral inhibition of caspase-8 unleashes the activation of RIPK3 upon RIPK1-mediated phosphorylation which set off the process of necroptosis (Dillon *et al*., 2012; Dillon *et al*., 2014).

All the necroptosis triggers lead to a shared downstream path involving the mixed lineage kinase domain-like pseudokinase (MLKL). MLKL is being phosphorylated at the activation loop by the RIPK3 kinase domain of the active necrosome, causing the exposure of a four helical bundle (4-HB). Additionally, a persistent phosphate residue in the hinge region between the 4-HB and the rest of the protein is being dephosphorylated (Murphy *et al*., 2013; Murphy *et al*., 2014; Rodriguez *et al*., 2016). The fully active protein, phospho-MLKL (pMLKL) binds to phosphatidylinositol-4,5-bisphosphate (PIP2) in the plasma membrane and by means yet to be clarified causes the loss of plasma membrane integrity (Dondelinger *et al*., 2014; Wang *et al*., 2014). However, membrane repair mechanisms formed by the endosomal sorting complexes required for transport (ESCRT-III) have been shown to be downstream of pMLKL. The presence of the ESCRT-III machinery extends the time until the plasma membrane ruptures (Gong *et al*., 2017). Absence of the ESCRT-III complex leads to MLKL-dependent necroptosis (Gong *et al*., 2017; Yoon *et al*., 2017; Zargarian *et al*., 2017).

Several molecules have been developed that inhibit necroptosis. Such molecules are referred to as “necrostatins”. For instance, the small molecule Necrostatin-1 (Nec-1) inhibits the RIPK1 kinase (Degterev *et al*., 2005; Degterev *et al*., 2013; Degterev and Linkermann, 2016). Apart from blocking necroptosis, Nec-1 has been shown to exhibit ferroptosis-inhibitory features (Friedmann Angeli *et al*., 2014a), a pathway that

is presented in more detail in section 1.1.4. A more necroptosis-specific molecule based on the structure of Nec-1 was developed and termed Nec-1s (Degterev *et al*., 2013). Other inhibitors of RIPK3 (e.g. GSK'840) (Mandal *et al*., 2014) and MLKL (e.g. necrosulfonamide) (Sun *et al*., 2012) have also been developed.

1.1.3. Pyroptosis

Pyroptosis is defined as an inflammasome-mediated pathway in which gasdermins are key mediators of cell death (**Figure *1*C**). It has been described in macrophages as a necrotic type of death where inflammasomes lead to caspase activation (Man *et al*., 2014). Inflammasomes are cytosolic, intracellular supramolecular complexes. Caspase-1 and caspase-11 mediate the proteolytic activity of inflammasomes in mice, and caspase-4 mediates the proteolytic activity of inflammasomes in humans (Broz and Dixit, 2016; de Vasconcelos *et al*., 2016). The interleukins pro-IL-1β and pro-IL-18 contain a cleavage site for caspase-1, while gasdermin D (GSDMD) can be cleaved by caspase-11 (Kayagaki *et al*., 2015; Shi *et al*., 2015; Ding *et al*., 2016). The N-terminus of the cleaved GSDMD forms a 28-fold single-ring pore, in a similar way as GSDMA, which represents another member of the gasdermin family able to execute necrotic cell death by pyroptosis (Ding *et al*., 2016; Ruan *et al*., 2018). The formation of this pore allows IL-1β and IL-18 to be released into the extracellular space (Ding *et al*., 2016). These two highly pro-inflammatory cytokines render pyroptosis the most pro-inflammatory RCD pathway described to date (Tonnus *et al*., 2018).

An important aspect of pyroptosis is its role in the response to infectious diseases. It has been shown that mice lacking GSDMD are protected from lipopolysaccharide-mediated shock (LPS shock). Interestingly, caspase-8 controls the cleavage of gasdermins (Fritsch *et al*., 2019; Newton *et al*., 2019b), an event that occurs upstream of inflammasome activation (Vince *et al*., 2012; Kang *et al*., 2013; Philip *et al*., 2014; Lawlor *et al*., 2015). In cell culture systems the death effector domain (DED) of caspase-8 was shown to bind to ASC (an inflammasome component) (Newton *et al*., 2019b). However, data demonstrating this in mice are lacking. Evidently, inflammasomes exert two major functions: the cytokine maturation and the GSDMD cleavage. These two events happen in a mechanistically distinct fashion, during which ASC oligomerization is required for IL-1β maturation, while absence of ASC allows the cleavage of GSDMD (Dick *et al*., 2016).

At least six members of the gasdermin family have been identified in humans: GSDMA, GSDMB, GSDMC, GSDMD, GSDME and DFNB59 (Wang *et al*., 2017). Other members of the gasdermin family have the potential of forming pores, such as GSDME, which can be activated by caspase-3 during apoptosis (Wang *et al*., 2017; Rogers *et al*., 2019). GSDMD also contains a caspase-3 cleavage site (Taabazuing *et al*., 2017) which is preventing the GSDMD N-terminal fragment pore formation (Wang *et al*., 2017; Rogers *et al*., 2019).

1.1.4. Ferroptosis

The term ferroptosis was first introduced in 2012 (Dixon *et al.*, 2012), and is an iron-catalysed type of RCD that leads to lipid peroxidation (Dixon *et al*., 2012a; Stockwell *et al*., 2017a). Ferroptosis differs from the other RCD pathways (apoptosis, necroptosis and pyroptosis) in many ways (**Figure *1*D**). No death receptors or DNA-sensors have been found to induce ferroptosis, while it remains unclear which specific signal triggers ferroptosis initiation *in vivo* (Davidson and Wood, 2020). Cellular concentrations of reactive oxygen species (ROS) may result from iron-catalysed or Fenton reactions, which can potentially lead to lipid peroxidation. Under healthy conditions, lipid peroxidation is prevented by diverse cellular anti-redox systems (Tonnus *et al*., 2021a). When these systems fail, then the plasma membrane will get oxidised leading to its rupture by poorly understood mechanisms (Dixon *et al.*, 2012; Dixon and Stockwell, 2014). Polyunsaturated fatty acids (PUFAs) are considered to be the primary targets of free radicals, such as ROS (Yin *et al*., 2011; Tonnus *et al*., 2021a). A hydrogen atom from the targeted PUFA is abstracted, yielding a carbon-centered radical that can react with O_2. The last reaction leads to a peroxyl radical that can propagate the chain reaction by interacting with another molecule or even itself. Interestingly, the number of double bonds of the lipids increases the complexity of the oxidised products, as PUFAs can be autooxidised (Yin *et al*., 2011).

The metabolism of amino acids is tightly linked to ferroptosis (Friedmann Angeli *et al*., 2017; Stockwell *et al*., 2017a). The antiporter system X_c^- exchanges a cysteine with a glutamate in a 1:1 ratio. High levels of glutamate inhibit the system X_c^- and therefore trigger ferroptosis (Dixon *et al*., 2012a). Cystine is metabolized intracellularly to cysteine, the rate-limiting amino acid for glutathione (GSH) synthesis (Sarhan *et al*., 2018b). GSH is synthesized from glutamate, cysteine, and glycine in two steps. The ATP-dependent cytosolic enzyme glutamate-cysteine ligase (GCL) produces a molecule of γ-glutamyl-cysteine, which with glycine will be utilised by the also ATP-dependent cytosolic enzyme glutathione synthetase (GSS) (Stockwell *et al*., 2017a). GSH is essential for the anti-ferroptotic function of the enzyme glutathione peroxidase 4 (GPX4), a selenoprotein, which inhibits the peroxidation of plasma membrane lipids (Stockwell *et al*., 2017b; Ingold *et al*., 2018). Metabolism of GSH results in the increase of intracellular levels of NADPH, which in certain types of cells such as renal tubular cells may diffuse freely through shared cytoplasms interconnected via gap junctions and tight junctions (Belavgeni *et al*., 2020). Depletion of the GSH or the NADPH levels will therefore lead to a dysfunction of GPX4 halting the reduction of continuously produced peroxidised lipids to PE-alcohol (Belavgeni *et al*., 2020). Consequently, GPX4 counterbalances the Fenton reactions maintaining homeostasis alongside low intracellular levels of H_2O_2.

Two other GSH-independent inhibitory systems have been reported: the ferroptosis-suppressing protein 1 (FSP1, also known as apoptosis-inducing factor mitochondrial 2) (Bersuker *et al*., 2019; Doll *et*

al., 2019) and prominin-2 (Belavgeni *et al*., 2019a; Brown *et al*., 2019). FSP1 is recruited to the plasma membrane by a myristoylation-binding motif and functions as an oxidoreductase that generates radical-trapping antioxidants (RTA) by reducing the coenzyme Q10 (CoQ10 otherwise known as ubiquinone-10), which counteract lipid peroxidation. FSP1 uses NAD(P)H to catalyse the generation of CoQ10 (Bersuker *et al*., 2019; Doll *et al*., 2019). Interestingly, GXP4 deficient mice are embryonically lethal (Ingold *et al*., 2018), while FSP1 deficient mice are viable and fertile (Bersuker *et al*., 2019). On the other hand, prominin-2 facilitates ferroptosis resistance via promoting the formation of ferritin-containing multivesicular bodies (MVBs) and exosomes that transport iron out of the cell, thus inhibiting ferroptosis. Consequently, this system regulates iron homeostasis and intracellular trafficking (Brown *et al*., 2019). However, to what extent the neighbouring cells might get sensitised to ferroptosis due to the increase of iron concentration in the microenvironment is unclear (Belavgeni *et al*., 2019a).

The repair mechanisms are essential in combating the peroxidation of membrane lipids, thereby counteracting cellular processes, which modulate the lipid peroxidation system. ACSL4 (Acyl-CoA Synthetase Long Chain Family Member 4) converts free fatty acids into fatty CoA esters (Doll *et al*., 2017). LPCAT3 (lysophosphatidylcholine acyltransferase 3) is involved in the biosynthesis of phospholipids. The products of ACSL4 and LPCAT3 are required for the onset of ferroptosis (Stockwell *et al*., 2017a). Consequently, loss of these genes leads to a resistance against ferroptosis (Dixon *et al*., 2015; Doll *et al*., 2017). Other systems such as oxidoreductases, including NADPH-cytochrome P450 reductase (POR) and NADH-cytochrome B5 reductase (CYB5R1), contribute to the sensitivity towards ferroptosis via the transferring of electrons from NAD(P)H to oxygen. This results in the production of H_2O_2, which reacts with iron generating reactive hydroxyl radicals. Concomitantly, these radicals react with PUFAs, thereby disrupting the membrane integrity leading to ferroptosis (Yan *et al*., 2021). Another system critically involved to the ferroptosis sensitivity is the regulation of the intracellular iron pool, by heme oxidase 1 (Zarjou *et al*., 2013), H-ferritin (Fang *et al*., 2020) and hepcidin (Scindia *et al*., 2015).

Ferroptosis inducers (FINs) have been developed, studied, and considered for a range of diseases such as cancer therapy or treatment of autosomal dominant polycystic kidney disease (ADPKD). Based on the mode of action four major classes of FINs have been proposed. Type I FINs inhibit the system X_c^-. Erastin, a small molecule found in a wide screen of compounds aiming to "eradicate" oncogenic RAS mutant cell lines belongs to this group (Dolma *et al*., 2003). Compounds that target the active center of GPX4, such as the small molecule RSL3 that confers increased lethality in the presence of oncogenic RAS (Yang and Stockwell, 2008), are categorized as type II FINs. Type III FINs, such as FIN56, degrade GPX4 (Shimada *et al*., 2016). Compounds belonging to the type IV FIN class, such as FINO2, cause indirect loss of the enzymatic activity of GPX4 while directly oxidizing iron (Gaschler *et al*., 2018). However, its exact mechanism remains unclear. Development of FINs is an ambitious field of research in pursuit of

therapeutics of a variety of diseases. For example, cancer cells that evade high H_2O_2 levels by upregulation of anti-ferroptosis pathways belonging to tumours that are resistant to initial chemotherapy are particularly sensitive to ferroptosis induction. Other types of cancer, such as adrenocortical carcinomas and clear cell carcinomas, show a high sensitivity towards ferroptosis induction (Yang and Stockwell, 2008; Zhou and Yuan, 2014; Belavgeni *et al*., 2019b).

On the other hand, small molecules have also been developed targeting ferroptosis (Skouta *et al*., 2014; Degterev and Linkermann, 2016; Martin-Sanchez *et al*., 2017a), with several of them representing high-quality compounds with promising pharmacodynamic and pharmacokinetic properties (Hofmans *et al*., 2016; Devisscher *et al*., 2018). Ferrostatin-1, also referred to as Fer-1, was found in a screen for inhibitors of erastin-induced ferroptosis in human fibrosarcoma (HT1080) cells (Dixon *et al*., 2012a). Fer-1 acts a lipid antioxidant and is the most used compound in studying ferroptosis. Interestingly, the necroptosis inhibitor Nec-1 was also found to function as an effective ferroptosis inhibitor (Friedmann Angeli *et al*., 2014a). The compound SRS11-92, a Fer-1 derivative, has been found to be effective in the prevention of tubular necrosis (Skouta *et al*., 2014). Similarly, liproxtatin-1 (Lip-1) was investigated in a model of liver ischemia reperfusion injury (IRI) and showed strong beneficial effects (Friedmann Angeli *et al*., 2014a).

In certain cases ferroptosis has been observed to occur in a synchronized manner in renal tubules (Linkermann *et al*., 2014), cell culture (Kim *et al*., 2016; Riegman *et al*., 2020a) or in the tail fins of zebrafish upon wound response induction (Katikaneni *et al*., 2020). In the case of HAP1 cells, when challenged to undergo ferroptosis a calcium signal precedes the SYTOX green marker of dead cells (nucleic stain that enters the nuclear membrane only when it ruptures) (Riegman *et al*., 2020a).

1.1.5. Interconnections of the regulated cell death pathways

Necroptosis is of critical importance in cells infected with virus that express caspase inhibitors (Cho *et al*., 2009). Several viral proteins inhibit the proteolytic function of caspase 8, rendering it incapable of cleaving caspases 3, 6 and 7. Therefore, apoptosis is inhibited (Kaiser *et al*., 2013). At the same time, caspase-8 inhibition prevents the inactivation of RIPK1, which proceeds to trigger the necroptotic pathway (Cho *et al*., 2009; Newton *et al*., 2019a). Interestingly, caspase 8 deficient mice are embryonically lethal, a phenotype reversed upon additional deficiency to RIPK3 (Kaiser *et al*., 2011; Oberst *et al*., 2011) or MLKL (Alvarez-Diaz *et al*., 2016). The significance of the interconnection between apoptosis and necroptosis was demonstrated by mutations of RIPK1 preventing its cleavage by caspases which subsequently resulted in autoinflammatory diseases (Lalaoui *et al*., 2020). Additionally, the cleavage of RIPK1 does not only inhibit necroptosis, but also assists in the maintenance of the inflammatory homeostasis during development (Lalaoui *et al*., 2020).

Apoptosis and pyroptosis are also interconnected via caspase 8. Caspase 8 might directly recruit ASC through its DED, regulating inflammasome activation and therefore pyroptosis (Fritsch *et al*., 2019; Newton *et al*., 2019b). Whether caspase 8 can directly cleave and thereby activate GSDMD under certain circumstances is not entirely clear (Mandal *et al*., 2018; Orning *et al*., 2018; Sarhan *et al*., 2018a). Additionally, the proteolytic activity of caspase 3 directly cleaves GSDME at its linker, generating a GSDME-N fragment capable of forming pores in the plasma membrane and initiating pyroptosis (Wang *et al*., 2017). Furthermore, the cellular FLICE-inhibitory protein was shown to directly inhibit caspase 8-mediated GSDMD cleavage and protecting macrophages from LPS-induced pyroptosis (Muendlein *et al*., 2020). Concerning the sensitivity of cells towards necroptosis or pyroptosis the ESCRT-III complex prevents the loss of membrane integrity by releasing pMLKL (Gong *et al*., 2017; Yoon *et al*., 2017) or GSDMD-N terminal-containing microvesicles (Rühl *et al*., 2018), respectively.

Ferroptosis, on the other hand, is not shown to have any interconnections with the other three regulated pathways. The only known common feature of ferroptosis to necroptosis and pyroptosis is the loss of plasma membrane integrity, an event occurring due to the loss of the redox capacity of the cell (Tonnus *et al*., 2021a). Nevertheless, a connection of ferroptosis with the other pathways would be rather expected, since evidence from acute kidney injury models point towards the importance of both necroptosis and ferroptosis (Belavgeni *et al*., 2020). Clinical needs to inhibit acute kidney injury (AKI) have led, for instance, to the development of a dual inhibitor of necroptosis and ferroptosis termed as Nec-1f (Tonnus *et al*., 2021c).

1.2. The neuroendocrine system of the HPA axis: focus on the adrenal glands

1.2.1 The HPA axis

Under stress conditions, the human body activates multiple coordinated and dynamic processes aiming to restore homeostasis (Russell and Lightman, 2019). This system was evolutionary developed with the goal of better survival of the organism when the body is under threat or under physiological conditions dictated by the circadian rhythm. In such a case, a hormonal-neural network is mobilized to optimize the metabolic, immunological, cognitive and cardiovascular functions (Russell and Lightman, 2019). In the absence of stress, a circadian rhythm of the adrenocorticotropic hormone (ACTH) and glucocorticoid secretion is observed. The nadir and the quiescent phase of the ACTH and the secreted glucocorticoids are dictated by the waking and sleeping cycle of the organism (Lightman and Conway-Campbell, 2010; Russell and Lightman, 2019). This rhythm is tightly regulated from the suprachiasmatic nucleus of the hypothalamus (Reppert and Weaver, 2002) and has been observed in several mammals including humans (De Kloet and Sarabdjitsingh, 2008; Sarabdjitsingh *et al*., 2010). Pathophysiological conditions, such as arthritis, may alter the circadian corticosterone rhythm in rodents (Windle *et al*., 2001).

The system responsible for the regulation and secretion of the adrenal hormones is the hypothalamus-pituitary-adrenal (HPA) axis (**Figure 2**). Briefly, the suprachiasmatic nucleus (SCN) of the hypothalamus is responsible for the secretion of corticotropin-releasing hormone (CRH) and arginine vasopressin (AVP) to the portal blood vessel system. These hormones act on the anterior lobe of the pituitary, which in turn produces ACTH (also known as corticotropin). The adrenal glands respond to the ACTH signal via the production and release of glucocorticoids, such as cortisol. Once the levels of glucocorticoids are high enough, they act with negative feedback on the hypothalamus and the pituitary.

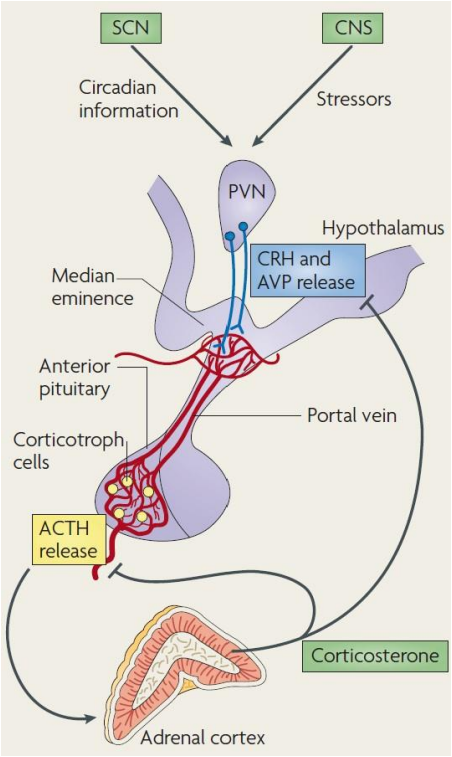

Figure 2. Schematic model of the HPA (hypothalamus-pituitary-adrenal) axis and the release of hormones. Inputs from the suprachiasmatic nucleus (SCN), physical stressors relayed from the central nervous system (CNS), negative feedback mediated by the secretion of glucocorticoids are a few features to which the hypothalamus responds. The paraventricular nucleus of the hypothalamus secretes corticotropin-releasing hormone (CRH) and arginine vasopressin (AVP), two adrenocorticotropic hormone (ACTH) secretagogues, at the portal vein that reaches the anterior pituitary. CRH and AVP activate the receptors of the corticotroph cells, which in turn will release ACTH. Subsequently, ACTH triggers the production and release of glucocorticoids, which elicit negative feedback at the level of CRH release of the hypothalamus and ACTH of the pituitary. (Image obtained from Lightman and Conway-Campbell, 2010).

1.2.2. The adrenal glands

The adrenal glands are complex polyfunctional bilateral organs situated above the kidneys. They are comprised of two distinct regions: an outer region termed cortex and an inner region termed medulla. The cortex comprises of three distinct histological zones. The *zona glomerulosa*, is comprised of cells arranged

in a rosette formation which are surrounded by a basement membrane. These cells are responsible for the production of mineralocorticoids, such as aldosterone (responsible for the regulation of blood pressure as part of the renin-angiotensin system and electrolyte balance). In the *zona fasciculata*, which comprises the bulk of the cortex, the lipid-laden cells are arranged radially in bundles of parallel cords (fasces). Cells of this *zona* produce glucocorticoids, cortisol and cortisone, important regulators of the immune system and metabolism. The innermost layer of the cortex, the *zona reticularis*, consists of a tangled network of cells and produces androgens that are converted to fully functional sex hormones in the gonads. The medulla consists of modified sympathetic ganglia, that respond to cholinergic preganglionic fibres releasing catecholamines: epinephrine (also known as adrenaline) and norepinephrine (also known as noradrenaline) (Goodman, 2009; Hahner *et al*., 2021). A schematic view of the adrenal gland zonation and the hormones produced from each zona are shown in **Figure 3**.

The outer layers of the cortex undergo homeostatic renewal and regeneration after injury. As a dynamic organ, the adrenal gland is able to adjust its size and function in order to respond to the varying physiological demands (Lyraki and Schedl, 2021). During this process, steroidogenic cells undergo lineage conversion from zona glomerulosa to zona fasciculata, altering their identity (Freedman *et al*., 2013). The capsule zone and the sub-capsule zone, which are highly proliferative, will replace the adrenal tissue in a span of 3 months depending on the sex. For instance female mice show three times higher turnover of the adrenal cortex compared to male mice (Grabek *et al*., 2019). Canonical WNT signalling (β-catenin-dependent) is crucial for the development of the *zonas* in the adrenal. A gradient of diminishing WNT ligand expression is observed from the outer to the inner adrenal cortex. Therefore, high levels of β-catenin accumulate in the *zona glomerulosa* (Walczak *et al*., 2014; Finco *et al*., 2018; Basham *et al*., 2019). In the outer cortex R-spondin 3 (RSPO3) counteracts the activity of the membrane-bound E3 ubiquitin-protein ligase ZNRF3 (Hao *et al*., 2012; Zebisch *et al*., 2013; Vidal *et al*., 2016). ZBRF3 promotes in the inner cortex the lysosomal degradation of Frizzled WNT receptors. Therefore, the WNT signalling pathway is inhibited in the inner cortex (Basham *et al*., 2019). Given the complexity of the adrenal microenvironment in terms of renewal it is important to bear the effects of sex hormones, e.g. testosterone, in mind, on its developmental process (Grabek *et al*., 2019), a concept that has started to evolve during the past few years.

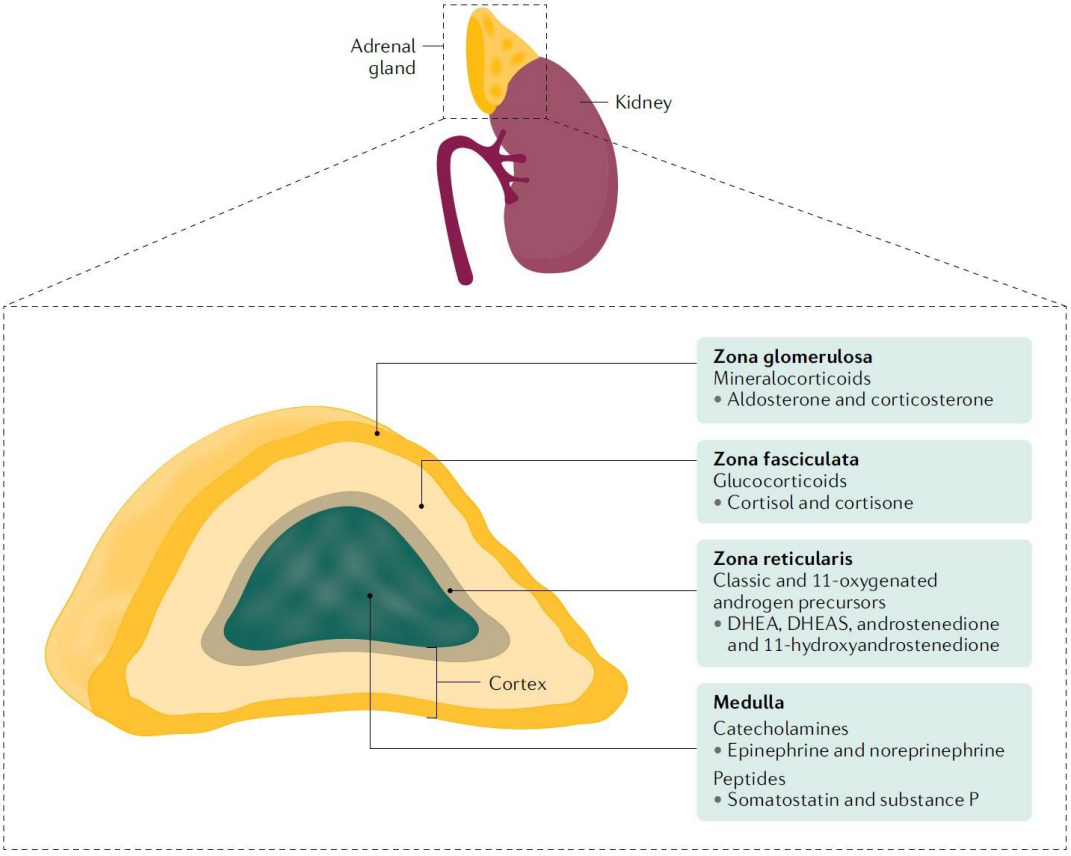

Figure 3. Schematic view of the adrenal gland zonation and the respective hormones produced from each *zona*. There are two major parts of the adrenal gland, the outer steroid-secreting cortex, and the inner neuroendocrine medulla. The cortex is further subdivided into three layers/zones. A capsule is covering the outermost *zona glomerulosa*, responsible for the production of mineralocorticoids. The intermediate *zona fasciculata* releases glucocorticoids, while the inner *zona reticularis* secretes adrenal androgen precursors. Catecholamines are being secreted by the medulla. DHEA; dehydroepiandrosterone, DHEAS; dehydroepiandrosterone sulfate. (Image obtained from Hahner *et al*., 2021).

1.2.2.1. Adrenocortical carcinomas

Adrenocortical carcinomas (ACCs) are rare, frequently aggressive tumours derived from the cortex of the adrenal glands. ACCs are recognized by the 2017 WHO (World Health Organization) classification as malignant epithelial tumours of adrenocortical cells (Lam, 2017; Lloyd *et al*., 2017). The incidence of ACCs is approximately one to two per million per year (Allolio and Fassnacht, 2006; Fassnacht *et al*., 2011; McAteer *et al*., 2013). A bimodal distribution of age has been observed for ACCs, with a peak before the age of five and a plateau between 40 and 60 years of age. Generally, the pace and aggressiveness of the disease progression are more severe in adults than in children (Ng and Libertino, 2003). The median overall survival of adult patients is approximately three to four years, while an approximate five year survival for the paediatric patients appears to be less than 60% (McAteer *et al*., 2013). Depending on the location of the ACC the survival might differ. For example, for patients whose ACC is limited to the adrenal cortex there

is a 60-80 % chance for a 5-year survival, while this number drops to 35-50 % for ACCs with locally advanced disease and 0-28 % when distant metastases are observed. These statistics reveal the importance of tumour staging for the prognosis of the disease (Fassnacht *et al*., 2009). The malignancy of the ACC is primarily determined by the Weiss scoring system (Weiss, 1984). The WHO recommends the use of the European Network for the Study of Adrenal Tumours (ENSAT), which is based on the size and the extent of the ACC (Fassnacht and Allolio, 2009). Additionally, the proliferation marker Ki-67, may be used to assess the proliferation rate of the tumour, making it an important prognostic factor (Fassnacht and Allolio, 2009).

An early diagnosis of the disease is challenging due to its rarity, combined with the lack of distinct alarming symptoms. Endocrine disturbances may occur in cases of hormone-secreting ACCs, representing the 50-60 % of cases. Clinically, hypercortisolism, or else referred to as Cushing syndrome (50-60 % of patients) and/or hyperaldosteronism (20-30% of female patients) are observed in the cases of hormone-secreting ACCs. A smaller percentage of patients show estrogen and/or mineralocorticoid excess (Fassnacht *et al*., 2018). Additionally, symptoms such as weight loss or gain, fatigue, insomnia, night sweating or fever are commonly observed and develop rapidly (usually between three to six months) (Ng and Libertino, 2003). Non-hormone-secreting ACCs or tumours with a modest production of steroids present with a clinical manifestation related to the growth of the tumour (e.g., abdominal pain) or with an incidentally found abdominal mass, which in this case is termed as incidentaloma. Apart from the evaluation of the hormone secretion, imaging using for examples computed tomography (CT) or magnetic resonance imaging (MRI) is used for differential diagnosis of a primary adrenal mass and potential metastases (Fassnacht and Allolio, 2009). Moreover, cytology from a specimen obtained by fine-needle aspiration (FNA) may not distinguish between a benign adrenal tumour and an ACC, but it can distinguish between an adrenal tumour and a metastatic tumour, providing more information concerning the staging of the disease (Jhala *et al*., 2004).

Most ACC cases appear to be sporadic, however, several hereditary cancer syndromes have been described as the cause of ACCs (Koch *et al*., 2002; Else and Rodriguez-Galindo, 2016). The Li-Fraumeni syndrome is inherited as an autosomal dominant disorder and is associated with inactivating mutations of TP53. This syndrome is detected in 50 % of the paediatric ACC tumours (Wasserman *et al*., 2015). Germline mutations at the TP53 are detected in 4-6 % of the adult patients (Herrmann *et al*., 2012; Raymond *et al*., 2013; Zheng *et al*., 2016). Mutations or deletions of genes at the chromosome 11p5.5 are associated with the Beckwith-Wiedemann syndrome, which is found in some cases of paediatric ACC (Weksberg *et al*., 2010). Interestingly, even though the mechanisms of many hereditary syndromes are rather well characterized, the molecular pathogenesis of sporadic ACCs is yet to be understood. Nevertheless, high chromosomal aneuploidy is a hallmark of ACC tumours, which separates them from adrenocortical

adenomas. The TCGA cohort identified three subgroups of ACCs: “chromosomal” with gains or deletions, “noisy” with high number of chromosomal breaks and “quiet” with few somatic copy number alterations (Zheng *et al*., 2016). It is estimated that ACCs rank among the top five tumours with the highest levels of chromosomal aneuploidy (Taylor *et al*., 2018). In addition, irregular cell cycle, impaired chromatin and DNA repair, and alterations of signalling pathways, such as the WNT-β-catenin pathway, are considered to be some of the molecular hallmarks of the ACC biology (Tissier *et al*., 2005).

The only curative option for patients with ACC currently is complete surgical resection of the tumour (adrenalectomy). According to the ENSAT guidelines, patients must undergo a hormonal profiling to determine the secretory activity of the tumour. This knowledge is important for cases of cortisol-producing tumours due to the potential suppression of the HPA axis, which could lead to a postoperative adrenal insufficiency (Fassnacht *et al*., 2018). Removal of the peritumoral lymph nodes has additionally been shown to increase the survival rate of patients with ACCs (Reibetanz *et al*., 2012).

Patients with inoperable or advanced ACC are treated with the only drug approved by the European Medicines Agency and the FDA, mitotane (Crona and Beuschlein, 2019). Mitotane is a derivative of the pesticide DDT (1,1-(dichlorobiphenyl)-2,2-dichloroethane) and even though it has been used for more than 70 years, its mode of action remains unclear (Paragliola *et al*., 2020). As an adrenocorticolytic drug, mitotane treatment seems to be more successful for patients with less aggressive tumours (Fassnacht *et al*., 2018). A combination of mitotane with other cytotoxic agents, such as etoposide, doxorubicin and/or cisplatin, may be used for the primary therapy of unresectable tumours and for the treatment of the recurrence of the disease (Fassnacht *et al*., 2018). Concerning the duration of the mitotane used as an adjuvant treatment there are no clear guidelines, especially for patients with low-risk disease (Fassnacht *et al*., 2013; Fassnacht *et al*., 2018). Even though mitotane seems to be beneficial in certain cases of ACC, a high spectrum of side effects has been observed. These include fatigue, lethargy, dizziness, nausea, vomiting, anorexia, skin rash, diarrhoea, leukopenia, haematuria, to name a few (Allolio and Fassnacht, 2006). While adrenolytic drugs (e.g., mitotane) might be beneficial for the clearance of the tumour, the steroidogenesis of the normal adrenal cells is inhibited, thereby causing steroid deficiency. Adrenal insufficiency is treated by administration of glucocorticoids (Fassnacht *et al*., 2018; Paragliola *et al*., 2020).

1.2.2.2. Regulated cell death in the adrenal glands

Adrenocortical tumours seem to show high levels of DNA double-strand breaks, as detected via TdT-mediated dUTP-biotin nick end-labelling (TUNEL) staining (Wachenfeld *et al*., 2001). This observation has led to interpretation of TUNEL positivity as a sign of apoptosis (Tonnus *et al*., 2021a). However, every cell death pathway (including the ones mentioned in section 1.1) exhibits TUNEL positivity. Therefore, a scientific interpretation concerning the regulated cell death pathway which could be triggered to eliminate

ACC cells is not yet possible. As mentioned already in section 1.1., necrotic cells release DAMPs that may trigger different inflammatory responses. A hormone producing tumour dying by necrosis would therefore not only release DAMPs, but also hormones that might be associated with necrotic death. This phenomenon is referred to as damage-induced release of endocrine factors (DIRE) (Tonnus *et al.*, 2021a). Those factors can potentially cause systemic consequences mediated by hormone signalling or interfere with the progression of regulated cell death pathways, as shown for dexamethasone effects on ferroptosis sensitivity (Lau *et al*., 2022; von Mässenhausen *et al*., 2022). Analysis of the supraphysiological concentrations of DIRE in the serum of patients could provide the scientific field with information on the underlying mechanism of necrosis and therefore dictate a better treatment strategy (Tonnus *et al*., 2021a).

The importance of GPX4 during ferroptosis was mentioned above (section 1.1.4). Other members of the glutathione peroxidase family (GPX3, GPX7 and GPX8) were found to be amongst the most frequently mutated genes in ACCs (Giordano *et al*., 2009; Zheng *et al*., 2016). Interestingly, those studies found lipoxygenases (e.g., ALOX12) to be mutated, while thioredoxin reductases were overexpressed (Giordano *et al*., 2009; Zheng *et al*., 2016). Such mutations of the cancer cells could indicate a strategy of the tumor to avoid on the one hand ferroptosis and lipid peroxidation on the other hand. However, a connection of the ACC with regulated cell death pathways, other than apoptosis, has not been thoroughly investigated.

1.3. Structure of the kidney

Up to two thirds of the human body consist of water. The normal organ function is maintained via the fluid balance attributed to the function of the kidneys (Wallace, 1998). The human kidneys are located in the retroperitoneal space of the posterior abdominal wall on each side of the spine at the level between the twelfth thoracic and third lumbar vertebrae and are bean-shaped (Wallace, 1998; Du *et al*., 2018). The right kidney lies slightly lower than the left one due to the displacement by the liver (Wallace, 1998). A cushion of fat keeps the kidneys in position, while their position between the abdominal organs and the muscles of the back protect them from trauma (Wallace, 1998). Blood enters through the paired renal arteries and exits through the paired renal veins, while the end-product of the kidney, the urine, is transported to the bladder through the ureters. Each kidney has three distinct structures enclosed by a fibrous capsule: the cortex, the medulla, and the pelvis (**Figure 4A**) (Du *et al*., 2018). The medulla is divided into a series of wedges, termed as renal pyramids, that open into the renal calyces. The major calyces join forming the renal pelvis, the extension of the upper end of the ureter. Renal columns extend from the cortex down between the renal pyramids (**Figure 4A**) (Wallace, 1998).

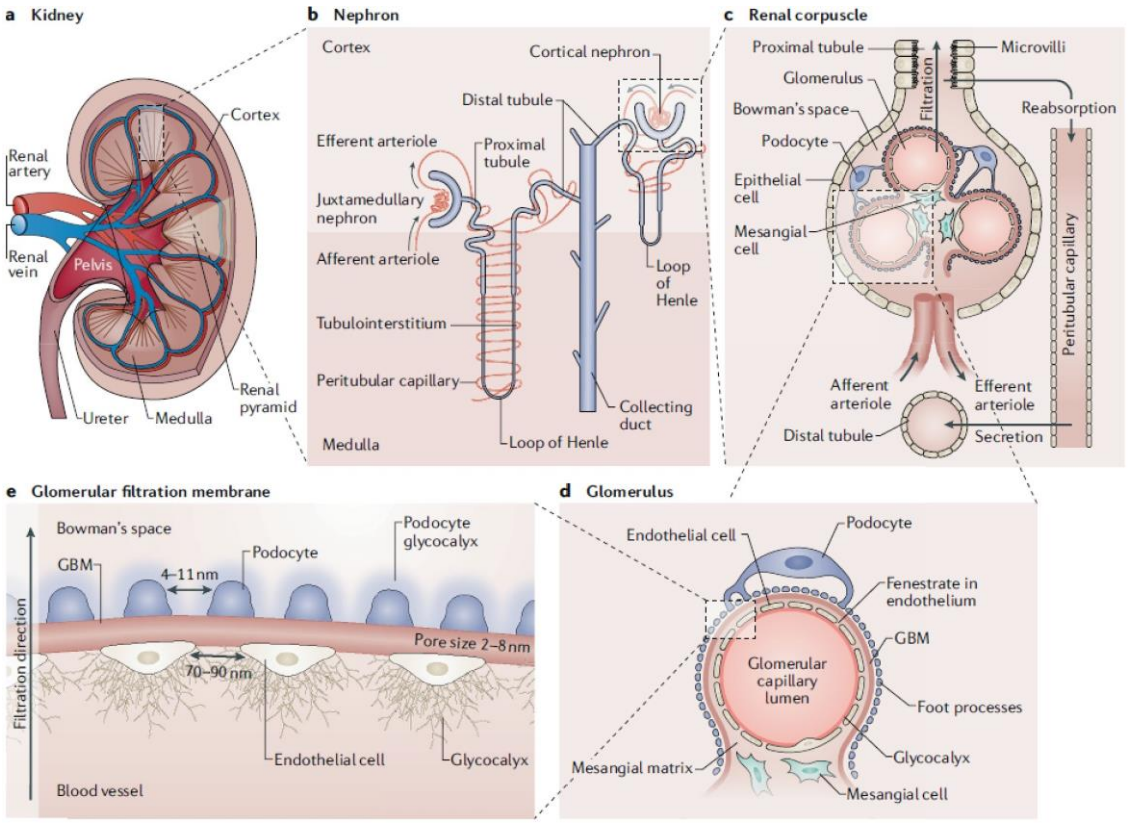

Figure 4. The structure of the kidney. A. Three main structures can be observed in the kidney: cortex, medulla, and the pelvis. Blood enters via the renal artery and exits via the renal vein. The secreted urine is transported through the ureter to the bladder. **B.** The basic structural and functional unit of the kidney is the nephron. It consists of the glomerulus and Bowman's capsule, and the renal tubules (with the order of sequence; proximal tubule, loop of Henle, distal tubule, collecting ducts) and the peritubular capillaries surrounding the renal tubules. **C.** Detailed illustration of the nephron. The afferent arteriole transfers blood into the glomerulus, while the high blood pressure in the glomerular cavity triggers the filtration of fluid, solutes, and waste from the blood into the Bowman's space and then into the proximal tubules (cells located in this part have characteristic microvilli). The efferent arteriole transports the filtered blood. **D.** Between the glomerular capillary lumen and the Bowman's capsule is the glomerular filtration barrier. It consists of endothelial cells carrying glycocalyx structures, the glomerular basement membrane (GBM) and podocytes. The distance between the endothelial cells, the pore size of the GBM and the distance of the podocytes limit the size of proteins that can be filtered under physiological conditions. The endothelial fenestrations are between 70-90 nm, the GBM has 2-8 nm size pores. **E.** The endothelial glycocalyx is consisted of glycosaminoglycans and associated proteoglycans, that line the vascular lumen. The podocytes face the Bowman's space and are arranged in a monolayer with their foot processes featuring 4-11 nm gaps. (Image obtained from Du *et al*., 2018).

The main functions of the kidneys can be divided into five different activities. Firstly, the kidneys regulate the total amount of water in the body, the inorganic ion composition, the acid-base balance, as well as the fluid volume of the internal environment. This is achieved by the excretion of water and inorganic ions, keeping the concentrations of these substances within a narrow range in the body. Secondly, the kidneys are responsible for the excretion of waste metabolic products, in order to prevent them from

accumulating in the body. These include urea, produced from the catabolism of proteins, uric acid, produced from nucleic acids, and creatinine, produced from the muscle creatine. As a third function, foreign chemicals, such as drugs, pesticides, food additives etc. and their metabolites, are being excreted with the urine. Another function of the kidneys is the gluconeogenesis, which occurs after prolonged periods of fasting. Glucose is synthesized from amino acids and their precursors and then released into the blood. Lastly, kidneys are responsible for the release of two hormones: erythropoietin (important for the maturation of red blood cells) and 1,25-dihydroxyvitamin D (important for the regulation of plasma Ca^{2+}), while the secretion of the enzyme renin is important for the control of blood pressure and sodium balance (Widmaier *et al*., 2019).

Approximately 1.2 million functional units, called nephrons, are contained in each kidney (**Figure 4B**). Each nephron consists of an initial filtering component, the renal corpuscle, and the tubule component, that extends from the renal corpuscle. All the renal corpuscles are located in the cortex of the kidneys, while the tubules extend from the cortex with varying lengths into the medulla (Widmaier *et al*., 2019). The renal corpuscle contains the glomerulus, a compact tuft of interconnected capillary loops, which is surrounded by the fluid-filled Bowman's capsule (Wallace, 1998; Widmaier *et al*., 2019). The kidneys are highly vascularised organs with a perfusion rate of approximately 1,200 mL of blood per minute (Wallace, 1998). Blood is filtered from the afferent arteriole into the renal corpuscle to the glomeruli. The high blood pressure in the glomerular cavity results in the filtration of the fluid and its components (containing small molecular size solutes and waste) into the Bowman's space (**Figure 4C**). The glomerular filtrate lacks cells, large polypeptides, and proteins, that are too large to pass through the pores formed by a filtration barrier. This barrier consists of three difference components: the single-celled capillary endothelium (cells that have glycocalyx structures), the basement membrane (non-cellular proteinaceous layer) and the single-celled epithelial lining of Bowman's capsule (cells referred to as podocytes) (**Figure 4D,E**) (Wallace, 1998; Du *et al*., 2018; Widmaier *et al*., 2019). Podocytes are characteristic for their "octopus-like" structure with a large number of foot processes (Widmaier *et al*., 2019). The unfiltered residual fluid is effused through the efferent arteriole, thereby entering the peritubular capillaries, the renal vein and then the main bloodstream (Du *et al*., 2018). Around 80 % of the renal plasma flows through the efferent arterioles to the peritubular capillaries, while the remaining 20 % is filtered at the glomerulus and passes into the Bowman's capsule (Wallace, 1998). The filtration of the plasma per unit of time, represents an important parameter of the physiological function of the kidneys and is referred to as the glomerular filtration rate (GFR). The clearance of creatinine is a method that assesses glomerular filtration with sufficient accuracy for clinical use. Urine formation starts with the glomerular filtration of the plasma (Wallace, 1998). Blood enters the kidney through the cortex, where only 10 % of blood vessels branch off to supply the medulla. This

anatomic structure of blood vessels creates a gradient in the cortico-medullary oxygen pressure. This high osmotic concentration in the medulla facilitates the urine concentration (Scholz *et al*., 2021).

The second step in urine formation is the selective reabsorption of filtered substances, which is achieved by active (energy consuming) and passive (non-energy consuming) transport mechanisms. Among the filtered substances are electrolytes (such as sodium, calcium, potassium, magnesium, phosphate, bicarbonate and chloride), non-electrolytes (such as glucose, amino acids, urea, uric acid and creatinine), and water (Wallace, 1998). The filtered fluid that drains from the Bowman's capsule passes through the proximal tubules where the bulk of the fluid and solutes is reabsorbed (Scholz *et al*., 2021). Concentration of the urine and regulation of salt excretion takes place at the distal nephron segments (Scholz *et al*., 2021). Following the proximal tubule is the loop of Henle, which is a sharp, hairpin-like loop consisting of a descending and an ascending limb. The ascending limb passes between the afferent and the efferent arterioles of that loop's own nephron (**Figure 4C**) (Du *et al*., 2018). The cells located at the transition to the distal convoluted tubules are referred to as macula densa. Most of the water is reabsorbed by the proximal tubule and the loop of Henle. The ascending limb of the loop of Henle leads to the next tubular segment, the distal convoluted tubules. Fluid from the distal convoluted tubules flows into the collecting duct system, which is comprised of the cortical collecting duct and the medullary collecting duct (Widmaier *et al*., 2019). The reabsorption and excretion of metabolic substances are fine tuned by the different tubular parts. For instance, the secretion of the mineralocorticoid aldosterone from the adrenal glands acts on the ascending portion of the Henle loop, the distal convoluted tubule, and the collecting duct increasing sodium ion reabsorption and potassium and hydrogen ion excretion (Wallace, 1998). While each nephron is a separated unit, ultimately multiple collecting ducts merge and the urine drains into the renal pelvis, the kidney's central cavity (Widmaier *et al*., 2019).

1.3.1. Regulated cell death in kidney diseases

A dysregulation or damage of the kidneys can lead to an inadequate filtration of the blood resulting in severe health consequences, such as heart diseases, stroke, anaemia, or increased occurrence of infections. The deterioration of kidney function is defined by a decline in the glomerular filtration rate, tubular necrosis and nephron loss (Venkatachalam *et al*., 2015; Romagnani *et al*., 2017; Ruiz-Ortega *et al*., 2020). Necrosis is a main feature of different acute and chronic renal disorders (Belavgeni *et al*., 2020). Necroptosis, pyroptosis and ferroptosis play an important role in the pathophysiology of kidney diseases (Tonnus *et al*., 2019; Belavgeni *et al*., 2020; Tonnus *et al*., 2021a), as well as the necroinflammation following these types of regulated cell death (Sarhan *et al*., 2018b; Tonnus *et al*., 2018).

Kidney diseases, such as acute kidney injury (AKI) represent a global burden (Hoste *et al*., 2018). AKI is frequently associated with acute tubular necrosis (ATN) and results in nephron loss, as well as permanent deterioration of the renal function in an AKI to chronic kidney disease (CKD) (Venkatachalam

et al., 2015; Agarwal *et al*., 2016). Even though it is possible that more than one RCD pathways might be important for the progression of renal failure, increasing evidence points towards ferroptosis as the main pathway involved, especially in tubular necrosis (Martin-Sanchez *et al*., 2017b; Huang *et al*., 2019; Su *et al*., 2019; Hu *et al*., 2020; Mishima *et al*., 2020). In fact, isolated renal tubules perfused with a ferroptosis inducer, were shown to undergo a cell death that propagated in a synchronized manner (Linkermann *et al*., 2014), which looks similar to the clinical manifestation in humans. Also, experimental intravital microscopy videos do point towards a cell death occurring in a "wave" (Kim *et al*., 2016; Riegman *et al*., 2019). The speculation as to how this death propagates is that the carriers of intracellular redox capacity (primarily NADPH) diffuse through intercellular junctions. Across a line of living and dying cells a NADPH gradient forms, increasing the risk of the neighbouring cells to undergo ferroptosis (**Figure 5**) (Tonnus *et al*., 2021a).

The pathways involved in renal dysfunction have intrigued the field of science, as well as the involvement of the gender of the organisms. Even though it is clear that male rodents are more sensitive to kidney injury as shown in the models of ischemia-reperfusion injury (Müller *et al*., 1999a; Park *et al*., 2004; Silva Barbosa *et al*., 2020), the reason behind such observation remains unclear. Whether testosterone has a sensitizing effect (Park *et al*., 2004; Kim *et al*., 2006), or β-estradiol has a protective effect (Squadrito *et al*., 1997; Barbosa *et al*., 2020), remains to be further investigated.

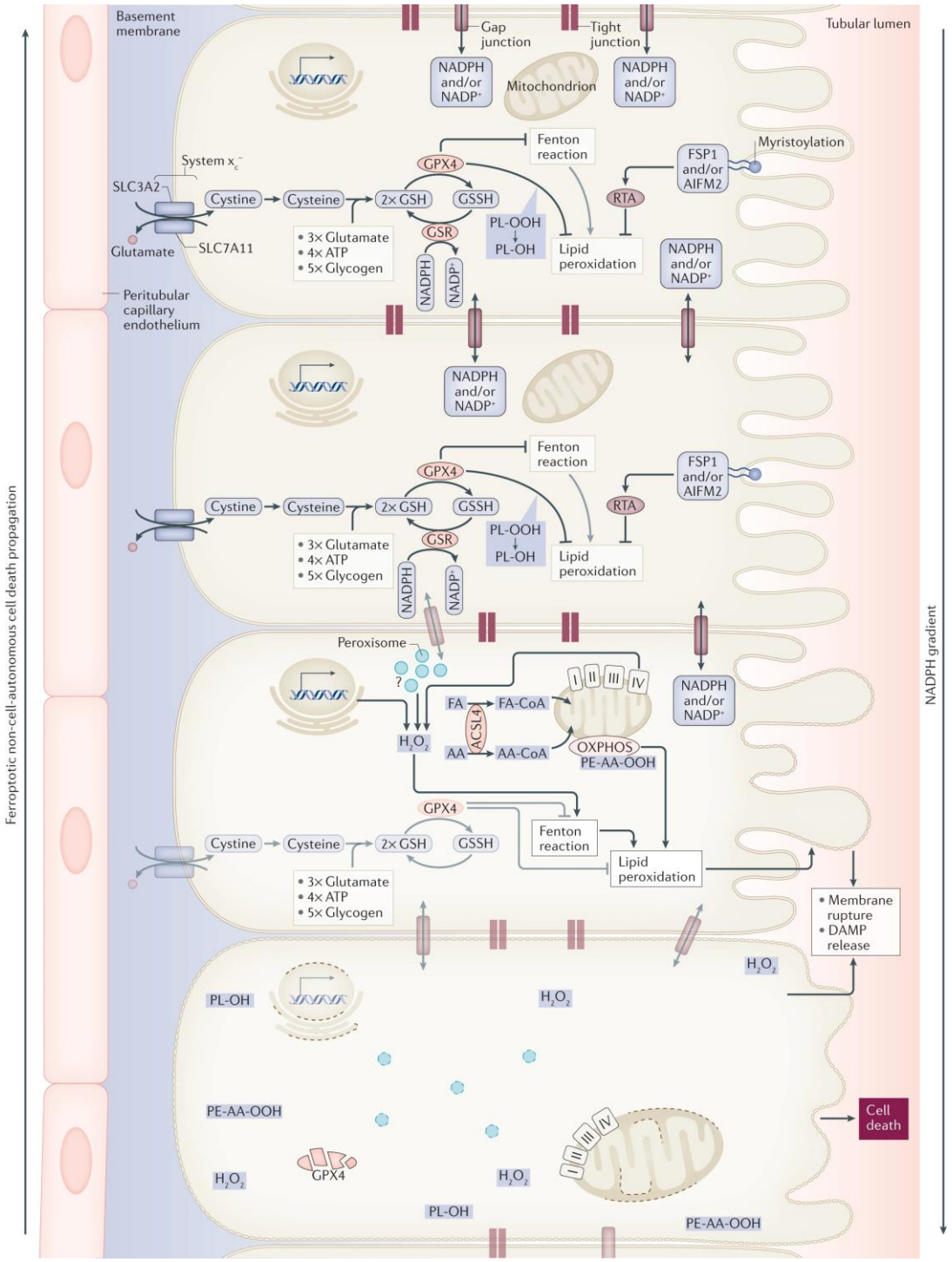

Figure 5. Synchronized regulated necrosis in renal tubules. Graphical representation of renal tubules undergoing ferroptosis. A propagation of death in a "wave-like" manner is being portrayed. It is assumed that a gradient of the redox capacity, specifically the concentration of NADP(H), establishes along the living and dying cells. Consequently, a neighbouring cell has increased risk of dying in a regulated cell death manner. AA, arachidonic acid, FA, fatty acid; GSH, glutathione; GSR, glutathione-disulphide reductase; GSSG, glutathione disulphide; HMGCR, 3-hydroxy-3-methylglutaryl-CoA reductase; PL-OH, phospholipid alcohol; PL-OOH, phospholipid hydroperoxide; RTA, radical trapping antioxidant. (Image obtained from Tonnus *et al*., 2021a).

1.4. Aims

Despite the growing knowledge in the cell death field, the integration of this scientific evidence into a clinical context remains challenging.

In the field of cancer research, detailed knowledge of the mechanisms leading to cell death and the strategies of the cells to evade cell death is of critical importance for understanding the biology of these cells. Furthermore, insights into different cell death modalities are essential in the development of chemotherapeutic agents to be used in the treatment of neoplastic diseases. ACCs have been treated with mitotane for more than 70 years, though the molecular mechanism of action remains unclear. Emphasizing the importance identifying and unravelling specific cell death pathways is provided by numerous studies that used unspecific experimental methods and thereby came to false conclusions regarding the cell death modality. As a consequence, apoptosis is wrongly presented as the main pathway for the action of mitotane. In the first part of this thesis, the principal aim is to understand the mechanisms by which mitotane eliminates ACC cells. To this end, different types of RCD inhibitors were utilized to identify the relevant molecules. The reporting of potential superior therapeutic targets against ACCs was an additional aim of this thesis.

Kidney diseases and their relevance to RCD represent another field of high interest, which as of now is insufficiently studied. Understanding the role of the different RCD pathways in the kidney under physiological and pathophysiological conditions is of utmost importance. Therefore, the principal aim of the second part of this thesis was to investigate the involvement of RCD in a system of isolated renal tubules that undergo spontaneous necrosis. These studies were extended to investigate gender-specific differences of renal tubules, due to the knowledge that female mice are less sensitive to AKI in comparison to male mice. The main difference of male and female organisms is observed at the level of sex hormones. To this end, the effect of testosterone and β-estradiol in the progression of RCD was studied.

Materials and Methods

2. Materials and Methods

2.1. Reagents

Table 1. Substances used during experimental procedures.

Chemicals	Source	Identifier
DMSO	Sigma Aldrich	Cat#D2650
Ethanol	Carl Roth	Cat#64-17-5
ITS+1 Liquid Media Supplement	Sigma Aldrich	Cat#I2521
ITS Liquid Media Supplement	Gibco	Cat#41400045
ITS Liquid Media Supplement (100x)	Sigma Aldrich	Cat#I3146
Insulin from bovine pancreas	Sigma Aldrich	Cat#I6634
Transferrin human	Sigma Aldrich	Cat#T8158
Sodium selenite	Merck Millipore	Cat#214485
Selenium standard solution	Merck Millipore	Cat#1.19796.0100
β-estradiol	Sigma Aldrich	Cat#E2758
Testosterone	Sigma Aldrich	Cat#86500
Mitotane	Sigma Aldrich	Cat#SML1885
MIA602	Andrew V. Schally	N/A
Erastin (type 1 FIN)	Sigma Aldrich	Cat# E7781
RSL3 (type II FIN)	Selleckchem	Cat#S8155
FIN56 (type III FIN)	Sigma Aldrich	Cat#SML1740
FINO2 (type IV FIN)	Keith Wörperl, Brent Stockwell	N/A
Ferroptocide (FTC)	Paul Hergenrother	N/A
Ferrostatin-1 (Fer-1)	Merck Millipore	Cat#341494
TNFα human	BioLegend	Cat#570108
Birinapant	Chemietek	Cat#CT-BIRI
zVAD-FMK	BD Biosciences	Cat#550377
Emricasan	MedChemExpress	Cat#HY-10396
Necrostatin-1 (Nec-1)	Sigma Aldrich	Cat#480065
7-O-Cl-Nec-1 (Nec-1s)	Merck Millipore	Cat#5.04297.0001
SYTOX™ Green Nucleic Acid Stain	Life Technologies	Cat# S7020
BioTracker™ 609 Red Ca^{2+} AM dye	Merck Millipore	Cat#SCT021
7-AAD	BD Biosciences	Cat# 559925
Annexin-V-FITC	BD Biosciences	Cat# 556420
Annexin-V binding buffer	BD Biosciences	Cat# 556454
Kits		
Bradford assay	Fisher Scientific	Cat#G1780
ECL™ Prime Western Blotting System	Fisher Scientific	Cat#GERPN2232
LDH release assay	Promega	Cat# G1780

Bovine insulin, human transferrin and sodium selenite were diluted in Earle's Balanced Salts medium (Sigma Aldrich, E2888) prior to their use. Testosterone and β-estradiol were diluted in ethanol, while all the other substances were diluted in DMSO.

2.2. Antibodies

Table 2. Antibodies used during experimental procedures.

Antibodies	Dilution	Source	Identifier
Anti-Fas (clone 7C11)	10 ng/ml	Merck Millipore	Cat#05-201
Rabbit monoclonal anti-ACSL4 (anti FACL4); human, mouse	1:5000	Abcam	Cat#ab155282
Rabbit polyclonal anti-GPX4 (EPNCIR144); human	1:5000	Abcam	Cat#ab125066
Rabbit polyclonal anti-cleaved caspase 3 (Asp175); human, mouse	1:1000	Cell Signaling	Cat#9661
Rabbit monoclonal anti-RIP1; human, mouse	1:1000	Cell Signaling	Cat#3493
Rabbit polyclonal anti-RIP3; human, mouse	1:1000	Novis	Cat#NBP1-77299
Rabbit polyclonal anti-MLKL C-term; human, mouse	1:250	Abgent	Cat#AP14272b
Rabbit monoclonal anti-MLKL (phosphor-ser358), (EPR9814); human	1:1000	Abcam	Cat#ab187091
Mouse monoclonal anti-β-actin (8H10D19); human, mouse	1:1000	Cell Signaling	Cat#3700S
Rabbit monoclonal anti-GAPDH (14C10); human, mouse	1:1000	Cell Signaling	Cat#2118S
Anti-mouse IgG; HRP-linked antibody	1:5000	Cell Signaling	Cat#7076S
Anti-rabbit IgG; HRP-linked antibody	1:5000	Cell Signaling	Cat#7074S

2.3. Experimental models: Cell lines and mice

Table 3. Cell lines used during experimental procedures.

Cell line	Origin	Source
Human: NCI-H295R	Adrenocortical carcinoma	Provided by Waldemar Kanczkowski (8.9.2017)
Human: Jurkat T cells	Acute T cell leukemia	Provided by Angela Rösen-Wolff (1.2.2018)
Human: HT29	Colorectal adenocarcinoma	Provided by Simone Fulda (11.10.2017)
Human: HT1080	Fibrosarcoma	ATCC (CCL-121)
Mouse: NIH-3T3	Embryonic fibroblasts	ATCC (ERL-1685)
Mouse: L929	Adipose tissue	Provided by Simone Fulda (29.8.2017)

Human: HEK	Embryonic epithelial kidney cells	Leibniz Institute DSMZ-German Collection of Microorganisms and Cell Cultures (ACC-305)
Human: CD10-135	Kidney tubular epithelial cells	Provided by Rafael Kramann (5.2020)
Mice	Type of mice	Source
C57B1/6N	Wild type (WT)	Charles River, Germany
MLKL/GSDMD^{DKO}	Necroptosis and pyroptosis deficient	MLKL-KO: provided by James M. Murphy and Warren S. Alexander (The Walter and Eliza Hall Institute of Medical Research, Australia) GSDMD-KO: provided by Feng Shao (NIBS, Bejing, China)

2.4. Cell culture conditions

NCI-H295R cells (gender: female) were cultured in DMEM/F12 (modified) medium (Gibco, 11330032) supplemented with 2.5 % Nu-Serum (Corning Nu-Serum Culture Supplement, 355500) and 1 % penicillin-streptomycin (Gibco, 15140122). HT29, HT1080, L929, NIH-3T3 and HEK cells were cultured in DMEM (modified) medium (Gibco, 4966029) supplemented with 10% FBS (Gibco, 10270106) and 1 % penicillin-streptomycin. Jurkat T cells were cultured in RPMI (modified) medium (Gibco, 21875091) supplemented with 10 % FBS and 1 % penicillin-streptomycin. For maintenance of the culture, the cells were split in appropriate ratio after reaching 75 % confluency.

2.5. Plating and treatment of cells

For detaching NCI-H295R cells from the flasks Accutase (Thermo Fisher, 00455556) was used, while for all other adherent cell lines Trypsin-EDTA (Gibco, 25200056) was used. Cells were washed with their respective medium (as mentioned at section 2.4) and centrifuged in a Ficoll Paque Plus (Sigma Aldrich, GE17-1440-02) gradient. Cells collected from the corresponding Ficoll fraction were then seeded in six-well plates (Sarstedt, 83.3920) (5 x 10^5 for NCI-H295R cells and 8 x 10^5 for the other cell lines) in their respective medium. The following day the medium was removed, and cells were washed with 1 ml 1X PBS. Substances for treatments were dissolved in vehicle medium (as mentioned in section 2.1.), diluted in fresh medium and added in the established concentrations in 1 ml total volume. After treatment for indicated time points cells were harvested as described above and processed for flow cytometry or western blot (see sections 2.8.1 and 2.8.2)

For experiments involving testosterone or β-estradiol treatment the set-up was adjusted due to the long duration of the experiment. Unless otherwise stated, 1 x 10^5 cells were seeded in six-well plates and 4 h later 10 μM testosterone or β-estradiol was added to the medium for 12 h. Type I (erastin; 5 μM) and II

(RSL3; 1.13 μM) FINs, were then added for indicated time points. Cells were harvested for flow cytometry analysis (see section 2.8.1).

2.6. Mice

8 - 12-week-old C57B1/6N (wild type) male or female mice were co-housed with 2 - 5 mice/cage in individually ventilated cages (IVCs) in the animal facility at the Medizinisch-Theoretisches Zentrum (MTZ) at the Medical Faculty of the Technische Universität Dresden (TU Dresden). Wild type mice (C57Bl/6N) were provided by Charles River, Sulzfeld, Germany, at the age of 6 - 7 weeks. MLKL/GSDMD^{DKO} mice were generated in the lab by crossing previously published MLKL^{KO} mice (von Mässenhausen *et al*., 2018) kindly provided by James Murphy (WEHI, Melbourne, Australia) to GSDMD-ko mice (Shi *et al*., 2015) kindly provided by Feng Shao (NIBS, Bejing, China). All mouse experiments were performed according to German animal protection laws and were approved by the ethic committees and local authorities in Kiel (Germany) and Dresden (Germany).

2.6.1 Isolation of primary murine renal tubules

Primary murine renal tubules were isolated following an adapted protocol that was previously published (Tonnus *et al*., 2021c). Briefly, murine kidneys were removed, washed with PBS (1X), decapsualized and sliced in four to five slices. Kidney slices of each kidney were transferred in 2 ml Eppendorf tubes containing 2 mg/ml collagenase type II in incubation solution (48 μg/ml trypsin inhibitor, 25 μg/ml DNAse I, 140 mM NaCl, 0.4 mM KH_2PO_4, 1.6 mM K_2HPO_4 x 3 H_2O, 1 mM $MgSO_4$ x 7 H_2O, 10 mM CH_3COONa x 3 H_2O, 1 mM a-ketoglutarate and 1.3 mM Ca-gluconate). Slices were digested in a thermoblock for 5 min at 37°C at 850 rpm. These digestion periods were repeated and the supernatant containing isolated tubules was collected after each 5-minute incubation. After each supernatant removal, 1 ml of fresh digestion solution (2 mg/ml collagenase type II in incubation solution was added on the kidney slices). In order to reduce the number of damaged tubules the first and second supernatants were discarded. The third resulting supernatant was collected and transferred in a 2 ml Eppendorf tube containing 1 ml ice-cold sorting solution (0.5 mg/ml bovine serum albumin in incubation solution). The tubes were left for 5 min on ice for the tubules to precipitate. The supernatant was removed, and the tubules were washed twice with ice-cold incubation solution. Once tubules precipitated the supernatant was removed and ice-cold sorting solution was added (volume was adjusted depending on the number of samples needed for the experiment). Tubules were thendistributed in a twenty four-well plate containing DMEM/F12 Nutrient Mixture without glycine and phenol red (DMEM/F12, custom-made medium provided by Cell Culture Technologies LLC), supplemented with 0.01 mg/ml recombinant human insulin, 5.5 μg/ml human transferrin, 0.005 μg/ml sodium selenite (ITS without linoleic acid, Sigma Aldrich), 50 nM hydrocortisone,

100 U/ml penicillin, and 100 μg/ml streptomycin (Pen/Strep, Thermo Fisher). Images of the isolated tubules were obtained using a 20x/0.30 PH1 objective on a Leica DMi1 microscope.

2.6.2. Induction of cell death on isolated murine tubules

All the experiments performed contain a negative control to assess LDH release at 0 h of incubation as a quality control for the tubule isolation procedure. No more than 10% LDH release in these controls was tolerated. Isolated murine renal tubules were placed in twenty-four-well plates containing the respective agents diluted in DMEM/F12 Nutrient Mixture without phenol red (DMEM/F12, custom-made medium provided by Cell Culture Technologies LLC), supplemented with 0.01 mg/ml recombinant human insulin, 5.5 μg/ml human transferrin, 0.005 μg/ml Na_2SeO_3 (ITS without linoleic acid, Sigma Aldrich), 50 nM hydrocortisone, 100 U/ml penicillin, and 100 μg/ml streptomycin (Pen/Strep, Thermo Fisher). After the indicated time points, the medium of each well was collected and prepared for the LDH release assay. Images of the treated murine renal tubules were obtained using a 20x/0.30 PH1 objective on a Leica DMi1 microscope.

2.6.3. Generation, culture and induction of cell death in primary murine tubular cells

Murine tubular cells were generated by outgrowth from isolated renal tubules (as mentioned at section *2.6.1*). Primary murine tubules were placed in six-well plates containing DMEM/F12 Nutrient Mixture without glycine and phenol red (DMEM/F12, custom-made medium provided by Cell Culture Technologies LLC), supplemented with 0.01 mg/ml recombinant human insulin, 5.5 μg/ml human transferrin, 0.005 μg/ml sodium selenite (ITS without linoleic acid, Sigma Aldrich), 50 nM hydrocortisone, 100 U/ml penicillin, and 100 μg/ml streptomycin (Pen/Strep, Thermo Fisher). After two to three days the outgrown primary murine tubular cells were washed with PBS and fresh medium was added. When the confluency of primary murine tubular cells had reached 60 – 70 %, cells were washed with PBS and treated with the four types of FINs (as mentioned in detail at sections 1.1.4 and 2.1). After 24 hours, medium was collected and prepared for LDH release assay (as mentioned in section 2.8.5).

2.7. Generation of a 3D-printed double chamber

For specific live imaging experiments (see section 2.8.3) of isolated tubules 3D-printed double chambers were used.

The chambers consist of a border including a retainer for a glass wall and a glass wall, which is separating the two chambers. The border was printed using a silicone elastomere (SE 1700; Dow Corning) with the 3DDiscovery bioprinter from RegenHU using a conical nozzle with an inner diameter of 250 μm.

Print layouts were developed using the BIOCAD software (RegenHU). The printing speed and extrusion pressure was adjusted to get the thickness of the printed line around 500 μm and a height of 8mm.

The borders of the chamber were printed on top of a silinized microscope slide and cured at 100°C for 30 minutes. A line of SE1700 was printed in the center of the chambers using higher printing speed thus making it thinner than the border of the chambers (around 200 μm). SE1700 was applied to the retainer manually (via a syringe with a conical needle) to bond the glass wall. For the glass wall a cover slip (20 x 20 mm, thickness 0.12 mm) was cut to a size of 8 x 20 mm, cleaned with ethanol, and treated with air plasma for 10 seconds using a cold-plasma generator Piezobrush PZ2-i equipped with a Nearfield nozzle from Relyon Plasma. Then the glass wall was inserted into the retainer and pushed down until it was in direct contact with the thin line of SE1700. This structure was again cured at 100 °C for 30 minutes. The structure was removed from the microscope slide and its bottom side as well as the inside of a six-well plate was treated with air plasma for around 10 seconds (using Piezobrush PZ2-i). Then the structure was attached to a six-well plate and kept at 60 °C for 2 hours for bonding. In some cases, certain places of the border were poorly linked to the surface. These places were sealed with SE1700 manually and then the structure was placed again at 60 °C for 4 hours.

The generation of the 3D-chamber was supported by the Microstructure Facility, a Core Facility of the CMCB Technology Platform at TU Dresden

2.8. Experimental procedures

2.8.1. Fluorescence activated cell sorting (FACS)

NCI-H295R cells were removed from the six-well plates (Sarstedt, 83.3920) with Accutase (Thermo Fisher, Cat#00455556) while all other adherent cell lines were removed with Trypsin-EDTA (Gibco, Cat#25200056). Cells were then resuspended in their respective medium (as mentioned at section 2.4). The obtained pellets were washed twice with PBS (1X) and filtered using polystyrene round-bottom tubes with cell-strainer caps (Corning, Cat#352235). Subsequently, cells were stained with 5 μl of annexin-V-FITC (BD Biosciences) and 5 μl of 7-AAD (BD Biosciences) added to 100 μl annexin-V binding buffer (BD Biosciences). After a 15 min incubation with the staining solution, the cells were analyzed using the BD Biosciences LSRII with the FACS Diva 6.1.1 software (BD Biosciences). The data were analyzed using the FlowJo v10 software (Tree Star).

Flow cytometry experiments were supported by the Flow Cytometry Facility, a Core Facility of the CMCB Technology Platform at TU Dresden.

2.8.2. Western Blotting (WB)

Cell pellets were lysed in ice-cold 10 mM Tris-HClO, pH 7.5, 50 mM NaCl, 1% Triton X-100, 30 mM sodium pyrophosphate, 50 mM NaF, 100 μM 100 μM Na_3VO_4, 2 μM $ZnCl_2$, and 1 mM phenylmethylsulfonyl fluoride (PMSF, modified Frackelton buffer) for 30 min on ice. Samples were centrifugated (14,000 g) for 30 min at 4 °C to remove insoluble material and the supernatant was transferred to a clean tube. Protein concentration was determined using a commercial Bradford assay kit according to the manufacturer's instructions (Thermo Fisher). Subsequent preparation of samples included their denaturation with ROTI Load (Carl Roth, K929) at 95 °C for 5 min. Samples were kept on ice until they were loaded in equal amounts of protein (typically 30 – 35 μg per lane) on a 4 – 15 % gradient SDS/PAGE gel. Following the transfer of proteins on a PVDF membrane (Biorad), membranes were blocked with either 5 % w/v BSA (Carl Roth, Cat#8076.4) or 5 % powder milk (AppliChem ITW Reagents, Cat#271-045-3) in TBS 0.1 % Tween. Primary antibody incubation was performed overnight at 4 °C for anti-ACSL4 (Abcam, Cat# ab155282, 1:5000), anti-GPX4 (Abcam, Cat#ab125066, 1:5000), anti-cleaved-caspase 3 (Cell Signaling, Cat#9661, 1:1000), anti-RIP1 (Cell Signaling, Cat#3493, 1:1000), anti-RIP3 (Novis, Cat#NBP1-77299, 1:1000), anti-MLKL (Abgent, Cat#AP14272b, 1:250), anti-pS358-MLKL (Abcam, Cat#ab187091, 1:1000), anti-β-actin (Cell Signaling, Cat#3700S, 1:1000) and anti-GAPDH (Cell Signaling, Cat#2118S, 1:1000). Secondary antibodies (anti-mouse, HRP-linked antibody, Cell Signaling, Cat#70756S; anti-rabbit, HRP-linked antibody, Cell Signaling, Cat#7074S) were applied in a 1:5000 dilution in BSA or milk and incubated for 1 hour at room temperature. Blots were visualised by enhanced chemiluminescence (ECL; Amersham Biosciences).

2.8.3. Time lapse imaging and processing of the time lapse data

NCI-H295R cells were plated in either 6-well plates or 8-well glass-bottom slides (Ibidi 15 μ-slide 8 well, Cat#80827), treated as mentioned at the section 2.5 and subsequently stained with 50 nM SYTOX green nucleic acid stain (Life Technologies).

Videos of primary murine tubules stained with 50 nM SYTOX green with or without 150 nM Ca^{2+} AM dye (Merck Millipore) were obtained by using an oil-immersion 63x/0.3 EC Plan Neofluar objective. For some live imaging experiments with murine tubules high quality plastic-bottom slides (Ibidi 15 μ-slide 8-well, Cat#80826,) were used. The comparison of female and male tubules was performed using a 2.5x/0.3 EC Plan Neofluar objective. The isolated murine tubular cells were placed in the single 3D-printed well separated by a glass slide and stained with SYTOX green nucleic acid stain. Proliferating cells were generally interpreted as outgrown primary tubular cells and were imaged using a 5x/0.3 EC Plan Neofluar objective. An Axiovert 200M equipped with a large incubation chamber (37°C), 5% CO_2 and humidity

control were used for all time lapse imaging experiments. Transmitted light and fluorescent images (GFP BP filter cube, RFP double filter cube) were acquired by using an Orca flash camera.

Processing of the time lapse data was performed with the open-source image processing software Fiji. The fluorescent channels for SYTOX green or Ca^{2+} AM dyes in the time lapse videos of renal tubules were processed using the Surface Plot plugin in Fiji. This results in a time lapse video showing the intensity on the y' axis and the dimensions of the sample on the x' and z' axis, from which representative images are shown. Lookup tables for SYTOX green and Ca^{2+} AM dyes were adjusted for color-blind individuals, when necessary.

The live imaging procedure was supported by the Light Microscopy Facility, a Core Facility of the CMCB Technology Platform at TU Dresden.

2.8.4. Assessment of SYTOX positivity in freshly isolated renal tubules

Isolated renal tubules from male or female mice were incubated in a single 3D-printed well separated by a glass slide, stained with SYTOX green nucleic acid stain. Transmitted light and fluorescent time lapse images (GFP BP filter cube) were acquired (described in more detail in the time lapse imaging and processing of the time lapse data section above). Every 30 minutes the images were assessed for the number of tubules exhibiting more than 90 % of SYTOX green positivity. Tubules with less than 90% SYTOX positivity were counted as "negative" in the analysis, while debris were not included in the analysis. The total numbers of male and female tubules were calculated manually. Data are presented as the percentage of tubules with equal or more than 90 % of SYTOX positivity over time.

2.8.5. LDH release assay

LDH release of freshly isolated kidney tubules or primary tubular cells was measured according to manufacturers' instructions (Promega, Cat# G1780) at indicated time points. Briefly, an aliquot of the supernatant was taken, and Lysis Solution was added for 45 minutes to induce maximal LDH release before another aliquot of the supernatant was taken. Subsequently, the supernatants were incubated with CytoTox 96® Reagent for 15 minutes protected from light at room temperature. Stop Solution was added and the absorbance was measured at 490 nm. Percentage (%) of LDH release was measured by using the formula: % of LDH = 100 * (supernatant LDH/maximal LDH).

2.8.6. Electron microscopy

Electron microscopy was performed by our collaborator Dr. Jan Ulrich Becker. Briefly, murine tubules were isolated with the protocol mentioned above and placed in 4 % buffered paraformldehyde for fixation. Afterwards, tubules were subjected to another fixation in glutaraldehyde and 1 hour of post-

fixation/contrasting with osmium tetroxide. They were then embedded in Epon resin through graded ethanols and propylene oxide. Blocks were polymerized at 80 °C overnight. Semi-thin sections were stained with methylene blue and azure blue. Thin sections were stained with lead citrate and uranyl acetate. Transmission electron microscopy was performed on a Zeiss Electron Microscope.

2.9. Statistics

Statistical analyses were performed using Prism 8 (GraphPad software, San Diego, CA, USA). In all experiments, unpaired student t-test with Welch's correction was used. The difference of means was considered significant when * $p < 0.05$, ** $p < 0.01$, *** $p < 0.001$, **** $p < 0.0001$.

Results

3. Results

3.1. Part I: The sensitivity of adrenocortical carcinoma cells towards regulated cell death pathways

3.1.1. NCI-H295R cells are sensitive to mitotane

The first established cell line for studying ACC was the NCI-H295, prepared from a female patient diagnosed with adrenocortical carcinoma (Gazdar *et al*., 1990). Even though the NCI-H295 cells could produce a variety of steroids (Gazdar *et al*., 1990), problems during their slow growth in culture conditions lead to the establishment of three new ACC cell lines (H295R-S1, H295R-S2 and H295R-S3), distinct from each other based on their medium supplementation (Rainey *et al*., 2004; Wang and Rainey, 2012). From the three aforementioned cell lines the strain H295R-S1 (mentioned throughout the text as NCI-H295R cells) that grows in DMEM7/F12 supplemented with Nu-Serum was selected for the adrenal-related experiments of this thesis, due to their maintenance of several steroids being produced (Rainey *et al*., 2004; Wang and Rainey, 2012).

Mitotane, an insecticide dichlorodiphenyltrichloroethane (o,p'DDT) derivative, acts as an adrenocytolytic drug and is currently the only therapeutic option approved by the US Food and Drug Administration (FDA) and the European Medicine Executive Agency (Schteingart *et al*., 2005; Paragliola *et al*., 2018; Paragliola *et al*., 2020). Mitotane is used as the main drug in the clinical practice for the treatment of ACCs. Aiming to determine n optional concentration of mitotane that should be used throughout the rest of the adrenal-related experiments, different concentrations varying from 25 μM to 100 μM of mitotane were tested. NCI-H295R cells and other cell lines were plated, and flow cytometry analysis (FACS) was utilised to assess the occurrence of cell death (scheme shown in **Figure 6A**). For FACS analysis, the cells were stained withfluorescently labelled annexin V, which reliably detects the phosphatidylserine on the plasma membrane, and 7AAD, which intercalates with DNA thereby labelling the nuclei of necrotic cells. Different concentrations of mitotane were used to treat the cells for 24 h (**Figure 6B**). Cell lines used to study regulated cell death pathways, such as Jurkat T cells used for apoptosis, HT29 cells used for necroptosis, HT1080 cells used for ferroptosis, exhibited no sensitivity to mitotane for concentrations up to 50 μM. Similar data were obtained when other cells lines (NIH-3T3, L929, HEK) were tested in a similar experimental set-up. On the contrary, NCI-H295R cells showed low sensitivity to concentrations of mitotane up to 50 μM. At a mitotane concentration of 100 μM, NCI-H295R cells, Jurkat T cells and L929 cells showed increased sensitivity (36 %, 29 % and 12 % double negative stained cells respectively) compared to their corresponding vehicle control. Investigating the temporal component of the cytotoxic activity of mitotane another set of experiments was set up, incubating this time only the NCI-

H295R cells with either 50 µM or 100 µM mitotane for 2, 4 or 6 h (**Figure 6C**). Both concentrations showed similar results, while the 6 h treatment time point was the optimal in terms of cytotoxic effects of mitotane.

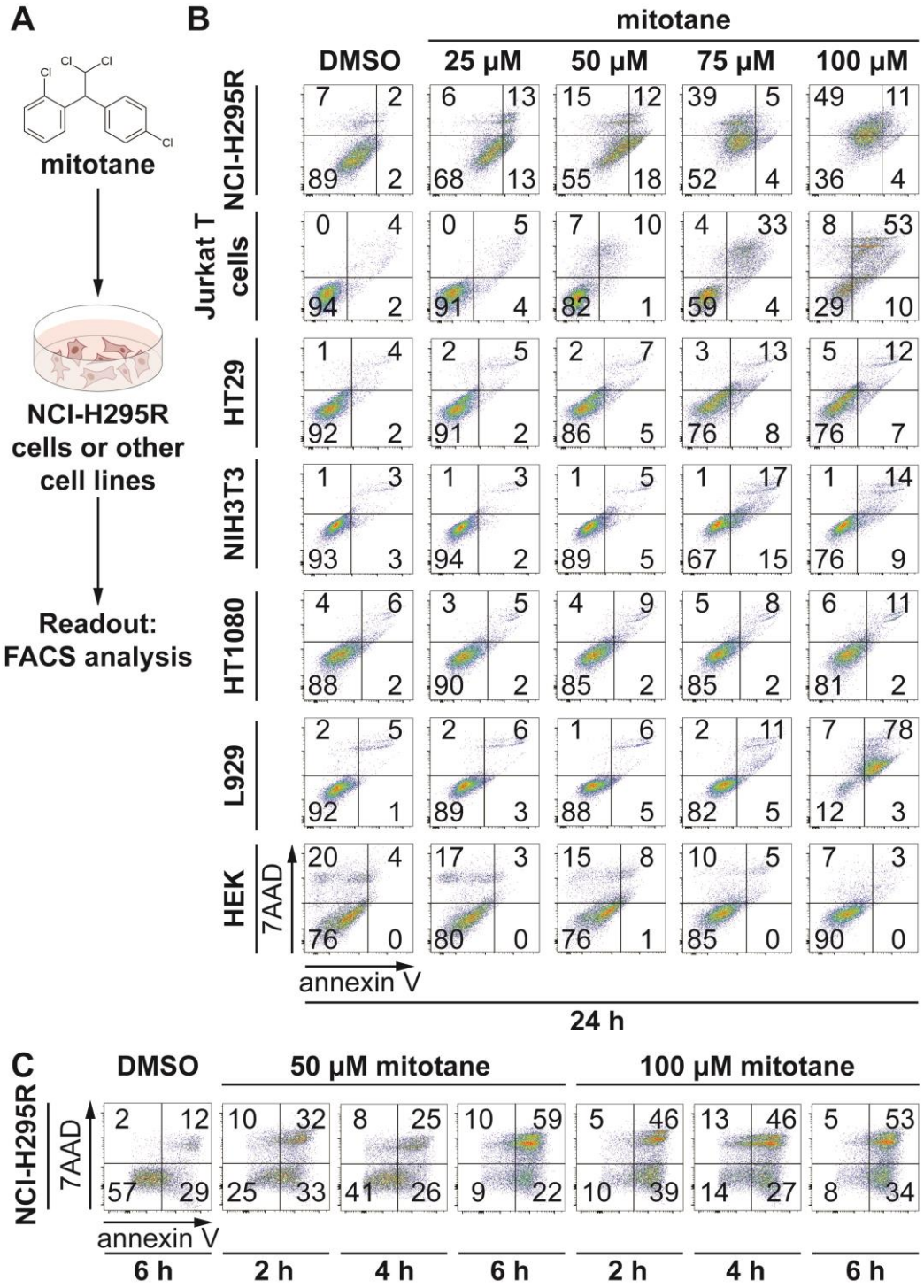

Figure 6. NCI-H295R cells are sensitive to mitotane. A. Protocol followed for testing different concentrations of mitotane on different cell lines. **B.** NCI-H295R, Jurkat T, HT29, NIH-3T3, HT1080, L929

and HEK cells treated for 24 h with 25, 50, 75 or 100 μM mitotane. **C.** NCI-H295R cells treated for 2, 4 or 6 h with 50 μM or 100 μM mitotane. Cells were stained for the phosphatidylserine on the plasma membrane with annexin V and for DNA of impaired nuclei with 7AAD. Representative FACS plots from at least three independent experiments are shown.

The ACC cell line, NCI-H295R, showed cytotoxicity even at the lowest tested concentration, a result that comes in line with the literature (Lehmann *et al*., 2013). Collectively, these data indicate a stronger effect of mitotane's cytotoxicity towards the ACC cell line. Any cell death observed with concentrations above 50 μM were accounted to toxic effects of mitotane. Therefore, the 50 μM were chosen as the closest to the clinical practice relevant concentration (14 mg/L) (Paragliola *et al*., 2018), while the 6 h were chosen as the earliest time point that more than 70 % of the cells were necrotic. Consequently 50 μM mitotane treatment for 6 h was chosen as the standard treatment of the ACC cell line.

3.1.2. Mitotane does not induce apoptosis or necroptosis

Even though mitotane has been in clinical use for many years, its mechanism of action is not yet understood. In order to gain further insight into which pathway might play the major role in mitotane-induced cytotoxicity, various inhibitors specific for aforementioned RCD pathways were tested. As mentioned before (section 1.1), several inhibitors have been established for the known regulated cell death pathways. To this end, the pan-caspase inhibitors, zVAD-fmk (referred in the rest of the text as zVAD) and emricasan, and the RIPK1 inhibitor necrostatin-1s (Nec-1s) were used at concentrations 20 μM, 5 μM and 10 μM, respectively (**Figure 7A**). Flow cytometry analysis of NCI-H295R cells treated with mitotane (50 μM) and co-treated with either zVAD or emricasan showed a reduction of the double negative stained cells (13 % and 12 %, respectively) compared to mitotane-only treated cells (27 %) (**Figure 7B**). Jurkat T cells were used as a positive control for the induction of apoptosis using the well established monoclonal antibody anti-Fas (100 ng/ml) (Nagata, 1996). The presence of pan-caspase inhibitors served as the protection control. Cell lysates of the aforementioned experimental set-up were used for western blot analysis against cleaved caspase 3, a marker of apoptosis induction. The positive control of Jurkat T cells indicated the specific bands of cleaved caspase 3 which were partially present in the mitotane-treated NCI-H295R cells (**Figure 7C**).

Necroptosis is another form of regulated cell death, described in detail in section 1.1.2. This pathway relies on the proteins RIPK1 and 3 and MLKL. The latter will get phosphorylated (p-MLKL), locate to the membrane and by unknown means lead to its rupture (Linkermann and Green, 2014; Sarhan *et al*., 2018b). Nec-1s has been shown to inhibit RIPK1 (Takahashi *et al*., 2012), and therefore was used for the inhibition of necroptosis. Following a similar experimental set-up, co-treatment of NCI-H295R cells with Nec-1s and 50 μM mitotane showed no difference to mitotane-treated cells (23 % double-negative stained cells and 27

% double-negative stained cells, respectively). Similar results were obtained when zVAD and Nec-1s were used together as a co-treatment with mitotane (12 % double-negative stained cells) (**Figure 7D**). For the positive control of necroptosis induction the human colorectal adenocarcinoma cells, HT29, were used and treated with the combination of TNFα (20 ng/ml), smac mimetic birinapant (1 μM) and the pan-caspase inhibitor zVAD (20 μM) (TSZ referred to as an abbreviation), as proposed in the literature (Tait *et al*., 2013; Ousingsawat *et al*., 2016). Western blot analysis of cell lysates obtained from the presented experiment showed no phosphorylated MLKL in mitotane-treated NCI-H295R cells, compared to the positive control of HT29 cells treated with TSZ (**Figure 7E**). Time lapse analysis of NCI-H295R treated with mitotane (50 μM) in the presence of the necrosis marker SYTOX green, that stains the DNA of a necrotic cell, revealed membrane blebbing within 6 hours of treatment. In the presence of zVAD the phenomenon was completely abolished. Nec-1s did not affect the membrane blebbing process (**Figure 7F**).

The hypothesis of apoptosis or necroptosis being the underlying mechanism of action of mitotane was challenged with the co-treatment of mitotane and the pan-caspase inhibitors, zVAD and emricasan, or the co-treatment with the necroptosis inhibitor, Nec-1s. All the three inhibitors failed to prevent the mitotane-induced necrosis. Even though WB analysis revealed low expression of cleaved caspase 3, the failure of caspase inhibitors to block mitotane-induced cell death fail to overall support the hypothesis that apoptosis is involved. Additionally, no presence phosphorylated MLKL was detected, disapproving the hypothesis of necroptosis as the involved pathway. Hypothesising that blockade of apoptosis during a mitotane treatment might unleash necroptosis or the other way around, the combined treatment of the apoptosis inhibitor, zVAD, and the necroptosis inhibitor, Nec-1s, in mitotane-treated NCI-H295R cells was tested. However, the mitotane-induced cell death was not blocked. Collectively, these data suggest that mitotane induces a necrotic type of cell death that does not involve apoptosis or necroptosis.

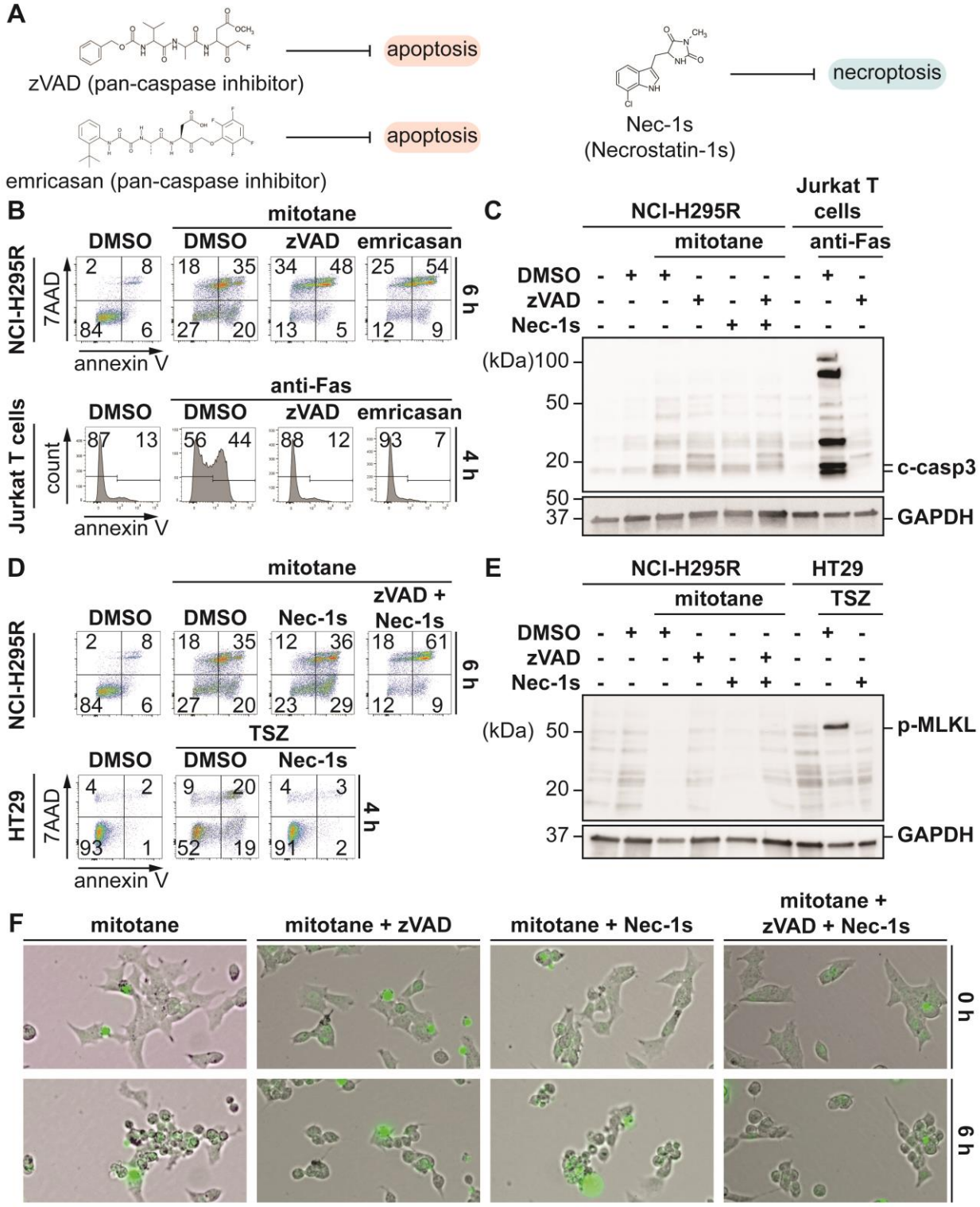

Figure 7. Mitotane does not induce apoptosis or necroptosis. A. The chemical structure of the pan-caspase inhibitors, zVAD-fmk and emricasan, which inhibit apoptosis and of the necrostatin-1s (Nec-1s) that inhibits necroptosis. **B.** FACS analysis of NCI-H295R cells treated with 50 μM mitotane and co-treated with zVAD (20 μM) or emricasan (5 μM) for 6 h. Jurkat T cells were treated with 100 ng/ml anti-Fas antibody. **C.** NCI-H295R cells were treated with mitotane (50 μM) and co-treated with zVAD (20 μM)

and/or Nec-1s (10 μM) for 6 h. Western Blot against cleaved caspase 3 (c-casp3) after treatment as used in B. Samples of Jurkat T cells treated with anti-Fas antibody (100 ng/ml) and co-treated with zVAD (20 μM) were lysed and served the positive control for cleaved caspase 3. **D.** FACS analysis of NCI-H295R cells treated with 50 μM mitotane and co-treated with Nec-1s (10 μM) or the combination of zVAD and Nec-1s (20 μM and 10 μM, respectively) for 6 h. HT29 cells were treated with TNF-α (20 ng/ml), smac mimetics birinapant (1 μM) and zVAD (20 μM) (together referred to as TSZ). **E.** NCI-H295R cells were treated with 50 μM mitotane and co-treated with Nec-1s (10 μM) or the combination of zVAD and Nec-1s (20 μM and 10 μM, respectively) for 6 h. The samples were lysed for WB against phosphorylated MLKL (p-MLKL). Lysates from samples of HT29 cells treated with TSZ (as mentioned in D) served as the positive control for p-MLKL. **F.** Still images of time lapse analysis of NCI-H295R cells treated with mitotane (50 μM) in the presence or not of the co-treatments of zVAD (20 μM), Nec-1s (10 μM) or the combination of zVAD and Nec-1s for a total of 6 h. Cells were stained for the phosphatidylserine on the plasma membrane with annexin V and for DNA of impaired nuclei with 7AAD. Representative data from at least three independent experiments are shown.

3.1.3. Mitotane does not induce ferroptosis

Ferroptosis was first mentioned in 2012 as an iron-dependent form of non-apoptotic cell death (Dixon *et al*., 2012b) (described in detail in section 1.1.4). Induction of ferroptosis can be achieved with the use of the four types of FINs (ferroptosis inducers) (Tonnus *et al*., 2021b). Among the FINs, RSL3 was described as the first direct inhibitor of GPX4, the glutathione peroxidase 4 that plays a key role in the execution of ferroptosis (Yang *et al*., 2014). Ferroptosis inhibitors were also developed, such as Ferrostatin-1 (Fer-1) (Skouta *et al*., 2014), while other compounds such as necrostatin-1 (Nec-1), were shown to inhibit both necroptosis (Degterev *et al*., 2005) and ferroptosis (Friedmann Angeli *et al*., 2014a). The hypothesis whether mitotane induces ferroptosis was addressed by using the necroptosis/ferroptosis inhibitor Nec-1 and the ferroptosis inhibitor Fer-1, the structure of which is shown in **Figure 8A**. Flow cytometry analysis showed that neither Nec-1 (30 μM) or Fer-1 (1 μM) prevented the mitotane-induced type of death. The observed double negative stained population for annexin V and 7AAD were very similar in all three samples; 11 % for cells treated with mitotane, 9 % when treated with mitotane and Fer-1, and 11 % for cells treated with mitotane and Nec-1. The human fibrosarcoma cell line, called HT1080, is used as the standard cell line to study ferroptosis. Therefore, these cells served as positive control for RSL3-induced ferroptosis, while the co-treatment with Nec-1 and Fer-1 served as the protection controls (**Figure 8B**).

To test whether mitotane might induce a ferroptosis-related type of cell death, ferroptosis inhibitors (Nec-1 and Fer-1) were used in mitotane-treated NCI-H295R cells. However, neither of them was able to reverse the cell death induced by mitotane, indicating that ferroptosis might not be the pathway involved in mitotane-induced necrosis.

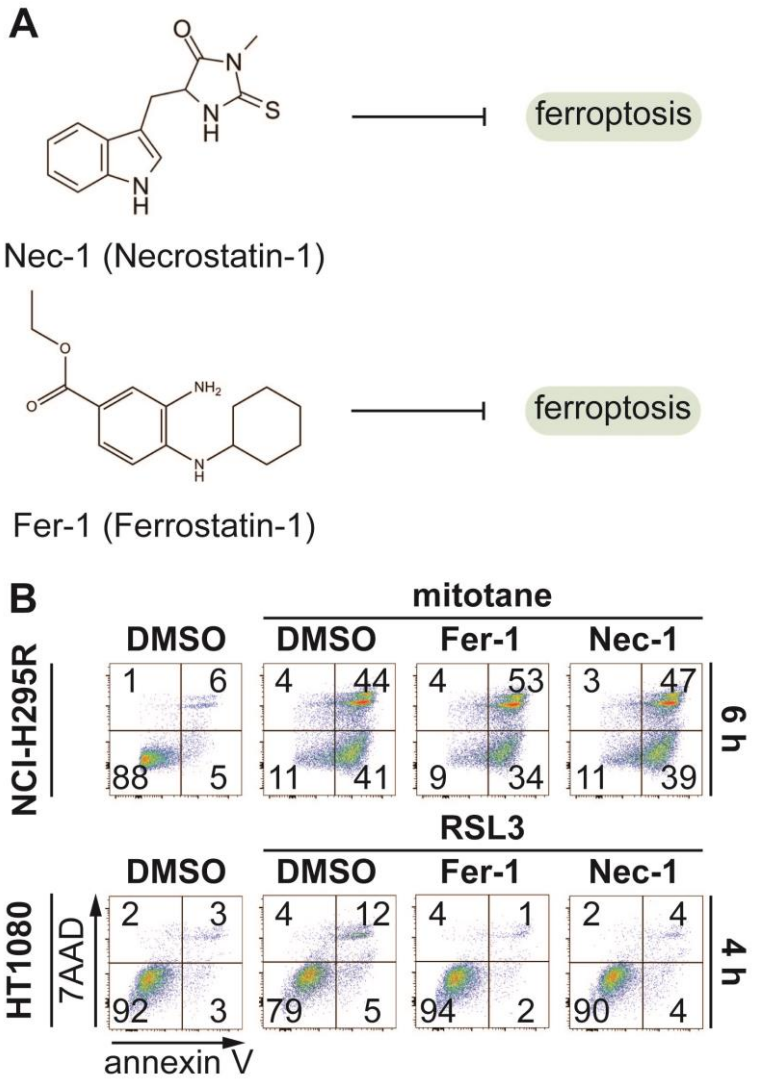

Figure 8. Mitotane does not induce ferroptosis. A. Chemical structures of the ferroptosis inhibitors necrostatin-1 (Nec-1) and ferrostatin-1 (Fer-1). **B.** FACS analysis of NCI-H295R cells treated with 50 μM mitotane and co-treated with the ferroptosis inhibitors, Fer-1 (1 μM) or Nec-1 (30 μM) for 6 h. HT1080 cells were used as positive controls for ferroptosis induction (treatment with 1.13 μM RSL3) or inhibition (co-treatment with Fer-1 or Nec-1). Cells were stained for the phosphatidylserine on the plasma membrane with annexin V and for DNA of impaired nuclei with 7AAD. Representative data from at least three independent experiments are shown.

3.1.4. Medium supplementation with ITS+1 rescues the NCI-H295R cells from mitotane-induced cell death

Previously established culture conditions of NCI-H295R cells indicate the supplementation of the basal medium with ITS+1 (Rainey *et al*., 2004). ITS stands for human insulin, transferrin, sodium selenite (Na_2SeO_3) or selenium (Se). The presence of linoleic acid is indicated with the +1 (**Figure 9A**). Since the presence of such supplements may influence not only the growth of cells, but also their sensitivity to RCD, different concentrations of ITS+1 were tested in cultured NCI-H295R cells for 6 h. The 5 % of supplementation indicated concentrations of 114.6 nM human insulin, 2.78 µM transferrin, 144 nM Na_2SeO_3 and 83.8 µM linoleic acid are contained. Flow cytometric analysis of annexin V and 7AAD-stained cells showed healthy double negative populations in the cells treated with either 5 % or 10 % ITS+1 compared to cells that were incubated in DMEM/F12 medium without any supplementation (DMSO/control: 73 % double negative stained cells, addition of 5 % ITS+1 supplementation: 80 % double negative stained cells, addition of 10 % ITS+1 supplementation: 74 % double negative stained cells) (**Figure 9B**). Based on these data 5 % supplementation of ITS+1 was chosen for the following experiments. The respective ITS compounds and all possible combinations at concentrations indicated for the 5 % ITS+1 were tested on NCI-H295R cells in the presence or absence of 50 µM mitotane. All ITS compounds and their combinations, apart from the combination of insulin + selenium and transferrin + selenium, showed similar double negative stained cells compared to the vehicle control. Interestingly, supplementation of the medium with 5 % ITS+1 resulted in the protection of NCI-H295R cells against mitotane (87 % double negative stained cells compared to 19 % double negative stained cells treated with mitotane only). However, none of the distinct compounds or their combinations showed a protective effect (**Figure 9C**). To investigate the hypothesis that the presence of linoleic acid is responsible for the protective features of ITS+1 against mitotane-induced necrotic cell death, ITS without linoleic acid was tested. The flow cytometry analysis revealed that only the ITS+1 was protective against mitotane (Figure 4D). Time lapse imaging of NCI-H295R cells treated with mitotane in the presence or absence of ITS+1 confirmed the data, showing no SYTOX positivity when ITS+1 was present (**Figure 9E**).

Taken together, none of the tested cell death inhibitors not individual components of ITS and their combinations were able to prevent mitotane-induced cell death. However, the presence of PUFAs in the culture medium of NCI-H295R cells were able to reverse the cell death. This finding could point towards a potential oxidative type of cell death induced by mitotane.

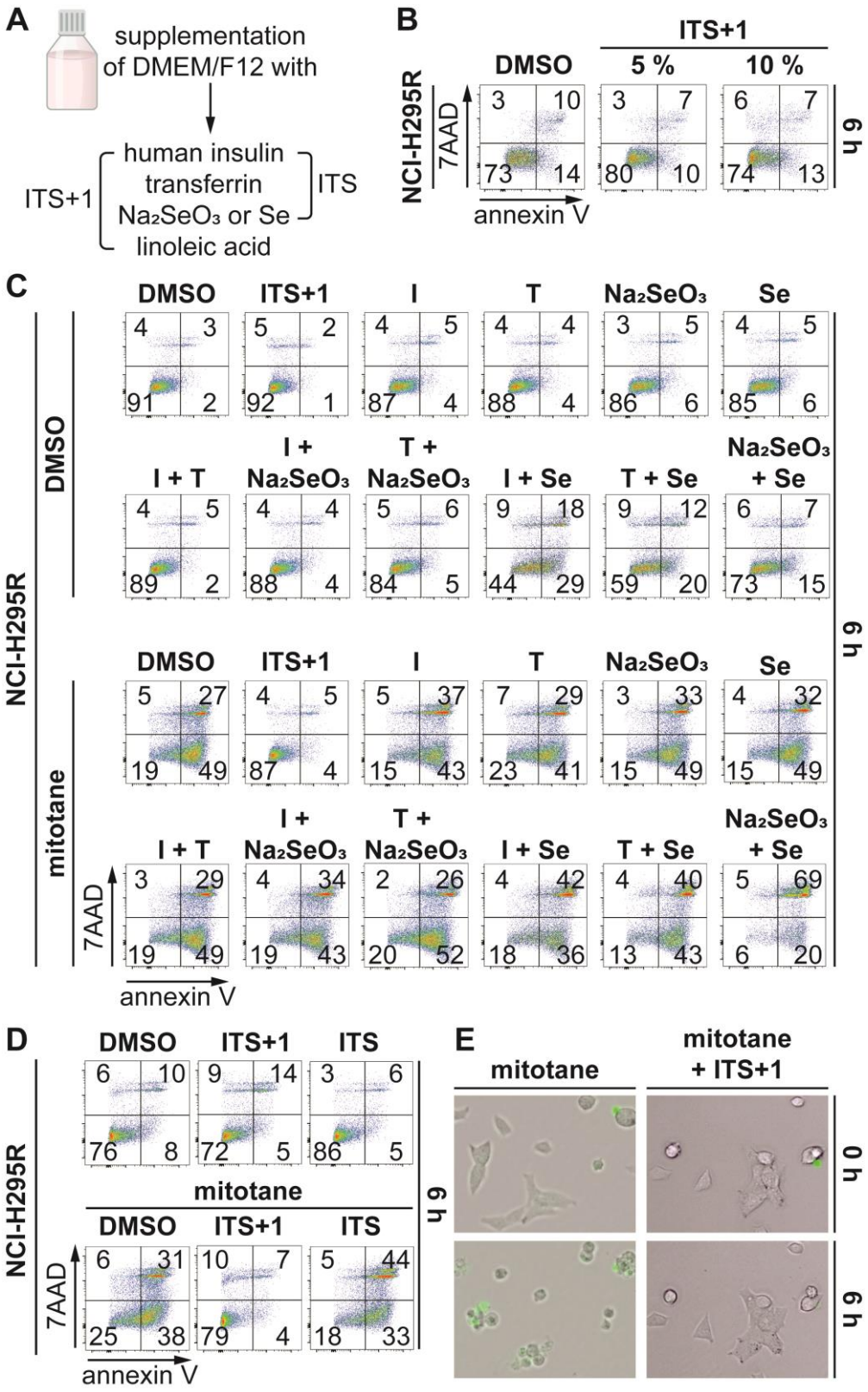

Figure 9. ITS+1 supplementation inhibits mitotane-induced cell death of NCI-H295R cells. A. Cartoon representing the compounds contained in ITS+1 or ITS supplementation recommended for the culture of

NCI-H295R cells. ITS+1 contains insulin, transferrin, selenium (Se) and linoleic acid, while ITS contains insulin, transferrin, and sodium selenite (Na2SeO3). **B.** FACS analysis of different concentrations of ITS+1 supplementation added to the medium of NCI-H295R cells. In the 5 % ITS+1 contains 114.6 nM human insulin, 2.78 µM transferrin, 144 nM Na_2SeO_3 and 83.8 µM linoleic acid are contained. 10 % ITS+1 229.2 nM human insulin, 5.56 µM transferrin, 288 nM Na_2SeO_3 and 167.6 µM linoleic acid are contained. **C.** FACS analysis of NCI-H295R cells treated with ITS+1 or its individual compounds alone and in different combinations in the presence or absence of mitotane (50 µM) for 6 h. **D.** FACS analysis of NCI-H295R cells treated with ITS+1 or ITS (8.61 µM human insulin, 0.34 µM transferrin, 0.42 µM Se) in the presence or absence of mitotane (50 µM) for 6 h. **E.** Still images of time lapse analysis of NCI-H295R cells treated with mitotane (50 µM) in the presence or absence of 5 % ITS+1 for a total of 6 h. Cells were stained for the phosphatidylserine on the plasma membrane with annexin V and for DNA of impaired nuclei with 7AAD. Representative data from at least three independent experiments are shown.

3.1.5. NCI-H295R cells are sensitive to ferroptosis induction

Aiming to further investigate key players of necroptosis and ferroptosis pathways, cell pellet lysates of NCI-H295R cells and other cell lines that served as positive controls were tested in western blot analysis. Of the main three necroptosis mediators RIPK1, RIPK3 and MLKL, only RIPK1 was detected in NCI-H295R cells, while RIPK3 and MLKL were absent (**Figure 10A-C**). Western blot analysis against ACSL4 in adrenocortical carcinoma cells and HT1080 cells, the standard cell line used to study ferroptosis, revealed equal expression levels. On the other hand, GXP4 expression was increased in the ACC cell line compared to HT1080 cells (**Figure 10D**). This finding lead to the hypothesis that the NCI-H295R might be sensitive to ferroptosis induction. The four types of FINS were tested in the presence or absence of Fer-1 for 6 or 24 h. The subsequent flow cytometry analysis showed no response of the NCI-H295R cells to the treatment with the type I FIN, erastin (5 µM) and some sensitivity to the type III FIN FIN56 (20 µM) (**Figure 10E**). Interestingly, high sensitivity of the ACC cell line was observed even after 6 h when treated with type II FIN RSL3 (1.13 µM), and type IV FIN FINO2 (5 µM) (**Figure 10E**). The addition of ferroptosis inhibitor, Fer-1 prevented the induced cell death.

The findings of ITS+1 supplementation in the medium of mitotane-treated NCI-H295R cells, lead to the hypothesis of ITS+1 blocking ferroptosis induction. Therefore, the medium of NCI-H295R cells was supplemented with 5 % ITS+1 (114.6 nM human insulin, 2.78 µM transferrin, 144 nM Na_2SeO_3 and 83.8 µM linoleic acid) or 5 % ITS (114.6 nM human insulin, 2.78 µM transferrin, 144 nM Na_2SeO_3) and treated with the four FINs (5 µM erastin, 1.13 µM RSL3, 20 µM FIN56, 5 µM FINO2). Erastin and FIN56 did not induce a significant necrosis (**Figure 10F**). RSL3 induced a necrotic type of death, which was reversed in the presence of Fer-1 (1 µM) (15 % compared to 68 % double negative stained cells, respectively). ITS+1 and ITS supplementation reversed the RSL3-induced cell death to similar percentages to the vehicle control (64 % and 59 % for the ITS+1 and ITS samples respectively, compared to 73 % double negative stained cells of the vehicle control). After FINO2 treatment only ITS+1 supplementation reversed the observed

death (10% for the FINO2 vs 63 % for the FINO2 and ITS+1 double negative stained cells). Supplementation of the medium with ITS, that did not contain linoleic acid, resulted in 22 % double negative stained cells, compared to 73 % double negative of the control (**Figure 10F**).

To investigate which pathways the ACC cells are susceptible to, a semi-quantitative method (WB) indicated that one of the main molecules important for the execution of necroptosis (MLKL) is absent. However, the main enzyme responsible for the prevention of ferroptosis was highly expressed in the NCI-H295R cells. Indeed, induction of ferroptosis with FINs (mainly types II and IV), showed a high sensitivity of the cells. Additionally, the prevention of ferroptosis induction when linoleic acid was present indicated the oxidation of PUFAs to be crucial for the execution of this cell death pathway.

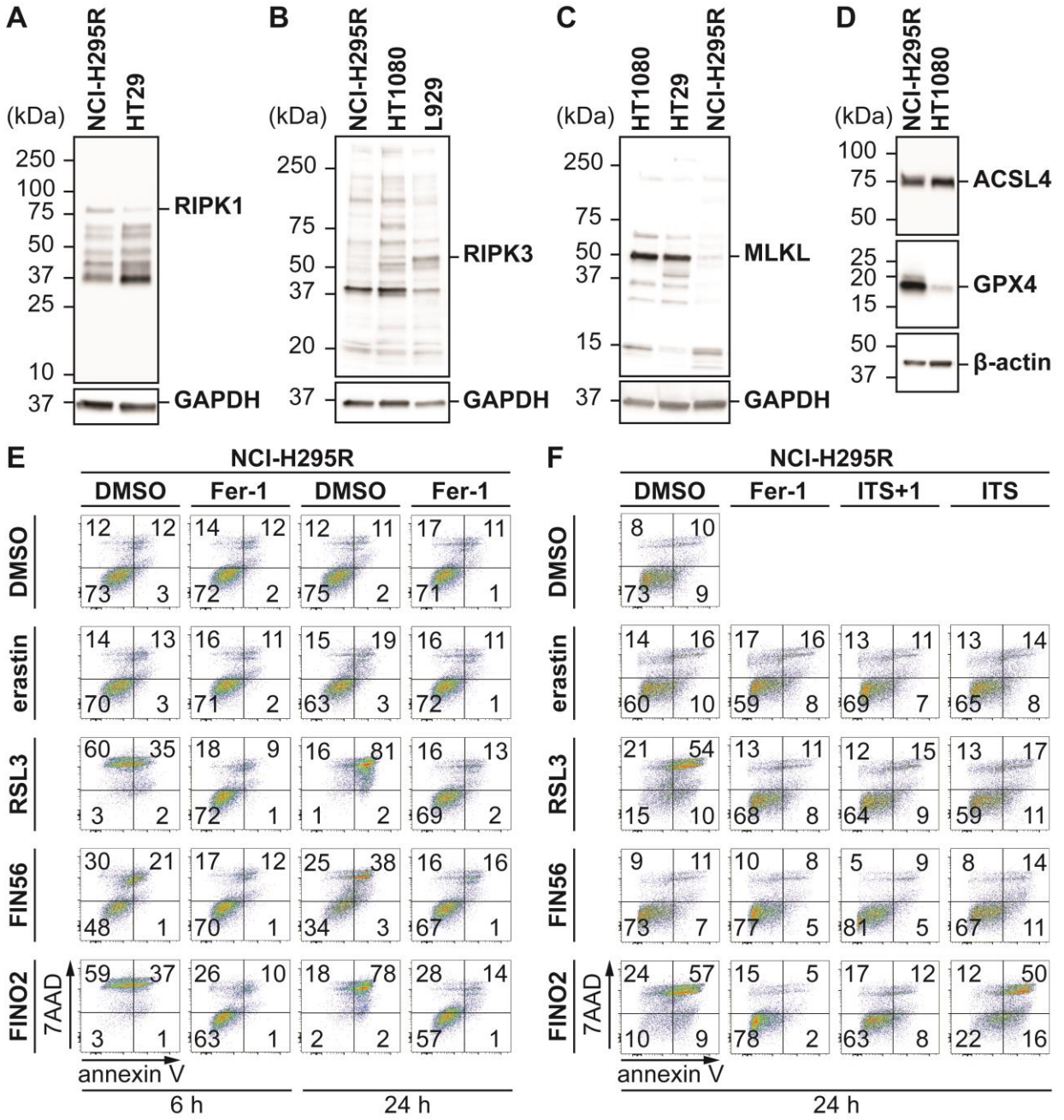

Figure 10. The NCI-H295R cells are sensitive to ferroptosis induction. A. Western blot analysis of NCI-H295R and HT29 lysates against RIPK1. The HT29 represent the positive control. **B.** Western blot analysis of cell lysates of NCI-H295R, HT1080 and L929 (positive control) against RIPK3. **C.** Western blot analysis of HT1080, HT29 (positive control) and NCI-H295R cells against total MLKL. **D.** Western blot analysis of NCI-H295R and HT1080 (positive control) cells against ACSL4 and GPX4. For all western blots GAPDH or β-actin were used as the loading control. **E.** Flow cytometry of NCI-H295R cells treated with the four different FINs (5 μM erastin, 1.13 μM RSL3, 20 μM FIN56, 5 μM FINO2) in the presence or absence of 1 μM Fer-1 for 6 or 24 hours. **F.** Flow cytometry of NCI-H295R cells treated with the four different FINs (concentrations mentioned in E) in the presence or absence of ITS+1 or ITS (5 % of the medium volume). Fer-1 (1 μM) was used as the protection control. Cells were stained for the phosphatidylserine on the plasma membrane with annexin V and for DNA of impaired nuclei with 7AAD. Representative data from at least three independent experiments are shown.

3.1.6. NCI-H295R cells are sensitive to other types of necrosis inducers

The high sensitivity of the ACC cell line towards ferroptosis lead to the hypothesis that these cells might be sensitive to other inducers of necrotic cell death. The growth hormone-releasing hormone (GHRH) has been studied as a potential target of synthesised antagonists for the elimination of pheochromocytomas (Ziegler *et al*., 2013). MIA602, a synthesised amino acid chain by the laboratory of Andrew Schally, is a potent GHRH inhibitor (Bellyei *et al*., 2010). Since NCI-H295R cells are shown to express the GHRH receptor (Giordano *et al*., 2009), different concentrations of MIA602 were tested for 24 h. Already at concentrations of 5 μM the majority of cells underwent necrotic cell death. This further increased with up to 13 % double negative stained cells when treated with 20 μM MIA602 compared to the 78 % double negative cells in the vehicle control (**Figure 11A**). Next, NCI-H295R cells were treated with 20 μM MIA602 in the presence of zVAD (20 μM), Nec-1s (10 μM), the combination of zVAD and Nec-1s, or Fer-1 (1 μM) to investigate the involvement of apoptosis, necroptosis or ferroptosis in the MIA602-induced necrotic death. However, none of the tested inhibitors blocked the observed cell death (**Figure 11B**).

Recently the group of Paul Hergenrother produced a compound called ferroptocide (FTC) that inhibits thioredoxin, a key component of the antioxidant system (Llabani *et al*., 2019a). Different concentrations FTC were tested on NCI-H295R for 24 h. Concentrations of 10 μM FTC resulted in 7 % double negative cells compared to 79 % double negative cells in the vehicle control (Figure 11**C**). Based on this experiment the concentration 10 μM FTC was chosen and its potential to cause necrotic cell death was challenged in the presence or Fer-1 (1 μM) or ITS+1 (114.6 nM human insulin, 2.78 μM transferrin, 144 nM Na_2SeO_3 and 83.8 μM linoleic acid). As shown at the flow cytometry analysis, both Fer-1 and ITS+1 successfully blocked the FTC-induced cell death, indicating the involvement of ferroptosis (**Figure 11D**).

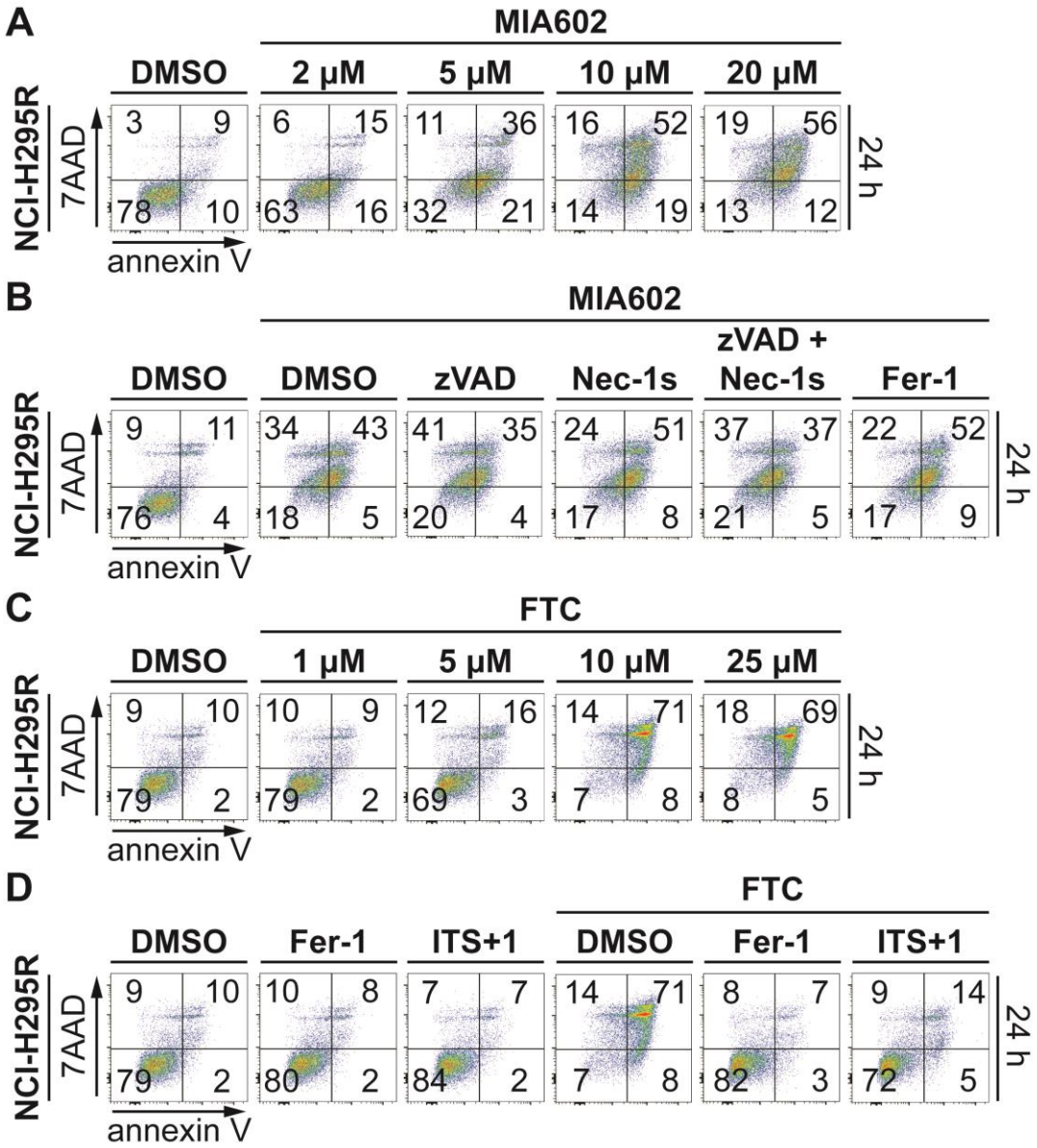

Figure 11. The NCI-H295R cells are sensitive to compounds inducing regulated necrosis. A. Flow cytometry analysis of NCI-H295R cells treated with different concentrations of the compound MIA602 for 24 h. **B.** Apoptosis, necroptosis and ferroptosis inhibitors (20 µM zVAD, 10 µM Nec-1s, 1 µM Fer-1) were used in combined treatment with MIA602 (20 µM) for 24 h and subsequently analysed via flow cytometry. **C.** Flow cytometry analysis of NCI-H295R cells treated with different concentrations of ferroptocide (FTC) for 24 h. **D.** Flow cytometry of NCI-H295R cells treated with 10 µM FTC for 24 h in the presence or absence of Fer-1 (1 µM) or 5 % ITS+1 (114.6 nM human insulin, 2.78 µM transferrin, 144 nM Na_2SeO_3 and 83.8 µM linoleic acid). Cells were stained for the phosphatidylserine on the plasma membrane with annexin V and for DNA of impaired nuclei with 7AAD. Representative data from at least three independent flow cytometry experiments are shown.

The results obtained so far lead to the question whether adrenocortical carcinomas mutate key players of regulated cell death pathways, such as ferroptosis. To answer this question, analysis of two published public databases (Giordano *et al*., 2009; Zheng *et al*., 2016) was performed. The analysis showed several ferroptosis-associated genes, such as the glutathione peroxidases 3 and 7 (GPX3, GPX7), the lipoxygenase L1 (LOXL1) and the phospholipid scramblase co-factor (XKR8), that were highly mutated and/or hypermethylated (**Figure 12A**). The second database (Giordano *et al*., 2009) confirmed those findings, while showing that GPX4 and of thioredoxin reductases 1 and 2 (TXNRD1 and 2) are highly expressed in ACCs, as well as adrenal adenomas and normal adrenal tissue (**Figure 12B**).

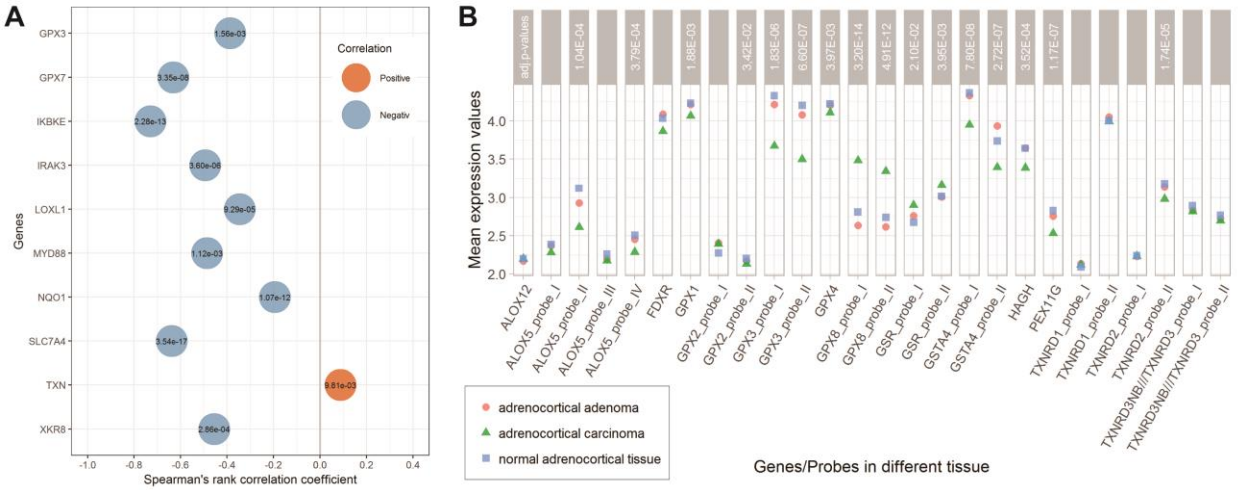

Figure 12. Data base analysis reveals ferroptosis-related genes highly mutated in ACCs. A. Samples of human adrenocortical carcinomas analysed for gene expression and DNA methylation according to Zheng *et al* (Zheng *et al*., 2016). **B.** Selected differentially expressed genes in tissues of adrenocortical carcinomas, adenomas, and normal human adrenal tissue.

Research on compounds that can eliminate the ACC cells, prove that the field for potential therapeutic directions for ACC can expand further from ferroptosis induction. The mutated genes involved in the protection against ferroptosis observed in human ACC samples highlight potential drug targets.

3.2. Part II: Investigation of murine kidney tubules towards spontaneous necrosis

3.2.1. Tubular necrosis is related to a non-random type of necrotic cell death

The process of regulated cell death in tissues such as the kidney is a source or many open scientific questions. Ferroptosis and necroptosis are involved in various pathologies related to the kidney (Tonnus *et al*., 2018; Tonnus *et al*., 2019; Belavgeni *et al*., 2020). Aiming to further understand the distinct role of kidney tubules in these pathologies a protocol for the isolation of fresh murine kidney tubules was established. This protocol can provide a large number of tubules that can be used in time lapse imaging, western blot analysis etc. To investigate whether isolated tubules undergo a random type of cell death, tubules from wild type mice were stained with the nucleic acid stain SYTOX green and observed under the microscope over time. The time lapse images revealed a propagation of the SYTOX signal in a non-random manner during their spontaneous death (**Figure 13A**). Further analysis of the SYTOX green signal via surface plot confirmed the observation of this signal propagating from the ends of the tubules inwards (**Figure 13B**). Adding a red fluorescent calcium indicator (Ca^{2+} AM dye) in the presence of SYTOX green during imaging, revealed a propagation of the calcium signal along the isolated tubules similar to the SYTOX green signal (**Figure 13C**). Analysis via surface plots showed that the propagation of both signals happened almost simultaneously (**Figure 13D**). Tubules that remained alive during the time lapse imaging, no positivity of SYTOX green or calcium was detected (**Figure 13E**).

To further visualise the state of individual compartments of the tubules, imaging of the intermediate necrotic part and the necrotic part of the tubules was assessed using electron microscopy. Representative images are shown in **Figure 13F**. Interestingly, throughout the tubules impaired mitochondria can be observed, with the damage to be more profound in the necrotic part (**Figure 13F-H**).

The wave of death as observed via a nucleic acid staining and a calcium dye, point towards a regulated process occurring during the spontaneous death of isolated murine tubules. Additionally, similarities between electron microscopy images of murine and human tubules (e.g., impaired mitochondria, and other cellular structures) show that the established protocol of the freshly isolated kidney tubules a helpful tool for understanding the physiology and pathology of renal tubules.

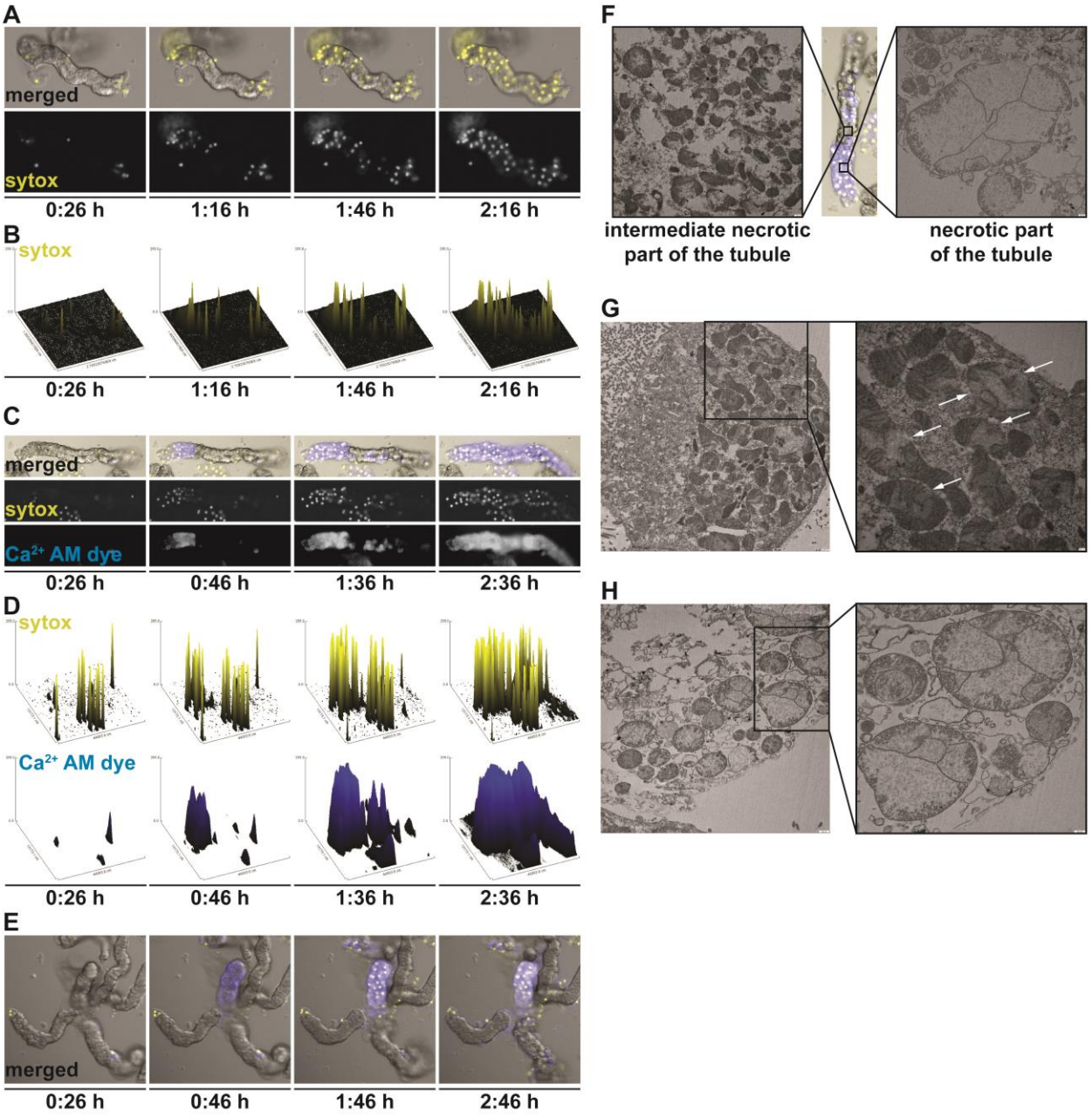

Figure 13. The spontaneous necrosis in murine tubules exhibits a non-random necrotic cell death propagation. A. Still images of time lapse imaging of freshly isolated murine kidney tubules stained with SYTOX green (pseudo-coloured in yellow) at different time points. **B.** Surface plots obtained from the analysis of the time lapse imaging mentioned in A. The plot indicates the intensity of the SYTOX green over time. **C.** Still images at different time pointes of time lapse imaging of freshly isolated tubules stained with SYTOX green (pseudo-coloured in yellow) and Ca^{2+} AM dye (pseudo-coloured in blue). D. Surface plots of the SYTOX green and Ca^{2+} AM dye from the time lapse imaging mentioned in C, indicating their intensity over time. **E.** Still images of freshly isolated murine renal tubules stained with SYTOX green (pseudo-coloured in yellow) and Ca^{2+} AM dye (pseudo-coloured in blue). **F.** Electron microscopy images obtained from the intermediate necrotic and the necrotic parts of the tubule (scaled at 250 nm). **G.** Electron microscopy image (scaled at 250 nm) of the intermediate transition part of a murine renal tubule. The

zoomed area (scaled at 100 nm) of the image focuses on the damaged mitochondria (indicated by the white arrows). **H.** Electron microscopy image (scaled at 250 nm) of the necrotic part of a murine renal tubule. The zoomed area (scaled at 100 nm) of the image focuses on the severely damaged mitochondria. Images for A-E were obtained with the use of a 63x lens. All freshly isolated murine tubules were isolated from male wild type mice.

3.2.2. Spontaneous tubular necrosis is partially mediated by ferroptosis

The role of regulated cell death pathways, such as necroptosis, pyroptosis and ferroptosis during the spontaneous cell death of murine tubules was assessed next. For addressing this, kidney tubules were from necroptosis and pyroptosis deficient mice (MLKL/GSDMD^{DKO}) and the spontaneous occurring necrotic death was compared with tubules isolated from WT mice. Careful examination of the tubules revealed that throughout the experimental time course necrotic tubules change their morphology and show a white appearance under the microscope. Microscopic examination between isolated WT and necroptosis/pyroptosis deficient tubules revealed no phenotypic differences (**Figure 14A**). Comparing the LDH release from these tubules also showed no significant difference (**Figure 14B**).

The hypothesis as to whether ferroptosis plays an important role during the spontaneous tubular necrosis was addressed using the ferroptosis inhibitor, Fer-1, in the medium of freshly isolated wild type tubules. Microscopic observation revealed the presence of less “whitened” tubules when Fer-1 was present (**Figure 14C**). Data obtained from the LDH release of WT tubules treated with 30 μM Fer-1 further supported this finding showing significantly lower LDH levels compared to vehicle-treated tubules. (**Figure 14**Error! Reference source not found.**D**). The susceptibility of tubules towards ferroptosis was further examined with the treatment of isolated wild type tubules with RSL3 (1.13 μM). Microscopic analysis (**Figure 14E**), as well as LDH release after 2 h of treatment showed increased tubular necrosis, which was reversed in the presence of Fer-1 (**Figure 14F**).

Genetic evidence as well as the cell death inhibitor Fer-1 used to investigate the role of necroptosis, pyroptosis or ferroptosis during the spontaneous tubular necrosis reveal the involvement of ferroptosis, even though the reversal of death was not 100 % complete. Moreover, the induction of ferroptosis via type II FIN RSL3 leads to increased damage of tubules which is reversed by the presence of the ferroptosis inhibitor Fer-1, data that strengthen the susceptibility of renal tubules to ferroptosis.

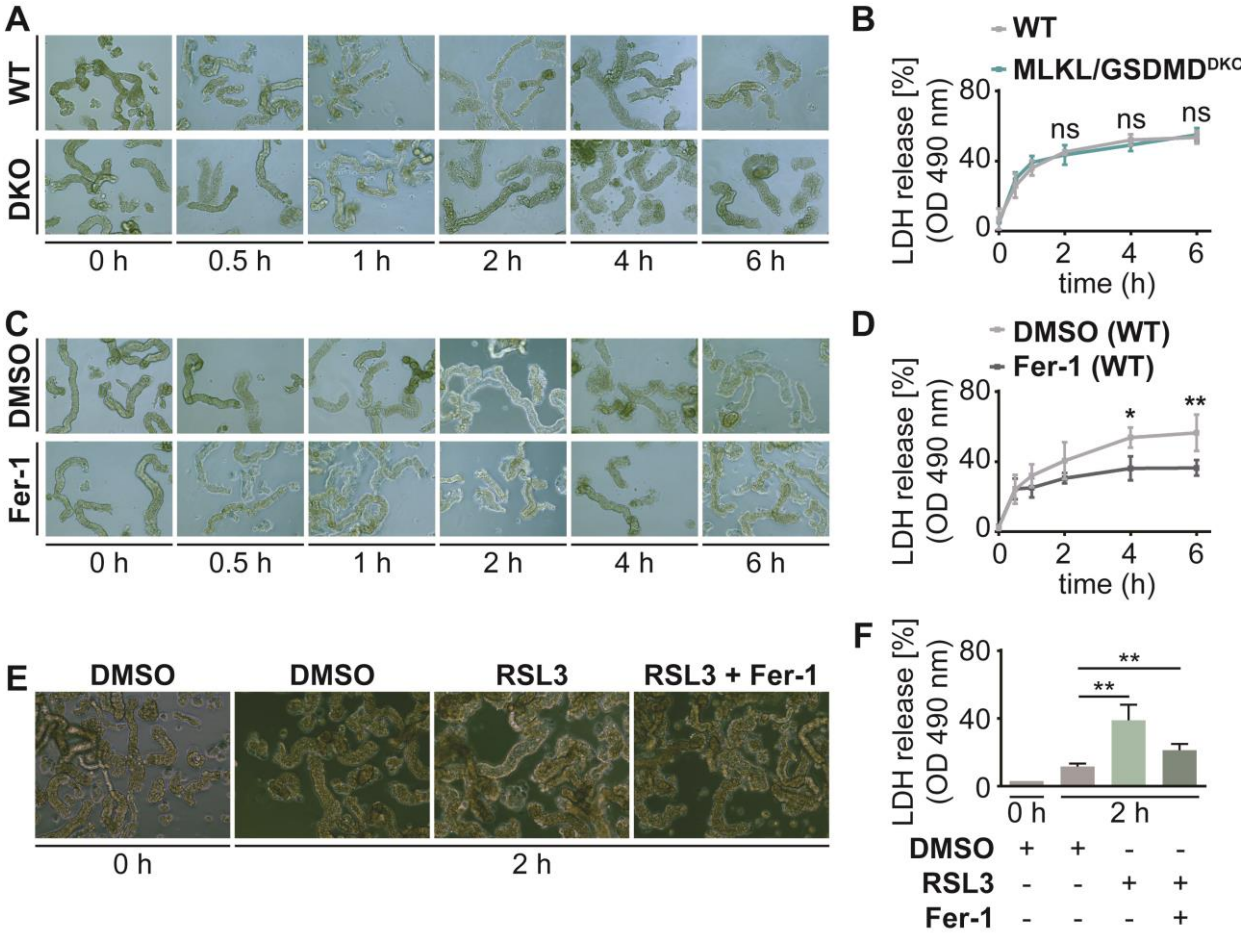

Figure 14. The presence of a ferroptosis inhibitor reduces the LDH release of tubules undergoing spontaneous necrosis. A. Representative images of freshly isolated tubules from wild type mice (WT) and MLKL/GSDMD^{DKO} mice (DKO) at indicated time points. **B.** LDH release from isolated tubules from WT and MLKL/GSDMD^{DKO} mice (n = 4). **C.** Representative images of isolated WT tubules treated with vehicle control or 30 µM Fer-1. **D.** LDH release from isolated tubules in the presence of 30 µM Fer-1 (n = 3) or vehicle control (n = 5). **E.** Representative images of isolated WT tubules treated with vehicle control for 0 and 2h, RSL3 (1.13 µM) and RSL3 with Fer-1 (10 µM) for 2h. **F.** LDH release from isolated WT tubules in the presence of RSL3 (1.13 µM) and in co-treatment with 10 µM Fer-1 for 2 h. DMSO at 0 h represents the starting point of LDH release (n = 5). All experiments were independently repeated at least 3 times. Graph plots show the mean +/- standard deviation (SD). * $p < 0.05$; ** $p <= 0.01$; ns = non significant. Statistical analysis was performed using unpaired student t-test with Welch's correction.

3.2.3. Tubules isolated from female mice are less sensitive towards spontaneous necrosis

The increased susceptibility of male mice towards kidney injury compared to female mice has been previously reported (Bairey Merz *et al.*, 2019). Aiming to further investigate this effect on the level of isolated tubules, a custom-made 3D-printed silicone chamber was generated. A glass slide was placed in the middle of the chamber dividing the silicone well in two halves rendering the communication between the two parts impossible (**Figure 15A**). This allowed for time lapse imaging of two different samples

without moving the stage of the microscope, while reducing any sheer stress. Female and male WT mice were sacrificed, kidney tubules were isolated and stained with the nucleic acid stain SYTOX green. The time lapse imaging showed a higher uptake of SYTOX green by male tubules compared to female tubules over time (**Figure 15B**). The percentage of tubules with equal or greater than 90 % SYTOX positivity was calculated for both male and female tubules. An example of the tubules fulfilling the criteria used to include or exclude tubules from the set criteria is shown in **Figure 15C**. Tubules that showed less than 90 % of SYOX positivity or debris were not included in the calculation. This analysis revealed a much faster increase and higher total percentage of male tubules with equal or greater than 90 % SYTOX positivity compared to female tubules (**Figure 15D**). These data were further supported by the LDH release assay from the samples used for live imaging, showing a higher LDH release from isolated male tubules (**Figure 15E**). In another set of experiments comparing the LDH release of female and male WT tubules alongside with their phenotypic changes under the microscope, the higher susceptibility of male tubules compared to female tubules towards spontaneous necrosis was statistically significant already after half an hour (**Figure 15F-G**).

The role of ferroptosis during spontaneous tubular necrosis of male tubules lead to the hypothesis that this pathway might also be involved during the spontaneous necrosis of female tubules. To address this hypothesis Fer-1 (30 μM) was added to the medium of freshly isolated WT female tubules. Microscopic observation did not reveal any phenotypic differences between the control and the Fer-1-treated tubules (**Figure 15H**). Alongside these findings, analysis of the LDH release showed no statistical significance between female tubules treated either with vehicle control or 30 μM Fer-1 (**Figure 15I**).

Collectively these data show that the sensitivity of male tubules towards spontaneous death compared to female tubules links the previously described findings of the literature in the context of male mice being more susceptible to models of AKI compared to female mice. Interestingly the already low levels of LDH release of female tubules could not be lowered further in the presence of Fer-1. A potential explanation to this outcome could be the presence of a molecule with anti-ferroptotic or antioxidant properties.

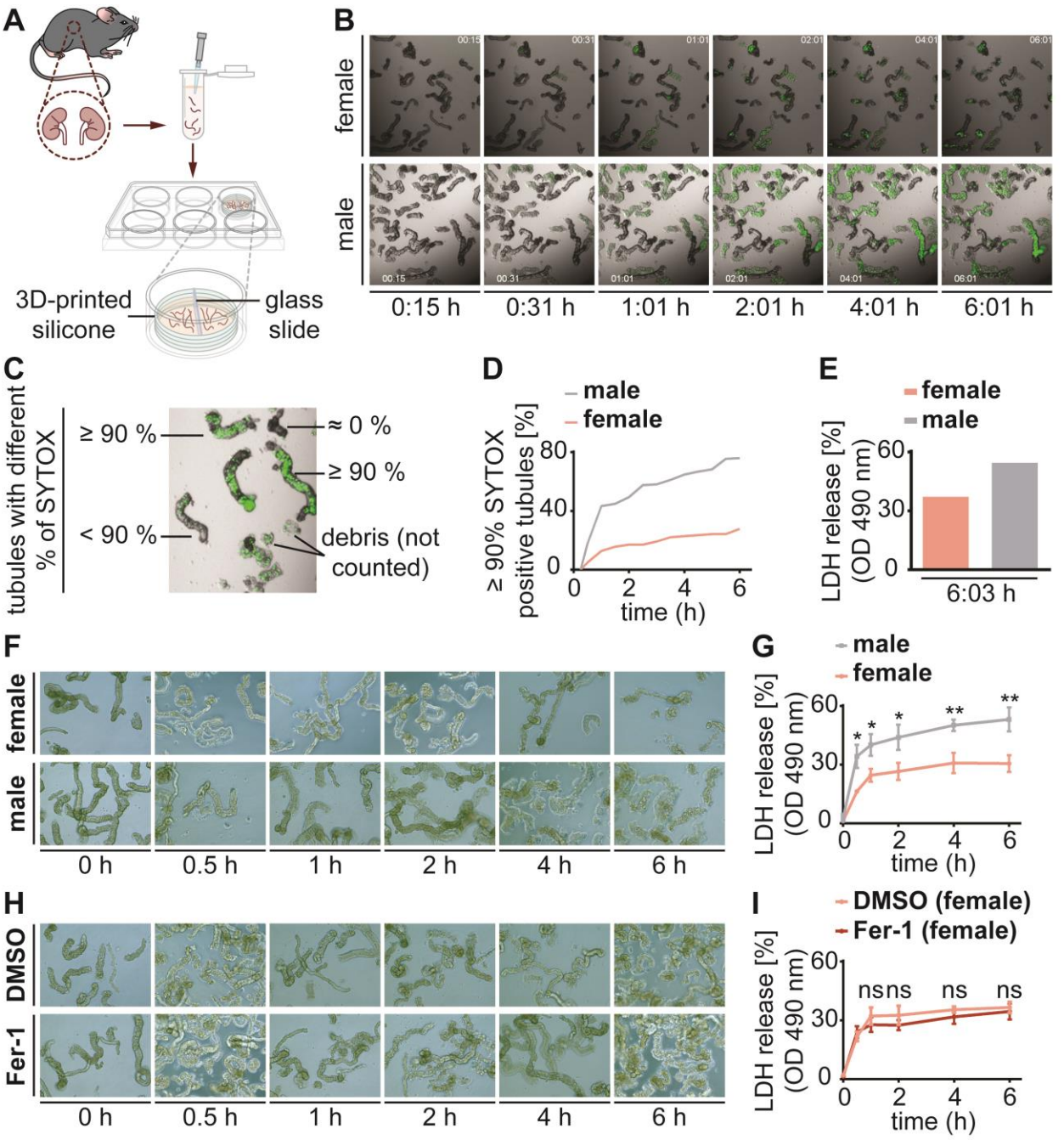

Figure 15. Female tubules are more resistant towards spontaneous tubular necrosis compared to male tubules. A. Cartoon representing the custom-made 3D printed chamber used to simultaneously monitor isolated tubules from female and male mice. The presence of the glass slide prevented any communication of the samples. **B.** Still images of the time lapse imaging of isolated kidney tubules from female and male mice. The tubules were stained with SYTOX green to visualise necrotic cells. Higher background in the female sample was caused by the low magnification used. **C.** Distinction of tubules with different percentages of SYTOX green positivity. **D.** Calculation of the percentage of necrotic tubules with equal or greater than 90 % SYTOX positivity based on the time lapse imaging shown in B. **E.** LDH release of samples obtained after the 6 h time lapse imaging experiment shown in B. **F.** Representative images of

freshly isolated kidney tubules from female and male mice at indicated time points. **G.** LDH release of male and female tubules during spontaneous necrosis (n = 4). **H.** Representative images of female tubules in the presence of vehicle or Fer-1 (30 μM) at indicated time points. **I.** LDH release of isolated female tubules treated with vehicle or 30 μM Fer-1 (n = 3). All experiments were independently repeated at least 3 times. Graph plots show the mean +/- the standard deviation (SD). * $p < 0.05$; ** $p <= 0.01$; ns = non significant. Statistical analysis was performed using unpaired student t-test with Welch's correction.

3.2.4. Primary tubular cells are susceptible to ferroptosis

Leaving isolated murine tubules in a culture dish would eventually lead to the outgrowth of primary cells from individual tubules. With the help of time lapse imaging this process was monitored over time (**Figure 16A**). When the outgrown cells reached a confluency of about 70 – 80 %, they were used for experiments. Primary tubular cells derived from either male of female mice were challenged with the four FINs for 24 h, to address the hypothesis that primary tubular cells are susceptible towards ferroptosis. LDH release assay revealed a low sensitivity of male and female primary cells towards erastin (5 μM) as well as its more stable derivate imidazole ketone erastin (IKE, 5 μM) (**Figure 16B**). On the contrary, RSL3-induced ferroptosis resulted in 36 % LDH release from female primary tubular cells and 58 % of LDH release in primary tubular cells generated from male tubules, which was statistically significant compared to their corresponding controls (**Figure 16C**). Treatment with 20 μM FIN56 did not result in a necrotic death in either female or male primary tubular cells (**Figure 16D**). Treatment with the type IV FIN FINO2 (10 μM), resulted in an increase of LDH release in both female and male primary tubular cells, which was statistically significant to their respective controls (**Figure 16E**). The thioredoxin inhibitor, ferroptocide (FTC, 10 μM), led to 39 % LDH release in female primary tubular cells and 48 % LDH release in male primary tubular cells (**Figure 16F**). Interestingly, in this case Fer-1, which was used as the protection control of all FINs and FTC, did not reduce the LDH of FTC-induced necrosis as successfully as in the cases of the type I-IV FINs. To test the involvement of necroptosis as an important pathway in the primary tubular cells, the cells were treated with a combination of TNFα and zVAD-fmk (referred to as TZ). LDH release showed no induction of necrosis in female or male primary tubular cells after 24 h of treatment (**Figure 16G**).

Another event that was observed during RSL3-induced cell death on primary tubular cells was a non-random necrotic death that was monitored with the help of time lapse imaging. This phenomenon was more profound when only the SYTOX green cells were visualised in inverted images with white background and the SYTOX green depicted in black (**Figure 16H**). The "wave of death" occurring from the outer part of the cell cluster is moving towards the centre, which resembled the same pattern observed in the tubules during spontaneous tubular necrosis (as shown in Figure 12**A**).

Cultivation of isolated tubules from male or female mice resulted in the outgrowth of primary cells, which were susceptible to RSL3, just like the tubules (Figure 13F), as well as to FINO2. Therefore, primary

tubular cells maintain susceptibility to ferroptosis induction as well as the feature of a “wave of death” pattern, proving them to be a good model for studying RCD.

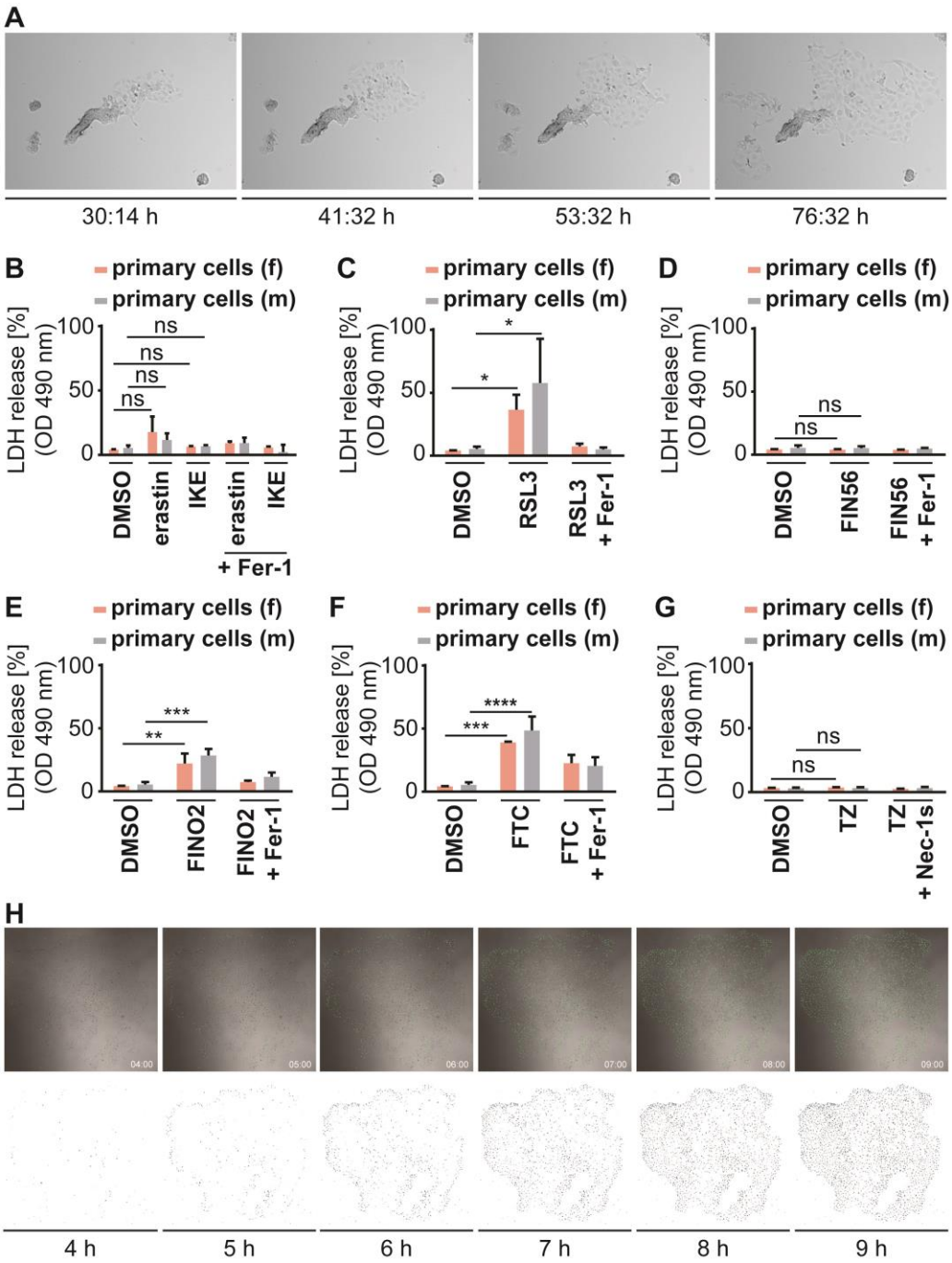

Figure 16. Primary tubular cells are sensitive to ferroptosis induction. A. Still images of time lapse imaging of primary cells growing out from isolated tubules. **B-G.** LDH release of primary tubular cells derived from female or male WT murine tubules treated with B. erastin or IKE (both at 5 µM), C. RSL3 (1.13 µM), D. FIN56 (20 µM), E. FINO2 (10 µM), F. FTC (10 µM) or G. with a combined treatment of 20 ng/ml TNFα and 20 µM zVAD (indicated as TZ) for 24 h. H. Still images of time lapse imaging of primary

tubular cells treated with RSL3 and stained with SYTOX green at indicated time points. The lower panel shows the SYTOX green positive cells (images with inverted colours to show SYTOX green in black colour). Fer-1 (10 μM) and Nec-1s (10 μM) were used as protection controls. All experiments were repeated independently at least 3 times. Graph plots show the mean +/- the standard deviation (SD). * $p < 0.05$; ** $p <= 0.01$; ns = non significant. Statistical analysis was performed using two-way ANOVA for multiple comparisons.

3.2.5. Testosterone does not promote ferroptosis

The increased sensitivity of male kidney tubules towards spontaneous necrosis compared to female kidney tubules, lead to the hypothesis that the sex hormones are involved in this phenomenon. To this end three well established cell lines for studying of ferroptosis were employed. A pre-treatment of 10 μM testosterone was performed 16 h before treatment with 5 μM erastin for 16, 18, 20 and 24 h, as shown in **Figure 17A**. Flow cytometry analysis showed no effect on the kinetics of annexin V and 7AAD staining in the murine fibroblasts NIH-3T3 (**Figure 17B**), the human fibrosarcoma cells HT1080s (**Figure 17C**), or the human kidney tubular epithelial cells CD10-135 (**Figure 17D**) regardless the time of erastin treatment.

In contrast with the literature that testosterone is responsible for the enhanced susceptibility of male mice to AKI (Park *et al*., 2004), these data do not support the hypothesis of an acceleration of cell death in three different cell lines. The use of the three cell lines to disapprove this hypothesis indicates a cell line independent effect of testosterone. Therefore, an investigation on how β-estradiol affects ferroptosis induction should be performed.

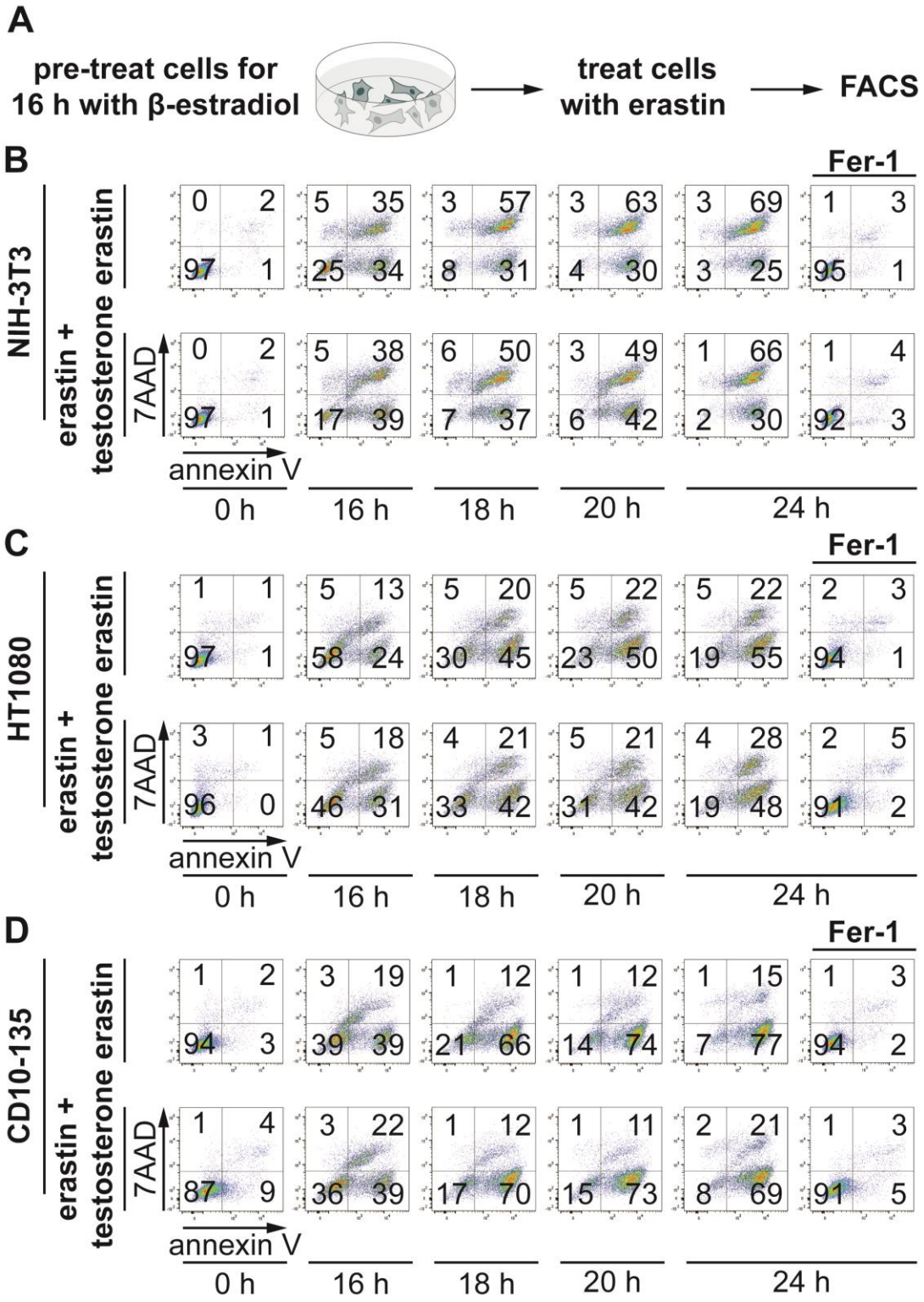

Figure 17. Testosterone does not affect ferroptotic cell death. A. Flow cytometry analysis of NIH-H3T3 cells pre-treated for 16 h with 10 μM testosterone and then treated with 5 μM erastin for indicated time points. **B**. HT1080 and **C.** CD10-135 cells treated as mentioned in A. Cells were stained with annexin V and 7AAD.

3.2.6. β-estradiol exhibits anti-ferroptotic properties

The female sex hormone, β-estradiol, was tested in a-similar experimental set-up to address the hypothesis that the presence of β-estradiol reduces the sensitivity towards ferroptosis. The murine fibroblast NIH-3T3, human fibrosarcoma HT1080 and the human kidney epithelial cells CD10-15 cell lines were employed to a pre-treatment of 10 μM β-estradiol of 16 h before a 5 μM erastin treatment for 16, 18, 20 and 24 h, as shown in **Figure 18A**. Flow cytometry analysis revealed a significant protection again erastin-induced ferroptosis in all cell lines (**Figure 18B-D**). Interestingly, even after 24 h of erastin treatment samples pre-treated with β-estradiol showed much higher percentage of double negative stained cells for almost all time points (49 % β-estradiol/erastin vs 2 % erastin-treated NIH-3T3 cells, 48 % β-estradiol/erastin vs 15 % erastin-treated HT1080 cells, 38 % β-estradiol/erastin vs 7 % erastin-treated CD10-135 cells after 24 h of erastin treatment).

To test whether the phenomenon observed when β-estradiol is present in erastin-containing medium is a general mechanism of β-estradiol preventing ferroptotic cell death, the type II FIN RSL3 was tested in a similar approach. Indeed, following a similar experimental approach (**Figure 19A**). Samples pre-treated with β-estradiol showed a higher percentage of double negative stained cells for all cell lines (**Figure 19B-D**). In all cell lines β-estradiol led to roughly 40% protection against RSL3-induced ferroptosis. Of notice, the increased incubation time with either erastin or RSL3 resulted in less double negative cells regardless the presence of β-estradiol. In all cases, Fer-1 was used as the protection control against ferroptosis induction.

The female hormone, β-estradiol is metabolized into different compounds, each of which bears different properties (Zhu and Conney, 1998). Even though estrogens react with their respective receptors, literature suggests that both β-estradiol and its metabolite 2-hydroxyestradiol (2-OHE2) inhibit lipid peroxidation (Miura *et al*., 1996). The difference of the two hormones is an additional hydroxide (-OH) at the second carbon molecule of the aromatic structure (**Figure 20A**). Therefore, the capacity of β-estradiol and 2-OHE2 in inhibiting RSL3-mediated cell death during a simultaneous treatment was tested (protocol showed as illustration in **Figure 20B**). Indeed, both hormones were able to inhibit RSL3-induced ferroptosis in all cell lines at 10 μM concentration (3T3, HT1080 and CD10) (**Figure 20C-E**). Different concentrations of the two hormones revealed a more potent effect of 2-OHE2 compared to β-estradiol.

Collectively, these data suggest a protective effect of β-estradiol against ferroptosis induction when cells are either pre-treated or treated simultaneously with β-estradiol and the FIN. The protective effect of β-estradiol and 2-OHE2 during a simultaneous treatment with RSL3 points towards antioxidant features. Such features could be due to the presence of the aromatic ring structure that offers double bonds that could be oxidized.

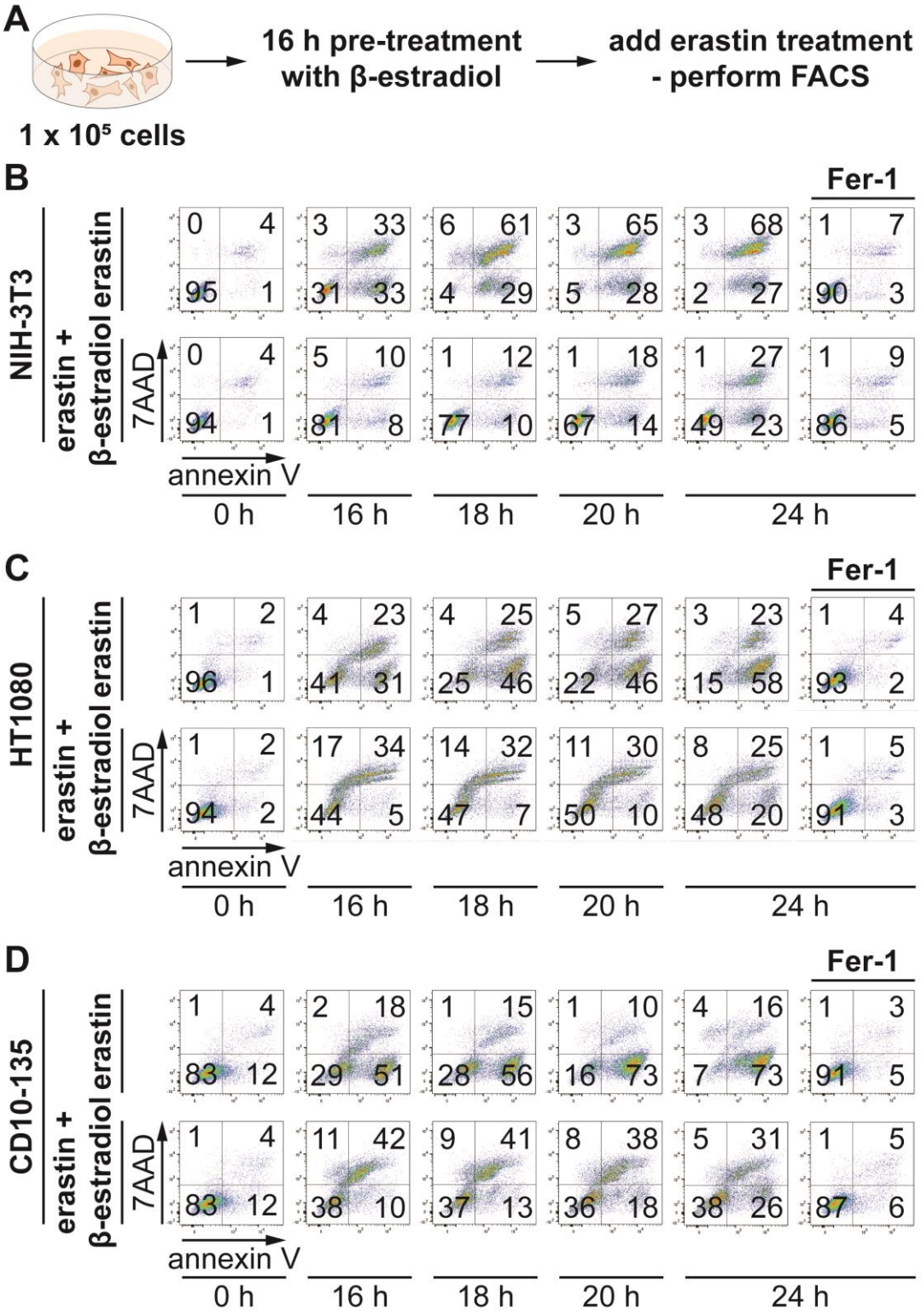

Figure 18. β-estradiol inhibits erastin-induced cell death. A. Illustration indicating the protocol followed for parts B-D of this figure. **B.** Flow cytometry analysis of NIH-H3T3 cells pre-treated for 16 h with 10 μM β-estradiol and then treated with 5 μM erastin for indicated time points. **C**. HT1080 and **D.** CD10-135 cells treated as mentioned in part A. Cells were stained with annexin V and 7AAD.

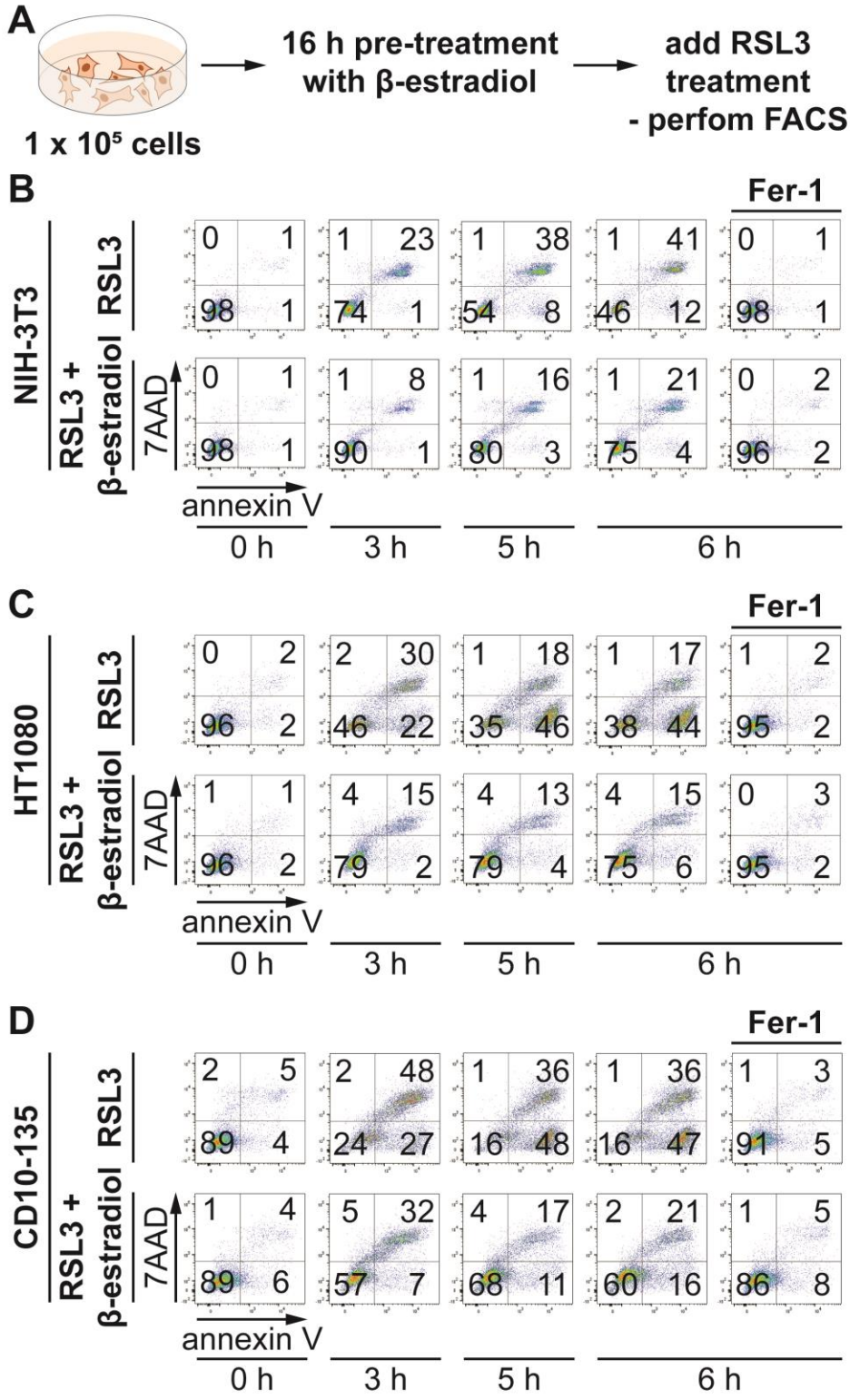

Figure 19. β-estradiol inhibits RSL3-induced cell death. A. Illustration indicating the protocol followed for parts B-D of this figure. **B.** Flow cytometry analysis of NIH-H3T3 cells pre-treated for 16 h with 10 μM β-estradiol and then treated with 1.13 μM RSL3 for indicated time points. **C**. HT1080 and **D.** CD10-135 cells treated as mentioned in part A. Cells were stained with annexin V and 7AAD.

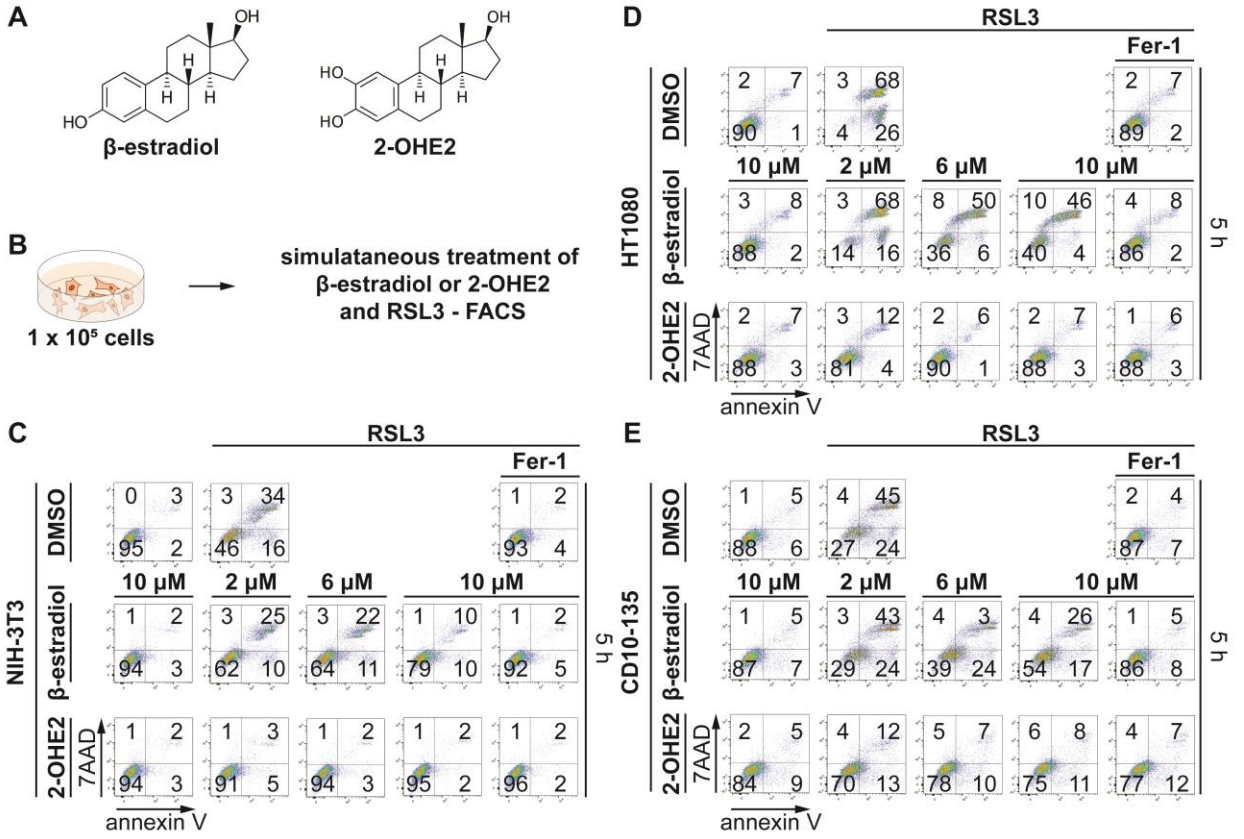

Figure 20. Simultaneous treatment of β-estradiol or 2-hydroxestradiol protects cells from RSL3-induced cell death. A. Chemical structure of β-estradiol and 2-hydroxyestradiol. **B.** Illustration indicating the protocol followed for parts B-D of this figure. **C.** Flow cytometry analysis of NIH-H3T3 cells treated simultaneously with 10 μM β-estradiol or 2-hydroxyestradiol (2-OHE2) and 1.13 μM RSL3 for 5 h. **D**. HT1080 and **E.** CD10-135 cells treated as mentioned in part A. Cells were stained with annexin V and 7AAD.

Discussion

4. Discussion

4.1. Part I: Adrenocortical carcinomas and key findings

Adrenocortical carcinoma (ACC) is a rare type of tumour located in the cortex of the adrenal glands. For many years, the best curative option is surgical removal either of the tumour or the whole adrenal glands. Other treatment options include the use of mitotane, a derivative of the pesticide DDT. Even though mitotane has been used for more than 60 years in the clinical practice its mechanism of action is not understood. Up to date, several laboratories that study the pharmacodynamics of mitotane have attributed its action to the inhibition of steroidogenesis (Lehmann *et al*., 2013), the destruction of mitochondria (Hescot *et al*., 2017) and ER stress (Sbiera *et al*., 2015). Apoptosis has also been proposed as the mechanism of action of mitotane (Pereira *et al*., 2019). This assumption has been derived from assays such as the activity of caspase 3 and 7 (Lehmann *et al*., 2013), assays labelling annexin V (Sbiera *et al*., 2015), and TUNEL assays (Kanczkowski *et al*., 2010). However, such results ought to be interpreted with caution, since it has been shown that TUNEL positivity occurs in many regulated cell death pathways beyond the classical apoptosis pathway (Galluzzi *et al*., 2014; Galluzzi *et al*., 2018). Data presented in this dissertation fail to clearly place the mode of action of mitotane in the one of the three RCD pathways analysed here, namely apoptosis, necroptosis, and ferroptosis. Inhibitors used to block apoptosis, necroptosis or ferroptosis did not reverse the mitotane-induced cell death, while western blot analysis indicated no cleavage of caspase3 (indicating the execution of apoptosis) or phosphorylated MLKL (indication for necroptosis execution). However, presence of linoleic acid, a PUFA, completely abrogated the effects of mitotane as evaluated with flow cytometry analysis and live imaging. This event could potentially point towards an oxidative type of death or a non-classical ferroptosis pathway, given the fact that the addition of Fer-1 was not sufficient to prevent this necrotic death. This hypothesis is supported by the finding that mitotane induces lipid peroxidation in ACC cells (Weigand *et al*., 2020).

Regulated cell death pathways, such as ferroptosis, might be more related to endocrine diseases than previously assumed (Tonnus *et al*., 2021a). Investigation of GPX4, one of the main regulators of ferroptosis, in the ACC cell line NCI-H295R revealed a much higher expression compared to the standard cell line used to study ferroptosis (HT1080). This finding led to the hypothesis that ACC cells are particularly sensitive to ferroptosis. Indeed, agents from the type II and IV FINs (see section 1.1.4) were able to induce cell death, which was reversed in the presence of Fer-1 or in the presence of PUFAs. Literature on three adrenocortical cell lines reported their high susceptibility to type II FIN RSL3 (Weigand *et al*., 2020). The high sensitivity of ACCs towards ferroptosis, as well as data supporting that ACC patients at low to intermediate risk of recurrence after surgery do not benefit significantly from mitotane treatment (Berruti *et al*., 2022), could point towards better targeted therapy strategies by

the induction of ferroptosis. Thereby this could offer a promising alternative to the currently broadly used therapeutic options with a suboptimal side effect profile (e.g., mitotane).

The exquisite sensitivity of ACCs to ferroptosis induction, is further supported by the analysis of two public databases, containing expression profiles of human ACC samples (Giordano *et al*., 2009; Zheng *et al*., 2016). According to this analysis, glutathione peroxidases (GPX3 and GPX7) are highly mutated in ACCs, which indicates an attempt of the tumour to evade ferroptotic cell death or alter its sensitivity to ferroptosis. The absence or the inhibition of GPX4 is in fact sufficient to kill kidney tubular cells (Linkermann *et al*., 2014). In line with these data, mutation of the selenocysteine required at the active center of GPX4 to its functional redox-competent analogue cysteine, renders mice more susceptible to AKI compared to WT mice (expressing the wild type version of GXP4) (Tonnus *et al*., 2021c), indicating the importance of GXP4 not only in the adrenal gland but also in other organs. Additionally, the cystathionine gamma lyase (cystathionase) indirectly regulates the sensitivity to ferroptosis, representing another potential clinical target for the control of the ferroptosis set point in ACCs. As mentioned in the introduction (section 1.2.2.1.), p53 is highly mutated in ACCs. Recently, p53 has also been associated with the regulation of ferroptosis (Jiang *et al*., 2015; Chen *et al*., 2017), establishing another link of ACCs and ferroptosis.

4.2. Part II: Kidney tubules, spontaneous necrosis, and key findings

In renal tubules, ferroptosis induction exhibits unique dynamics referred to as a “wave-of-death” or synchronized regulated necrosis (Linkermann *et al*., 2014; Tonnus *et al*., 2021a). In contrast to the procedure followed in this thesis, this phenomenon has been observed under micro-perfusion of the renal tubules and after direct infusion with erastin. Since the perfusion with erastin might not allow general conclusions on the physiological relevance of this cell death propagation, the spontaneous cell death was observed in isolated kidney tubules. Live imaging of isolated tubules undergoing spontaneous necrosis showed a clear “wave-of death” as indicated using nucleic stain (SYTOX green). Similar non-random cell death propagation has also been observed in cell culture models and the fins of zebrafish (Kim *et al*., 2016; Riegman *et al*., 2019; Katikaneni *et al*., 2020; Riegman *et al*., 2020b). Additionally, the live imaging data of this thesis show a calcium signal that propagates in parallel to the SYTOX green signal. In a different cell culture system it was shown that a ferroptosis predicting signal (rapid increase in calcium concentration) preceded the cell rupture and therefore the staining of the cells with SYTOX green (Riegman *et al*., 2020b). These two different observations might indicate two different types of cell death propagation.

Renal tubules are rich in mitochondria. The central role of mitochondria in tubular necrosis has been well established (Reimer and Jennings, 1971; Brooks *et al*., 2009). Therefore, maintenance of

mitochondrial homeostasis and quality control is vital for normal kidney function (Tang *et al*., 2021). Hence the high number of mitochondria observed in the electron microscopy images of isolated tubules was expected. These images further revealed a gradient of modestly damaged mitochondria to ballooned and highly damaged mitochondria following the propagation of the "wave-of-death" was highly interesting. These data are in line with the description of MOMP that has been associated with necrotic cell death and a calcium wave in proximal tubules (Weinberg *et al*., 1997; Feldkamp *et al*., 2009; Weinberg *et al*., 2016). Collectively, the data of this thesis and the existing literature further focus the spotlight on the mitochondria during the spontaneous tubular necrosis.

The vulnerability of kidney tubules in models of AKI has been shown and discussed at length (Linkermann *et al*., 2014; Linkermann, 2016). However, to what extent tubules contribute or how they are linked to the observed necrotic death is still not clear. Establishing a protocol for the isolation of murine renal tubules provided a tool free of immune system cells or vascular system interactions with the tubules, which are eliminated due to the extra washing steps of the tubules. Murine tubules die spontaneously in a non-necroptotic and non-pyroptotic manner, as shown in the genetically deficient model. However, small numbers of pMLKL positive cells observed in biopsies of transplanted human kidneys (Gong *et al*., 2017), while cleavage of GSDMD has been observed in mice undergoing cisplatin-induced AKI (Miao *et al*., 2019). Such findings indicate a potential role of necroptosis and pyroptosis in the kidney and do not support the data of this thesis. It is important to identify which compartment of the kidney is susceptible to necroptosis and/or pyroptosis. Partial involvement of ferroptosis in the spontaneous death of kidney tubular cells is implied by the finding that Fer-1 partially improved the viability of tubules when added directly to the medium. The existing literature points towards a strong presence of ferroptosis in the kidneys when mice are challenged with models of AKI (Linkermann *et al*., 2014; Tonnus *et al*., 2021c).

In this context, a discrepancy in the sensitivity of female and male mice to ischemia-reperfusion injury (IRI) of the kidney has been mentioned decades ago (Müller *et al*., 1999b; Park *et al*., 2004; Silva Barbosa *et al*., 2020). The protection of female mice was shown to be also characteristic of isolated murine tubules isolated from female mice. Female tubules undergoing spontaneous necrosis exhibited lower levels of LDH release compared to tubules isolated from male mice. In addition, primary tubular cells from female tubules were less susceptible to ferroptosis induction compared to primary tubular cells from male tubules. The difference between male and female organisms has been attributed to the sensitizing effects of testosterone (Hayward *et al*., 2000; Park *et al*., 2004; Kim *et al*., 2006), while by some other to the protective effects of estrogens (Ikeda *et al*., 2015; Singh *et al*., 2017; Tanaka *et al*., 2017; Silva Barbosa *et al*., 2020). This discord in the literature dictated the hypothesis that sex hormones affect the sensitivity to ferroptosis induction. The data of this thesis exploring this

hypothesis indicated no effect of testosterone on the potency of erastin-induced ferroptosis, while β-estradiol showed protective effects against type I (erastin) and II (RSl3) FIN-induced cell death. The fact that this protection was observed in three different cell lines indicated a cell line-independent effect of the hormone. Interestingly, a wide-range screening of CYP-substrates and hormones indicated that β-estradiol generally inhibits ferroptosis (Mishima *et al*., 2020). Furthermore, β-estradiol has been reported to regulate redox capacity in breast cancer cells by downregulating the lipoxigenase ALOX12B and upregulating oxidoreductases (e.g., cytochrome c) (Lin *et al*., 2004). The protection of β-estradiol against ferroptosis was not only observed after pre-treatment of cells, but also when cells were treated simultaneously with β-estradiol and the FINs. This points towards a general antioxidant effect of β-estradiol and should be further assessed in the future. In fact, metabolites of β-estradiol, such as 2-hydroxyestradiol show high antioxidant effects as well (Miura *et al*., 1996). Whether β-estradiol or one of its metabolites is transformed into its semiquinone derivative resulting in the recycling of the hormone and which enzymes play a role in this process is yet to be discovered.

4.3. Current understanding of the ferroptosis pathway

The interest in ferroptosis and its role in the physiology and the pathophysiology of various organs has increased extensively since 2012, when the term ferroptosis was introduced. It was shown that this type of death is caused by to lipid peroxidation, that will concomitantly lead to plasma membrane rupture. Which specific types of lipids are mainly involved during this process is an ongoing matter of debate (Zager and Foerder, 1992; Skouta *et al*., 2014; Yang *et al*., 2016; Li *et al*., 2017; Stockwell *et al*., 2017a; Ingold *et al*., 2018). Lipids that contain one or more double bonds (PUFAs) are prone to becoming a carbon-centered phospholipid radical (PL$^{\bullet}$). Subsequently a reaction with molecular oxygen would yield a phospholipid peroxyl radical (PLOO$^{\bullet}$). Such radicals can remove the hydrogen of another PUFA, thereby forming PLOOH. In case the lipid is not converted by GPX4 to its corresponding alcohol (PLOH), then PLOOH and lipid free radicals, such as PLOO$^{\bullet}$ and alkoxyl phospholipid radicals (PLO$^{\bullet}$), will react with PUFA-PLs propagating PLOOH production by further hydrogen atom removal and its concomitant reaction with molecular oxygen will form PLOOHs. Ultimately, this circle of reactions will lead to the formation of a myriad of lipid radicals and secondary products, such as breakdown products of lipids, oxidized and modified proteins. The increased modifications of the membrane lead to the loss of its stability and therefore to its breaking (Jiang *et al*., 2021). Baring this information in mind, it is expected that the presence of linoleic acid in medium containing FINs can reduce the percentage of necrotic cells, as seen in the experiments using the ACC cell line.

To which extent a cell can have oxidized lipids and the concomitant membrane modifications until it stops being functional and loses the membrane barrier is not yet clear. On the same note, the extent to which a cell can sustain lipid oxidization that is still reversible is particularly interesting. Is there a "lipid-point-of-no-return" for ferroptosis, like the "point-of-no-return" for apoptosis? Even though it has been shown that in some cases ferroptosis signals can propagate as a "wave-of-death" (Linkermann *et al*., 2014; Kim *et al*., 2016; Riegman *et al*., 2020a), the factor that confers this propagation is not known. One hypothesis is that this signal propagates via gap junctions. The decreased redox capacity of a dying cell results in an NAD(P)H gradient, meaning higher concentrations being observed inside the living cells and lower concentrations in the dying cells (Belavgeni *et al*., 2020; Tonnus *et al*., 2021a; Maremonti *et al*., 2022). Measurement and/or visualisation of the NAD(P)H gradient in a cell culture system or in isolated renal tubules could be performed via the fluorescence lifetime imaging microscopy (FLIM), allowing a better understanding of ferroptosis. Even though attempts at incorporating FLIM microscopy in studies related to kidney pathophysiology have been made (Ranjit *et al*., 2020), no relevant connection of its use with the field of ferroptosis exists.

During the membrane rupture of a cell DAMPs are being released (see section 1.1.), which are considered to induce an inflammatory response. A classification of these DAMPs and their immunogenicity has been established previously (Sarhan *et al*., 2018b; Tonnus *et al*., 2021a). Until recently it was considered that any kind of regulated cell death that results in the rupture of the cellular membrane results in an inflammatory response. To which extent the necrotic debris shape the immune response is not fully understood. As revised in the literature (Maremonti *et al*., 2022), necroptotically dying cells trigger a response from the adaptive immune system. The exposure of the debris to conventional dendritic cells (cDC1) stimulated cross-presentation of CD8-positive cytotoxic T cells (Giampazolias *et al*., 2021). In the microenvironment of tumours, soluble factors, such as gelsolin, interfere with actin binding to DNGR1 and thereby preventing an anti-tumour immune response (Giampazolias *et al*., 2021). Whether such a mechanism occurs during ferroptosis, for instance in an ischemic kidney, is not yet clear. Interestingly, even though previous literature suggests ferroptosis as an immunogenic necrosis pathway (Tang *et al*., 2020; Li *et al*., 2021; Turubanova *et al*., 2021), recent data implicate ferroptosis leading to the release of anti-immunogenic factors. Namely, T cells were paralysed by myeloid cells in high ROS conditions (Baumann *et al*., 2020), an effect mediated as a direct cell-to-cell contact between the T cells and the myeloid cells. This mechanism could explain the presence of adaptive immune cells and the paradoxical absence of an adaptive inflammatory response in histological samples of IRI-induced acute tubular necrosis, despite the high levels of tubular necrosis (von Mässenhausen *et al*., 2018; Tonnus *et al*., 2021c). Such findings are also in line with the absence of immune cell infiltration in mice with a dysfunctional GPX4 enzyme (Friedmann Angeli *et al*.,

2014a). Under conditions of active inhibition of the adaptive immune system the microenvironment of the kidney tubules would allow a regeneration process.

Understanding the pathophysiological features of ferroptosis in various diseases and other clinical implications is extremely valuable for developing new therapeutic strategies. The production of ROS or nitric oxide species (NOS) either in the cytosol of the cell or other cellular compartments, such as the mitochondria, the endoplasmic reticulum (ER), etc., does not necessarily lead to lipid peroxidation. However, ROS and oxidative stress have been tightly linked to ferroptosis (Stockwell *et al*., 2017a). The production of ROS plays a role in a wide variety of physiological responses, such as cellular proliferation, migration, angiogenesis, etc. (Sies and Jones, 2020; Sies *et al*., 2022). In fact, even beyond the cellular level, whole organisms such as mussels use ROS as a defence mechanism against xenobiotics or pathogens (Tsarpali *et al*., 2015; Belavgeni and Dailianis, 2017). Such an event might result in a triggered inflammatory response aiming to eliminate the pathogen without inflicting fatal damage to the host. Observations like this are leading to the open question regarding the physiological and evolutional role of ferroptosis. Why would a cell be prone to ferroptosis in physiological conditions? Which is the physiological role of ferroptosis? Until light is shed on these questions, they remain a promising avenue for research, setting perhaps ferroptosis as one of the most important pathways in almost all (if not all) the organisms of this world.

4.4. Ferroptosis and its significance in the endocrine system and beyond

The adrenal glands are tightly linked to ferroptosis, even beyond the high sensitivity of ACCs to this type of death. As mentioned in the introduction (see section 1.2.2.2.), a closer look into the cause of adrenal-related diseases might reveal their connection to ferroptosis, and even necroptosis and pyroptosis. Addison's disease, a primary adrenal insufficiency, can be caused by a haemorrhagic, ischemic, or surgical event, or by infection, or metastatic destruction of the adrenal tissue, or treatment of ACC (Merke *et al*., 2000; Bornstein, 2009; Husebye *et al*., 2021). In the pathophysiology of this disease a bleeding would result in increased free iron being released from damaged erythrocytes, an event that can lower the threshold for ferroptosis. Free iron can easily be oxidized via the Fenton reaction leading to an increase of ROS (Belavgeni *et al*., 2020; Tonnus *et al*., 2021a), that will oxidize the lipid membranes. Such an assumption remains a hypothesis, since it is unclear how most of the adrenal cells die during the progression of the disease. However, a therapeutic strategy using an RTA, such Fer-1 or Lip-1, might prove beneficial. Additionally, it would be of interest to investigate whether in a mouse model of Addison's disease administration of PUFAs would exhibit positive effects, while aiming at a better understanding of the biology of the adrenal glands.

Primary aldosteronism (PA, also known as Conn's syndrome), refers to the excess production of the mineralocorticoid, aldosterone. Aldosterone is important for the function of the renin-angiotensin system that regulates the blood pressure and its dysfunction confers a higher cardiovascular risk (Zennaro *et al*., 2020). The most common cause for PA is a unilateral aldosterone-producing adenoma (APA) or a bilateral adrenal hyperplasia (Zennaro *et al*., 2020). Genetically this disease has been linked to a chimeric gene, resulting from an unequal crossing-over event that fuses the regulatory regions of CYP11B1 and CYP11B2. CYP11B1 gene encodes the enzyme 11β-hydroxylase, while CYP1B2 encodes aldosterone synthase, making them the responsible genes for the last steps of cortisol and aldosterone biosynthesis, respectively (Lifton *et al*., 1992; Pascoe *et al*., 1992). The aldosterone-mediated cell death has been attributed to apoptosis (De Angelis *et al*., 2002; Yan *et al*., 2010). However, recent data on APAs indicated upregulation of BEX1, a protein involved in cell cycle progression. When BEX1 was stably expressed in human adrenocortical cells, a protection against type II-mediated ferroptosis was observed in comparison to BEX1 deficient cells (Yang *et al*., 2021). This establishes a new road for further investigation of the role of ferroptosis and the pathogenesis of APAs. Additionally, the role of aldosterone as a DIRE (section 1.2.2.2.) should be further investigated not only in the concept of damage arising in the adrenal gland but from a more systemic point of view. In this context of DIRE, it is worth mentioning that dexamethasone, a glucocorticoid analogue, was found to accelerate ferroptosis induction (von Mässenhausen *et al*., 2022). This indicates that clinical use of DIRE in combination with cell death-inducing drugs should be approached with caution and warrants further research, particularly in relation to the gender of the patients. Whether testosterone would prove to be a DIRE is yet to be investigated using a broader array of cell death inducers.

The inner part of the adrenal gland, the medulla, is prone to cancer formation as well. Pheochromocytomas (PCCs) and paragangliomas (PGLs) represent neuroendocrine tumours of the adrenal medulla. They are associated with high cardiovascular morbidity, due to their high production of catecholamines (Scriba *et al*., 2020). Catecholamines can also be included in the category of DIRE. Myocardial necrosis can be related to epinephrine release (Short and Padfield, 1976), while in extreme cases of PCC and PGL DIRE can lead to severe and eventually lethal shock (Delaney and Paritzky, 1969; Nyman and Wahlberg, 1970). Profiling of the DNA methylation of PCCs and PGLs revealed GXP3 as a frequently mutated prognostic marker (de Cubas *et al*., 2015). Even though GPX3 belongs to the glutathione peroxidation enzyme family, it is unclear which is its contribution to ferroptosis. Of particular interest in this regard are the findings of numerous mutations in this gene in both ACCs (as presented in this dissertation) and PCCs/PGLs. These findings are an essential clue in pursuit of better understanding of the microenvironment of the different parts of the adrenal gland. Given the systemic consequences of PCCs and PGLs, it is worth mentioning a case report that pointed to a potential link

between these type of tumors and acute tubular necrosis (Carpenter and Kunin, 1961). Whether ferroptosis could be the connecting link of the two diseases remains an unanswered question.

4.5. Pharmacologically harnessing ferroptosis

During the past decade, several compounds acting on RCD have been developed with the aim to be used in the therapy of diseases related with regulated necrosis (Degterev and Linkermann, 2016; von Mässenhausen *et al*., 2018). Some of those inhibitors, such as venetoclax, have since been applied to the clinical routine for the treatment of haematological cancers (Souers *et al*., 2013). Both necrostatins and ferrostatins are currently moving intro clinical trials (Tonnus *et al*., 2021a). On the other hand, inducers of regulated necrosis are just as important, for example in the treatment of cancer. Numerous of necroptosis, pyroptosis and ferroptosis (FINs) inducers have been developed (Stockwell *et al*., 2017b; Llabani *et al*., 2019b; Zhang *et al*., 2019). Further development of such molecules, aimed at introduction of novel drugs with more favourable side effect profiles, could be the next step in the treatment of adrenal-related cancers. The high sensitivity of ACCs to ferroptosis, as shown in this thesis, suggests a possibly similar nature of PCCs/PGLs in relation to ferroptosis. FINs could therefore contribute to the improvement of outcomes in patients with these tumours.

The ferroptosis inhibitor, Fer-1, has been shown to protect against AKI, as well as heart injury (Martin-Sanchez *et al*., 2017c; Tonnus *et al*., 2021c). Based on the chemical structure of Fer-1, other novel inhibitors have been developed, such as UCAM-3203/3206 (Devisscher *et al*., 2018). The iron chelator deferoxamine (DFO) inhibits cell death in isolated tubules from rabbits (Sogabe *et al*., 1996). The lipophilic antioxidant, diphenyl-p-phenylenediamine (DPPD), also exhibited a certain protective effect, in terms of LDH release, of isolated kidney tubules (Sogabe *et al*., 1996). The compound 11-92 was highly effective in the prevention of tubular necrosis, (Skouta *et al*., 2014), while the development of the compound 16-86 yielded strong effects in preclinical models of AKI (Linkermann *et al*., 2014). However, the plasma stability of 16-86 was not ideal. Liproxstatin-1 (Lip-1), successfully blocks ferroptosis-induced cell death in immortalized human renal proximal tubule epithelial cell line HK-2, as well as liver IRI (Friedmann Angeli *et al*., 2014a). Even though these inhibitors are unspecific, they could be used to further assess mitotane-induced cell death in NCI-H295R cells, given the hypothesis that the machinery of ferroptosis might be involved in a non-classical manner. On the other hand, treatment of tubules with different ferroptosis inhibitors could improve the current understanding of spontaneous necrosis. Finally, a more complete image of the ACC and tubule biology could be provided by genetic models, a field of future investigations. Overall, it is necessary to further improve the *in vivo* pharmacokinetics and efficacy.

Many different diseases have been reviewed and linked to ferroptosis. Interestingly, it seems like organs that are more prone to ischemic injury, such as the heart and the kidneys, are highly susceptible to ferroptosis (Tonnus *et al*., 2019; Tonnus *et al*., 2021a). For example, treatment with mitochondria-targeted antioxidant MitoTEMPO in an established murine model of doxorubicin (DOX) and ischemia/reperfusion (I/R)-induced cardiomyopathy, resulted in significant rescue against DOX cardiomyopathy (Fang *et al*., 2019). On the same spectrum, ferritin H, a spherical heteropolymer responsible for the storage of excess cellular iron, plays an important role in protection against cardiac ferroptosis and a subsequent heart failure, as shown in mice with cardiomyocytes lacking ferritin H (Fang *et al*., 2020). The importance of mitochondrial oxidative damage in cardiomyocytes, is in accordance with the finding that inhibition of the glutaminolysis process prevent heart injury induced by I/R (Gao *et al*., 2015).

Prevention of lipid peroxidation by Fer-1 was also shown to inhibit cell death in a cellular model of Huntington's disease (Skouta *et al*., 2014), while selenium supplementation improved behaviour in a haemorrhagic stroke model (Alim *et al*., 2019). Additional data concerning the connection of ferroptosis and stoke (Degterev *et al*., 2005; Tuo *et al*., 2017; Kenny *et al*., 2019), reveal a broader spectrum of the relevance of ferroptosis with different pathophysiological models in organs prone to ischemic injury. A deeper and more ferroptosis-oriented research will broaden the biology basis of such diseases, while exploring new direction for drug targeting strategies.

Before a connection of ferroptosis and kidney was established, necroptosis was thought to be the primary RCD pathway in murine AKI models. This hypothesis was supported by data showing Nec-1-mediated protection against contrast-induced murine AKI model (Linkermann *et al*., 2013). Considering the complexity of each organ, the involvement of more than one RCD pathways mut be considered. From a clinical approach, the use of dual or triple RCD inhibitors may prove more efficient than single RCD inhibitors. Such inhibitors are known for a while in the scientific community but have also been a source of misinterpretations. The necrostatin Nec-1 functions as a necroptosis as well as a ferroptosis inhibitor (Takahashi *et al*., 2012; Friedmann Angeli *et al*., 2014b). Based on the structure of Nec-1, another dual inhibitor of necroptosis and ferroptosis was constructed (termed Nec-1f). Nec-1f was also shown to have a similar effect on the recruitment of neutrophils and the cardiomyocyte cell death using a similar transplantation model (Tonnus *et al*., 2021c). Additionally, in the same paper it was shown that Nec-1f protects tubules from undergoing RSL3-induced cell death (Tonnus *et al*., 2021c), possibly exerting this effect to its anti-ferroptotic features. This is in line with the findings of this thesis concerning the protection of tubules in the presence of a ferroptosis inhibitor.

In transplantation medicine, an allograft must endure several unfavourable environments, occurring already from the explantation from the donor, during the organ preservation and during the

implantation-associated postischemic reperfusion injury (IRI) in the recipient. The development of ROS-mediated oxidative stress, in combination with the release of DAMPs can activate the innate immune system (Land *et al.*, 2016). Considering a potential anti-inflammatory response of cells dying by ferroptosis, and the inflammatory response of necroptotic cells, the prefusion of the organs with a dual necroptosis and ferroptosis inhibitor might represent the future of organ transplantation handling. Furthermore, this approach could prevent or reduce the complications of transplantation on the other organs in the recipient, as the cell death in the graft can trigger pathological events in distant organs. This is demonstrated particularly in an *in vivo* model of ischemic renal graft-mediated lung injury where the use of a PARP-inhibitor and the RIPK1 inhibitor Nec-1 resulted in some protection on their own, but the combination therapy proved to almost completely prevent pulmonary damage after kidney transplantation (Vanden Berghe and Linkermann, 2015; Zhao *et al.*, 2015). Therefore, crosstalk of ferroptosis with other types of necrosis, such as parthanatos (Linkermann, 2016), render the production of dual or even triple inhibitors important for the clinical approach of transplant-mediated remote death.

While the use of different mammalian or cell line models provides a better insight into the biology of different diseases, and many books have been written for human physiology, a clinical approach on how this knowledge would be best used proves to be a challenging question. Ultimately the balance of drug inducers and inhibitors remains a clinical issue. Which should be the dosage of an anti-cancer drug that induces ferroptosis without risking a renal failure or heart ischemia? Would a continuous use of ferroptosis inhibitors result in a ferroptosis-sensitive tumour? Additionally, genetic models should be established to clarify the specificity of the developed compounds/drugs. Such information would help the scientific community better understand the pathology of the targeted disease, as well as the molecular pathway that the drugs interfere with. Based on this knowledge, highly specific molecules could be developed, that can be used in low dosage and would therefore be more favourable in terms of their side effect profiles.

4.6. Sexual dimorphism in regulated cell death

Steroids are biologically active organic compounds with four interconnected carbon rings, composing the main skeleton of every steroid. Polar hydroxyl groups are attached to this ring structure, however in quantities unable to render steroids water-soluble. Steroid hormones (a word derived from the Greek-origin word ὁρμῶν, with the meaning “setting in motion”) are a class of signalling molecules that freely diffuse across lipid bilayers due to their lipophilic nature and are regulating numerous pathways. Cholesterol is the precursor of steroids, from which cortisol is produced in the adrenal glands. A major difference of male and female organisms can be observed on the production of sex hormones by the gonads. Males are characterized by higher levels of androgens, such testosterone and its

concomitant metabolites, while females show higher levels of estrogens, such as estradiol and its metabolites (Widmaier *et al*., 2019).

Hormones exert their effects via their corresponding receptors. The activation of the receptors in cells ultimately leads to alterations in molecular pathways, inhibition, or enhancement of gene expression. The androgen receptor (AR) offers a binding site for testosterone (Tan *et al*., 2014), while estrogen receptors alpha and beta (ESRα and ESRβ respectively) fashion a binding site for estradiol (Widmaier *et al*., 2019). Several NADPH-dependent cytochrome P450 enzymes are involved in steroid hormone production (Zhu and Conney, 1998; Peter Guengerich, 2019), which have been in the center of scientific attention concerning different diseases. Interestingly, not all enzymes are universally expressed in all tissues. Therefore, different sex hormone metabolites may be produced in different organs. The amount of hormones, e.g. stress hormones, in the different sexes also differ (Goel *et al*., 2014). It has already been indicated that sex hormones play a role in the contect of stress response, with higher levels of corticosterone in female rats compared to male littermates (Goel *et al*., 2014). On the other hand, their role in regulated cell death is an entirely new field of research.

Presently there is evidence that testosterone enhances the susceptibility of male mice to IRI (Park *et al*., 2004) and promotes cell death in renal tubular cells (Peng *et al*., 2019). Further supporting these findings, orchiectomy in mice was shown to diminish post-ischaemic oxidative stress and IRI (Kim *et al*., 2006). However, the findings in this thesis stand at contrast with these theories. Interestingly, examination of data derived from the United Network for Organ Sharing (UNOS) revealed an association of delayed graft function (DGF) in male recipients compared to female recipients (Aufhauser *et al*., 2016). In addition to this finding, a growing body of literature reports a reduced sensitivity of female rodents to IRI compared to males (Aufhauser *et al*., 2016; Singh *et al*., 2017; Tanaka *et al*., 2017), a protective role of 17β-estradiol during AKI (Silva Barbosa *et al*., 2020), and a reduction of myocardial necrosis and macrophage infiltration (Squadrito *et al*., 1997). These are further supported by the data of this thesis, showing the reduced sensitivity of tubules derived from female mice compared to tubules of male mice.

One hypothesis concerning the protective effects of 17β-estradiol is that the "presence of 17β-estradiol leads to a receptor-mediated upregulation of genes promoting cell survival or the downregulation of genes promoting cell death". However, the chemical structure of 17β-estradiol reveal an aromatic ring structure with three double bonds that could provide radical trapping functions (Zhu and Conney, 1998). In fact, literature supports the hypothesis that 17β-estradiol and its metabolite 2-hydroxyestradiol exhibit antioxidant effects, thereby inhibiting lipid peroxidation (Begoña Ruiz-Larrea *et al*., 1994; Miura *et al*., 1996). However, it is not clear how 17β-estradiol and certain metabolites may act as antioxidants at the chemical level. It is believed that 2- and 4-hydroxyestradiols

can generate reactive estrogen semiquinones/quinones (Zhu and Conney, 1998). Given the fact that quinones can be recycled by reductases, a recycling process of the hydroxyestradiol quinones generating estradiol might be happening intracellularly. Which exact NADPH-dependent oxidoreductase is involved in this prosses is yet to be found. The reaction of a semiquinone to a quinone yields superoxide anions ($O_2^{\bullet-}$), which as ROS may mediate protein, lipid and DNA damage etc (Zhu and Conney, 1998). However, if indeed the estradiol hormones are transformed to quinones, the cell should exhibit higher antioxidant capacities against ROS production. It would be of interest then, to investigate the basal expression of anti-ferroptosis genes, such as GPX4 and FSP1, in isolated tubules from male and female mice. If there is yet another mechanism to prevent these ROS from damaging the cells, it remains to be elucidated. Overall literature and data provided from this thesis concerning the protective effect of 17β-estradiol against a simultaneous RSL3 induction point towards a very potent anti-ferroptotic hormone highly present in female organisms. In that case 17β-estradiol and its metabolites would render them more protected against death. Medical approaches of cancer therapy, organ transplantation, etc., especially regarding their effects and outcome depending on the respective sex should be revisited. A better evaluation of transplantations taking gender into account might be crucial to achieve better transplant function. Even though the hypothesis points towards organs of female origin to be less prone to death, a perfusion with highly potent antioxidant estradiol metabolites might be a path to be considered. In fact, as mentioned in the previous section of the discussion, a perfusion with estrogens and dual cell death inhibitors (such as Nec-1f) could potentially prolong the viability of the transplanted organs while aiming at minimizing the side effects of both chemicals.

4.7. Outlook, future perspectives, and limitations of this thesis

Regulated cell death in the adrenal glands and the kidneys might at first glance seem to be unrelated events. Nevertheless, studies of the human body show that organs and cells can communicate in the most intricate ways. The hormones produced by the adrenal glands affect the physiological processes under normal conditions as well as in pathological conditions, such as cancer. Excessive production of hormones can lead to a potentiation of ferroptosis when ferroptosis-inducing drugs are present, as seen in the case of dexamethasone (Lau *et al*., 2022; von Mässenhausen *et al*., 2022). Other hormones and their metabolites, such as 17β-estradiol, exert anti-ferroptotic effects, a feature that could potentially explain the higher tolerance of female organisms to heart failure and kidney injury. The data provided in this thesis speak for a cascade of events unrelated to the estrogen receptors (ESRα and ESRβ) conferring this effect. The lack of respective knock out cell lines or even mice can be considered a limitation of the experimental approach used here. However, existing literature (Begoña Ruiz-Larrea *et al*., 1994; Miura *et al*., 1996) supports this hypothesis.

A genetic model for ferroptosis has been a challenge due to the fact that GXP4 knock out mice are embryonically lethal (Ingold *et al*., 2018). Alternative genetic models to study ferroptosis are the FSP1 knock out mice and mice that carry a manipulation of the active center of the GXP4 enzyme ($GPX4^{cys/-}$) (Tonnus *et al*., 2021c). These models could be an important addition to the data presented in this thesis and used to further validate them and better understand the role of ferroptosis both in the adrenal gland and the kidneys. The high sensitivity of an ACC cell line to ferroptosis might indicate a high sensitivity of the organ to regulated cell death. In fact, the adrenal glands exhibit high capacity of antioxidant enzymes against the constant production of hormones and the response to stress. So far, any attempts to study adrenal cells derived from normal human or mouse adrenal tissue were unsuccessful. Such cell lines would remove the bias created from the background of a cancer cell line. On the other hand, multicellular complex systems, such as renal tubules enable studying RCD in a more physiological setting. Limitations, such as lack of typical hormones or stimuli present in the kidney, cannot be avoided and hence, observations made in the kidney tubules cannot be directly linked to an *in vivo* effect. However, a system free of systemic effects of the body has its own advantages, depending on the scientific question.

Ultimately, the best approach to a scientific matter is to combine techniques, and use, if possible, all available material (cells, organoids, mice) in the most unbiased way possible.

References

References

Agarwal A, Dong Z, Harris R, Murray P, Parikh SM, Rosner MH, Kellum JA, Ronco C. 2016. Cellular and Molecular Mechanisms of AKI. J Am Soc Nephrol, 27(5):1288–1299 DOI: 10.1681/ASN.2015070740.

Alim I, Caulfield J, Chen Y, Swarup V, Geschwind D, Ivanova E, Seravalli J, Ai Y, Sansing L, Ste Marie E, Hondal R, Mukherjee S, Cave J, Sagdullaev B, Karuppagounder S, Ratan R. 2019. Selenium Drives a Transcriptional Adaptive Program to Block Ferroptosis and Treat Stroke. Cell, 177(5):1262-1279.e25 DOI: 10.1016/J.CELL.2019.03.032.

Allolio B, Fassnacht M. 2006. Clinical review: Adrenocortical carcinoma: clinical update. J Clin Endocrinol Metab, 91(6):2027–2037 DOI: 10.1210/JC.2005-2639.

Alvarez-Diaz S, Dillon CP, Lalaoui N, Tanzer MC, Rodriguez DA, Lin A, Lebois M, Hakem R, Josefsson EC, O'Reilly LA, Silke J, Alexander WS, Green DR, Strasser A. 2016. The Pseudokinase MLKL and the Kinase RIPK3 Have Distinct Roles in Autoimmune Disease Caused by Loss of Death-Receptor-Induced Apoptosis. Immunity, 45(3):513–526 DOI: 10.1016/j.immuni.2016.07.016.

De Angelis N, Fiordaliso F, Latini R, Calvillo L, Funicello M, Gobbi M, Mennini T, Masson S. 2002. Appraisal of the role of angiotensin II and aldosterone in ventricular myocyte apoptosis in adult normotensive rat. J Mol Cell Cardiol, 34(12):1655–1665 DOI: 10.1006/JMCC.2002.2115.

Aufhauser DD, Wang Z, Murken DR, Bhatti TR, Wang Y, Ge G, Redfield RR, Abt PL, Wang L, Svoronos N, Thomasson A, Reese PP, Hancock WW, Levine MH. 2016. Improved renal ischemia tolerance in females influences kidney transplantation outcomes. J Clin Invest, 126(5):1968–1977 DOI: 10.1172/JCI84712.

Bairey Merz CN, Dember LM, Ingelfinger JR, Vinson A, Neugarten J, Sandberg KL, Sullivan JC, Maric-Bilkan C, Rankin TL, Kimmel PL, Star RA. 2019. Sex and the kidneys: current understanding and research opportunities. Nat Rev Nephrol 2019 1512, 15(12):776–783 DOI: 10.1038/s41581-019-0208-6.

Barbosa ACS, Zhou D, Xie Y, Choi Y-J, Tung H-C, Chen X, Xu M, Gibbs RB, Poloyac SM, Liu S, Yu Y, Luo J, Liu Y, Xie W. 2020. Inhibition of Estrogen Sulfotransferase (SULT1E1/EST) Ameliorates Ischemic Acute Kidney Injury in Mice. J Am Soc Nephrol, 31(7):1496–1508 DOI: 10.1681/ASN.2019080767.

Basham KJ, Rodriguez S, Turcu AF, Lerario AM, Logan CY, Rysztak MR, Gomez-Sanchez CE, Breault DT, Koo BK, Clevers H, Nusse R, Val P, Hammer GD. 2019. A ZNRF3-dependent Wnt/β-catenin signaling gradient is required for adrenal homeostasis. Genes Dev, 33(3–4):209–220 DOI: 10.1101/GAD.317412.118.

Baumann T, Dunkel A, Schmid C, Schmitt S, Hiltensperger M, Lohr K, Laketa V, Donakonda S, Ahting U, Lorenz-Depiereux B, Heil JE, Schredelseker J, Simeoni L, Fecher C, Körber N, Bauer T, Hüser N, Hartmann D, Laschinger M, Eyerich K, Eyerich S, Anton M, Streeter M, Wang T, Schraven B, Spiegel D, Assaad F, Misgeld T, Zischka H, Murray PJ, Heine A, Heikenwälder M, Korn T, Dawid C, Hofmann T, Knolle PA, Höchst B. 2020. Regulatory myeloid cells paralyze T cells through cell-cell transfer of the metabolite methylglyoxal. Nat

Immunol, 21(5):555–566 DOI: 10.1038/S41590-020-0666-9.

Begoña Ruiz-Larrea M, Ma Leal A, Liza M, Lacort M, de Groot H. 1994. Antioxidant effects of estradiol and 2-hydroxyestradiol on iron-induced lipid peroxidation of rat liver microsomes. Steroids, 59(6):383–388 DOI: 10.1016/0039-128X(94)90006-X.

Belavgeni A, Bornstein SR, Linkermann A. 2019a. Prominin-2 Suppresses Ferroptosis Sensitivity. Dev Cell, 51(5):548–549 DOI: 10.1016/J.DEVCEL.2019.11.004.

Belavgeni A, Bornstein SR, Von Mässenhausen A, Tonnus W, Stumpf J, Meyer C, Othmar E, Latk M, Kanczkowski W, Kroiss M, Hantel C, Hugo C, Fassnacht M, Ziegler CG, Schally A V., Krone NP, Linkermann A. 2019b. Exquisite sensitivity of adrenocortical carcinomas to induction of ferroptosis. Proc Natl Acad Sci U S A, 116(44):22269–22274 DOI: 10.1073/PNAS.1912700116.

Belavgeni A, Dailianis S. 2017. The role of phosphatidylinositol-3-OH-kinase (PI3-kinase) and respiratory burst enzymes in the [omim][BF4]-mediated toxic mode of action in mussel hemocytes. Fish Shellfish Immunol, 68:144–153 DOI: 10.1016/J.FSI.2017.07.015.

Belavgeni A, Meyer C, Stumpf J, Hugo C, Linkermann A. 2020. Ferroptosis and Necroptosis in the Kidney. Cell Chem Biol, 27(4):448–462 DOI: 10.1016/j.chembiol.2020.03.016.

Bellyei S, Schally A V., Zarandi M, Varga JL, Vidaurre I, Pozsgai E. 2010. GHRH antagonists reduce the invasive and metastatic potential of human cancer cell lines in vitro. Cancer Lett, 293(1):31–40 DOI: 10.1016/J.CANLET.2009.12.014.

Vanden Berghe T, Linkermann A. 2015. Take my breath away: necrosis in kidney transplants kills the lungs! Kidney Int, 87(4):680–682 DOI: 10.1038/KI.2015.13.

Berruti A, Fassnacht M, Libè R, Lacroix A, Kastelan D, Haak H, Arlt W, Decoudier B, Lasolle H, Bancos I, Quinkler M, Fragoso MCBV, Canu L, Puglisi S, Bourdeau I, Baudin E, Berchialla P, Beuschlein F, Bertherat J, Terzolo M. 2022. First randomized trial on adjuvant mitotane in adrenocortical carcinoma patients: The Adjuvo study. https://doi.org/101200/JCO2022406_suppl001, 40(6_suppl):1–1 DOI: 10.1200/JCO.2022.40.6_SUPPL.001.

Bersuker K, Hendricks JM, Li Z, Magtanong L, Ford B, Tang PH, Roberts MA, Tong B, Maimone TJ, Zoncu R, Bassik MC, Nomura DK, Dixon SJ, Olzmann JA. 2019. The CoQ oxidoreductase FSP1 acts parallel to GPX4 to inhibit ferroptosis. Nat 2019 5757784, 575(7784):688–692 DOI: 10.1038/s41586-019-1705-2.

Bornstein SR. 2009. Predisposing Factors for Adrenal Insufficiency. N Engl J Med, 360(22):2328–2339 DOI: 10.1056/nejmra0804635.

Brooks C, Wei Q, Cho S, Dong Z. 2009. Regulation of mitochondrial dynamics in acute kidney injury in cell culture and rodent models. J Clin Invest, 119(5):1275–1285 DOI: 10.1172/JCI37829.

Brown CW, Amante JJ, Chhoy P, Elaimy AL, Liu H, Zhu LJ, Baer CE, Dixon SJ, Mercurio AM. 2019. Prominin2 Drives Ferroptosis Resistance by Stimulating Iron Export. Dev Cell, 51(5):575-586.e4 DOI: 10.1016/J.DEVCEL.2019.10.007.

Broz P, Dixit VM. 2016. Inflammasomes: mechanism of assembly, regulation and signalling. Nat Rev Immunol, 16(7):407–420 DOI: 10.1038/NRI.2016.58.

Carpenter AA, Kunin AS. 1961. Pheochromocytoma with acute tubular necrosis. Report of a case. N Engl J Med, 265(20):986–988 DOI: 10.1056/NEJM196111162652005.

Chen D, Tavana O, Chu B, Erber L, Chen Y, Baer R, Gu W. 2017. NRF2 Is a Major Target of ARF in p53-Independent Tumor Suppression. Mol Cell, 68(1):224-232.e4 DOI: 10.1016/J.MOLCEL.2017.09.009.

Cho YS, Challa S, Moquin D, Genga R, Ray TD, Guildford M, Chan FKM. 2009. Phosphorylation-driven assembly of the RIP1-RIP3 complex regulates programmed necrosis and virus-induced inflammation. Cell, 137(6):1112–1123 DOI: 10.1016/J.CELL.2009.05.037.

Crona J, Beuschlein F. 2019. Adrenocortical carcinoma — towards genomics guided clinical care. Nat Rev Endocrinol 2019 159, 15(9):548–560 DOI: 10.1038/s41574-019-0221-7.

de Cubas AA, Korpershoek E, Inglada-Pérez L, Letouzé E, Currás-Freixes M, Fernández AF, Comino-Méndez I, Schiavi F, Mancikova V, Eisenhofer G, Mannelli M, Opocher G, Timmers H, Beuschlein F, De Krijger R, Cascon A, Rodríguez-Antona C, Fraga MF, Favier J, Gimenez-Roqueplo AP, Robledo M. 2015. DNA Methylation Profiling in Pheochromocytoma and Paraganglioma Reveals Diagnostic and Prognostic Markers. Clin Cancer Res, 21(13):3020–3030 DOI: 10.1158/1078-0432.CCR-14-2804.

Damgaard RB, Walker JA, Marco-Casanova P, Morgan N V., Titheradge HL, Elliott PR, McHale D, Maher ER, McKenzie ANJ, Komander D. 2016. The Deubiquitinase OTULIN Is an Essential Negative Regulator of Inflammation and Autoimmunity. Cell, 166(5):1215-1230.e20 DOI: 10.1016/J.CELL.2016.07.019.

Davidson AJ, Wood W. 2020. Igniting the spread of ferroptotic cell death. Nat Cell Biol, 22(9):1027–1029 DOI: 10.1038/S41556-020-0570-4.

Degterev A, Huang Z, Boyce M, Li Y, Jagtap P, Mizushima N, Cuny G, Mitchison T, Moskowitz M, Yuan J. 2005. Chemical inhibitor of nonapoptotic cell death with therapeutic potential for ischemic brain injury. Nat Chem Biol, 1(2):112–119 DOI: 10.1038/NCHEMBIO711.

Degterev A, Linkermann A. 2016. Generation of small molecules to interfere with regulated necrosis. Cell Mol Life Sci 2016 7311, 73(11):2251–2267 DOI: 10.1007/S00018-016-2198-X.

Degterev A, Maki JL, Yuan J. 2013. Activity and specificity of necrostatin-1, small-molecule inhibitor of RIP1 kinase. Cell Death Differ, 20(2):366 DOI: 10.1038/CDD.2012.133.

Delaney JP, Paritzky AZ. 1969. Necrosis of a pheochromocytoma with shock. N Engl J Med, 280(25):1394–1395 DOI: 10.1056/NEJM196906192802508.

Devisscher L, Van Coillie S, Hofmans S, Van Rompaey D, Goossens K, Meul E, Maes L, De Winter H, Van Der Veken P, Vandenabeele P, Berghe T Vanden, Augustyns K. 2018. Discovery of Novel, Drug-Like Ferroptosis Inhibitors with in Vivo Efficacy. J Med Chem, 61(22):10126–10140 DOI: 10.1021/ACS.JMEDCHEM.8B01299/SUPPL_FILE/JM8B01299_SI_002.CSV.

Dick MS, Sborgi L, Rühl S, Hiller S, Broz P. 2016. ASC filament formation serves as a signal amplification mechanism for inflammasomes. Nat Commun, 7 DOI: 10.1038/NCOMMS11929.

Dillon CP, Oberst A, Weinlich R, Janke LJ, Kang TB, Ben-Moshe T, Mak TW, Wallach D, Green DR. 2012. Survival function of the FADD-CASPASE-8-cFLIP(L) complex. Cell Rep, 1(5):401–407 DOI: 10.1016/J.CELREP.2012.03.010.

Dillon CP, Weinlich R, Rodriguez DA, Cripps JG, Quarato G, Gurung P, Verbist KC, Brewer TL, Llambi F, Gong YN, Janke LJ, Kelliher MA, Kanneganti TD, Green DR. 2014. RIPK1 blocks early postnatal lethality mediated by caspase-8 and RIPK3. Cell, 157(5):1189–1202 DOI: 10.1016/J.CELL.2014.04.018.

Ding J, Wang K, Liu W, She Y, Sun Q, Shi J, Sun H, Wang DC, Shao F. 2016. Pore-forming activity and structural autoinhibition of the gasdermin family. Nature, 535(7610):111–116 DOI: 10.1038/NATURE18590.

Dixon SJ, Lemberg KM, Lamprecht MR, Skouta R, Zaitsev EM, Gleason CE, Patel DN, Bauer AJ, Cantley AM, Yang WS, Morrison B, Stockwell BR. 2012a. Ferroptosis: An Iron-Dependent Form of Nonapoptotic Cell Death. Cell, 149(5):1060–1072 DOI: 10.1016/J.CELL.2012.03.042.

Dixon SJ, Lemberg KM, Lamprecht MR, Skouta R, Zaitsev EM, Gleason CE, Patel DN, Bauer AJ, Cantley AM, Yang WS, Morrison B, Stockwell BR. 2012b. Ferroptosis: An Iron-Dependent Form of Nonapoptotic Cell Death. Cell, 149(5):1060–1072 DOI: 10.1016/J.CELL.2012.03.042.

Dixon SJ, Stockwell BR. 2014. The role of iron and reactive oxygen species in cell death. Nat Chem Biol, 10(1):9–17 DOI: 10.1038/nchembio.1416.

Dixon SJ, Winter GE, Musavi LS, Lee ED, Snijder B, Rebsamen M, Superti-Furga G, Stockwell BR. 2015. Human Haploid Cell Genetics Reveals Roles for Lipid Metabolism Genes in Nonapoptotic Cell Death. ACS Chem Biol, 10(7):1604–1609 DOI: 10.1021/ACSCHEMBIO.5B00245.

Doll S, Freitas FP, Shah R, Aldrovandi M, da Silva MC, Ingold I, Grocin AG, Xavier da Silva TN, Panzilius E, Scheel CH, Mourão A, Buday K, Sato M, Wanninger J, Vignane T, Mohana V, Rehberg M, Flatley A, Schepers A, Kurz A, White D, Sauer M, Sattler M, Tate EW, Schmitz W, Schulze A, O'Donnell V, Proneth B, Popowicz GM, Pratt DA, Angeli JPF, Conrad M. 2019. FSP1 is a glutathione-independent ferroptosis suppressor. Nat 2019 5757784, 575(7784):693–698 DOI: 10.1038/s41586-019-1707-0.

Doll S, Proneth B, Tyurina YY, Panzilius E, Kobayashi S, Ingold I, Irmler M, Beckers J, Aichler M, Walch A, Prokisch H, Trümbach D, Mao G, Qu F, Bayir H, Füllekrug J, Scheel CH, Wurst W, Schick JA, Kagan VE, Angeli JPF, Conrad M. 2017. ACSL4 dictates ferroptosis sensitivity by shaping cellular lipid composition. Nat Chem Biol 2016 131, 13(1):91–98 DOI: 10.1038/nchembio.2239.

Dolma S, Lessnick SL, Hahn WC, Stockwell BR. 2003. Identification of genotype-selective antitumor agents using synthetic lethal chemical screening in engineered human tumor cells. Cancer Cell, 3(3):285–296 DOI: 10.1016/S1535-6108(03)00050-3.

Dondelinger Y, Declercq W, Montessuit S, Roelandt R, Goncalves A, Bruggeman I, Hulpiau P, Weber K, Sehon CA, Marquis RW, Bertin J, Gough PJ, Savvides S, Martinou JC, Bertrand MJM, Vandenabeele P. 2014. MLKL compromises plasma membrane integrity by binding to phosphatidylinositol phosphates. Cell Rep, 7(4):971–981 DOI: 10.1016/J.CELREP.2014.04.026.

Dondelinger Y, Jouan-Lanhouet S, Divert T, Theatre E, Bertin J, Gough PJ, Giansanti P, Heck AJR, Dejardin E, Vandenabeele P, Bertrand MJM. 2015. NF-κB-Independent Role of IKKα/IKKβ in Preventing RIPK1 Kinase-Dependent Apoptotic and Necroptotic Cell Death during TNF Signaling. Mol Cell, 60(1):63–76 DOI: 10.1016/J.MOLCEL.2015.07.032.

Du B, Yu M, Zheng J. 2018. Transport and interactions of nanoparticles in the kidneys. Nat Rev Mater 2018 310, 3(10):358–374 DOI: 10.1038/s41578-018-0038-3.

Else T, Rodriguez-Galindo C. 2016. 5th International ACC Symposium: Hereditary Predisposition to Childhood ACC and the Associated Molecular Phenotype: 5th International ACC Symposium Session: Not Just for Kids! Horm Cancer, 7(1):36–39 DOI: 10.1007/S12672-015-0244-Z.

Fang X, Cai Z, Wang H, Han D, Cheng Q, Zhang P, Gao F, Yu Y, Song Z, Wu Q, An P, Huang S, Pan J, Chen HZ, Chen J, Linkermann A, Min J, Wang F. 2020. Loss of Cardiac Ferritin H Facilitates Cardiomyopathy via Slc7a11-Mediated Ferroptosis. Circ Res, 127(4):486–501 DOI: 10.1161/CIRCRESAHA.120.316509.

Fang X, Wang H, Han D, Xie E, Yang X, Wei J, Gu S, Gao F, Zhu N, Yin X, Cheng Q, Zhang P, Dai W, Chen J, Yang F, Yang H-T, Linkermann A, Gu W, Min J, Wang F. 2019. Ferroptosis as a target for protection against cardiomyopathy. Proc Natl Acad Sci, 116(7):2672–2680 DOI: 10.1073/PNAS.1821022116.

Fassnacht M, Allolio B. 2009. Clinical management of adrenocortical carcinoma. Best Pract Res Clin Endocrinol Metab, 23(2):273–289 DOI: 10.1016/J.BEEM.2008.10.008.

Fassnacht M, Dekkers OM, Else T, Baudin E, Berruti A, De Krijger RR, Haak HR, Mihai R, Assie G, Terzolo M. 2018. European Society of Endocrinology Clinical Practice Guidelines on the management of adrenocortical carcinoma in adults, in collaboration with the European Network for the Study of Adrenal Tumors. Eur J Endocrinol, 179(4):G1–G46 DOI: 10.1530/EJE-18-0608.

Fassnacht M, Johanssen S, Quinkler M, Bucsky P, Willenberg HS, Beuschlein F, Terzolo M, Mueller HH, Hahner S, Allolio B. 2009. Limited prognostic value of the 2004 International Union Against Cancer staging classification for adrenocortical carcinoma: proposal for a Revised TNM Classification. Cancer, 115(2):243–250 DOI: 10.1002/CNCR.24030.

Fassnacht M, Kroiss M, Allolio B. 2013. Update in adrenocortical carcinoma. J Clin Endocrinol Metab, 98(12):4551–4564 DOI: 10.1210/JC.2013-3020.

Fassnacht M, Libé R, Kroiss M, Allolio B. 2011. Adrenocortical carcinoma: a clinician's update. Nat Rev Endocrinol 2011 76, 7(6):323–335 DOI: 10.1038/nrendo.2010.235.

Feldkamp T, Park JS, Pasupulati R, Amora D, Roeser NF, Venkatachalam MA, Weinberg JM. 2009. Regulation of the mitochondrial permeability transition in kidney proximal tubules and

its alteration during hypoxia-reoxygenation. Am J Physiol Renal Physiol, 297(6) DOI: 10.1152/AJPRENAL.00422.2009.

Feoktistova M, Geserick P, Kellert B, Dimitrova DP, Langlais C, Hupe M, Cain K, MacFarlane M, Häcker G, Leverkus M. 2011. cIAPs block Ripoptosome formation, a RIP1/caspase-8 containing intracellular cell death complex differentially regulated by cFLIP isoforms. Mol Cell, 43(3):449–463 DOI: 10.1016/J.MOLCEL.2011.06.011.

Finco I, Lerario AM, Hammer GD. 2018. Sonic Hedgehog and WNT Signaling Promote Adrenal Gland Regeneration in Male Mice. Endocrinology, 159(2):579–596 DOI: 10.1210/EN.2017-03061.

Freedman BD, Kempna PB, Carlone DL, Shah MS, Guagliardo NA, Barrett PQ, Gomez-Sanchez CE, Majzoub JA, Breault DT. 2013. Adrenocortical zonation results from lineage conversion of differentiated zona glomerulosa cells. Dev Cell, 26(6):666 DOI: 10.1016/J.DEVCEL.2013.07.016.

Friedmann Angeli JP, Schneider M, Proneth B, Tyurina YY, Tyurin VA, Hammond VJ, Herbach N, Aichler M, Walch A, Eggenhofer E, Basavarajappa D, Rådmark O, Kobayashi S, Seibt T, Beck H, Neff F, Esposito I, Wanke R, Förster H, Yefremova O, Heinrichmeyer M, Bornkamm GW, Geissler EK, Thomas SB, Stockwell BR, O'Donnell VB, Kagan VE, Schick JA, Conrad M. 2014a. Inactivation of the ferroptosis regulator Gpx4 triggers acute renal failure in mice. Nat Cell Biol 2014 1612, 16(12):1180–1191 DOI: 10.1038/ncb3064.

Friedmann Angeli JP, Schneider M, Proneth B, Tyurina YY, Tyurin VA, Hammond VJ, Herbach N, Aichler M, Walch A, Eggenhofer E, Basavarajappa D, Rådmark O, Kobayashi S, Seibt T, Beck H, Neff F, Esposito I, Wanke R, Förster H, Yefremova O, Heinrichmeyer M, Bornkamm GW, Geissler EK, Thomas SB, Stockwell BR, O'Donnell VB, Kagan VE, Schick JA, Conrad M. 2014b. Inactivation of the ferroptosis regulator Gpx4 triggers acute renal failure in mice. Nat Cell Biol 2014 1612, 16(12):1180–1191 DOI: 10.1038/ncb3064.

Friedmann Angeli JP, Shah R, Pratt DA, Conrad M. 2017. Ferroptosis Inhibition: Mechanisms and Opportunities. Trends Pharmacol Sci, 38(5):489–498 DOI: 10.1016/J.TIPS.2017.02.005.

Fritsch M, Günther SD, Schwarzer R, Albert MC, Schorn F, Werthenbach JP, Schiffmann LM, Stair N, Stocks H, Seeger JM, Lamkanfi M, Krönke M, Pasparakis M, Kashkar H. 2019. Caspase-8 is the molecular switch for apoptosis, necroptosis and pyroptosis. Nature, 575(7784):683–687 DOI: 10.1038/S41586-019-1770-6.

Galluzzi L, Kepp O, Krautwald S, Kroemer G, Linkermann A. 2014. Molecular mechanisms of regulated necrosis. Semin Cell Dev Biol, 35:24–32 DOI: 10.1016/J.SEMCDB.2014.02.006.

Galluzzi L, Vitale I, Aaronson SA, Abrams JM, Adam D, Agostinis P, Alnemri ES, Altucci L, Amelio I, Andrews DW, Annicchiarico-Petruzzelli M, Antonov A V., Arama E, Baehrecke EH, Barlev NA, Bazan NG, Bernassola F, Bertrand MJM, Bianchi K, Blagosklonny M V., Blomgren K, Borner C, Boya P, Brenner C, Campanella M, Candi E, Carmona-Gutierrez D, Cecconi F, Chan FK-M, Chandel NS, Cheng EH, Chipuk JE, Cidlowski JA, Ciechanover A, Cohen GM, Conrad M, Cubillos-Ruiz JR, Czabotar PE, D'Angiolella V, Dawson TM, Dawson VL, De Laurenzi V, De Maria R, Debatin K-M, DeBerardinis RJ, Deshmukh M, Di Daniele N, Di Virgilio F, Dixit VM, Dixon SJ, Duckett CS, Dynlacht BD, El-Deiry WS, Elrod

JW, Fimia GM, Fulda S, García-Sáez AJ, Garg AD, Garrido C, Gavathiotis E, Golstein P, Gottlieb E, Green DR, Greene LA, Gronemeyer H, Gross A, Hajnoczky G, Hardwick JM, Harris IS, Hengartner MO, Hetz C, Ichijo H, Jäättelä M, Joseph B, Jost PJ, Juin PP, Kaiser WJ, Karin M, Kaufmann T, Kepp O, Kimchi A, Kitsis RN, Klionsky DJ, Knight RA, Kumar S, Lee SW, Lemasters JJ, Levine B, Linkermann A, Lipton SA, Lockshin RA, López-Otín C, Lowe SW, Luedde T, Lugli E, MacFarlane M, Madeo F, Malewicz M, Malorni W, Manic G, Marine J-C, Martin SJ, Martinou J-C, Medema JP, Mehlen P, Meier P, Melino S, Miao EA, Molkentin JD, Moll UM, Muñoz-Pinedo C, Nagata S, Nuñez G, Oberst A, Oren M, Overholtzer M, Pagano M, Panaretakis T, Pasparakis M, Penninger JM, Pereira DM, Pervaiz S, Peter ME, Piacentini M, Pinton P, Prehn JHM, Puthalakath H, Rabinovich GA, Rehm M, Rizzuto R, Rodrigues CMP, Rubinsztein DC, Rudel T, Ryan KM, Sayan E, Scorrano L, Shao F, Shi Y, Silke J, Simon H-U, Sistigu A, Stockwell BR, Strasser A, Szabadkai G, Tait SWG, Tang D, Tavernarakis N, Thorburn A, Tsujimoto Y, Turk B, Vanden Berghe T, Vandenabeele P, Vander Heiden MG, Villunger A, Virgin HW, Vousden KH, Vucic D, Wagner EF, Walczak H, Wallach D, Wang Y, Wells JA, Wood W, Yuan J, Zakeri Z, Zhivotovsky B, Zitvogel L, Melino G, Kroemer G. 2018. Molecular mechanisms of cell death: recommendations of the Nomenclature Committee on Cell Death 2018. Cell Death Differ 2018 253, 25(3):486–541 DOI: 10.1038/s41418-017-0012-4.

Gao M, Monian P, Quadri N, Ramasamy R, Jiang X. 2015. Glutaminolysis and Transferrin Regulate Ferroptosis. Mol Cell, 59(2):298–308 DOI: 10.1016/J.MOLCEL.2015.06.011.

Gaschler MM, Andia AA, Liu H, Csuka JM, Hurlocker B, Vaiana CA, Heindel DW, Zuckerman DS, Bos PH, Reznik E, Ye LF, Tyurina YY, Lin AJ, Shchepinov MS, Chan AY, Peguero-Pereira E, Fomich MA, Daniels JD, Bekish A V., Shmanai V V., Kagan VE, Mahal LK, Woerpel KA, Stockwell BR. 2018. FINO2 initiates ferroptosis through GPX4 inactivation and iron oxidation. Nat Chem Biol 2018 145, 14(5):507–515 DOI: 10.1038/s41589-018-0031-6.

Gazdar AF, Oie HK, Shackleton CH, Chen TR, Triche TJ, Myers CE, Chrousos GP, Brennan MF, Stein CA, La Rocca R V. 1990. Establishment and Characterization of a Human Adrenocortical Carcinoma Cell Line That Expresses Multiple Pathways of Steroid Biosynthesis. Cancer Res, 50(17).

Giampazolias E, Schulz O, Lim KHJ, Rogers NC, Chakravarty P, Srinivasan N, Gordon O, Cardoso A, Buck MD, Poirier EZ, Canton J, Zelenay S, Sammicheli S, Moncaut N, Varsani-Brown S, Rosewell I, Reis e Sousa C. 2021. Secreted gelsolin inhibits DNGR-1-dependent cross-presentation and cancer immunity. Cell, 184(15):4016-4031.e22 DOI: 10.1016/J.CELL.2021.05.021.

Giordano TJ, Kuick R, Else T, Gauger PG, Vinco M, Bauersfeld J, Sanders D, Thomas DG, Doherty G, Hammer G. 2009. Molecular Classification and Prognostication of Adrenocortical Tumors by Transcriptome Profiling. Clin Cancer Res, 15(2):668–676 DOI: 10.1158/1078-0432.CCR-08-1067.

Goel N, Workman JL, Lee TT, Innala L, Viau V. 2014. Sex Differences in the HPA Axis. Compr Physiol, 4(3):1121–1155 DOI: 10.1002/CPHY.C130054.

Gong YN, Guy C, Olauson H, Becker JU, Yang M, Fitzgerald P, Linkermann A, Green DR. 2017.

ESCRT-III Acts Downstream of MLKL to Regulate Necroptotic Cell Death and Its Consequences. Cell, 169(2):286-300.e16 DOI: 10.1016/J.CELL.2017.03.020.

Goodman HM. 2009. Adrenal Glands. In: Basic Medical Endocrinology. Academic Press, pp. 61–90 DOI: 10.1016/B978-0-12-373975-9.00004-5.

Grabek A, Dolfi B, Klein B, Jian-Motamedi F, Chaboissier MC, Schedl A. 2019. The Adult Adrenal Cortex Undergoes Rapid Tissue Renewal in a Sex-Specific Manner. Cell Stem Cell, 25(2):290-296.e2 DOI: 10.1016/J.STEM.2019.04.012.

Green DR. 2019. The Coming Decade of Cell Death Research: Five Riddles. Cell, 177(5):1094–1107 DOI: 10.1016/J.CELL.2019.04.024.

Haas TL, Emmerich CH, Gerlach B, Schmukle AC, Cordier SM, Rieser E, Feltham R, Vince J, Warnken U, Wenger T, Koschny R, Komander D, Silke J, Walczak H. 2009. Recruitment of the linear ubiquitin chain assembly complex stabilizes the TNF-R1 signaling complex and is required for TNF-mediated gene induction. Mol Cell, 36(5):831–844 DOI: 10.1016/J.MOLCEL.2009.10.013.

Hahner S, Ross RJ, Arlt W, Bancos I, Burger-Stritt S, Torpy DJ, Husebye ES, Quinkler M. 2021. Adrenal insufficiency. Nat Rev Dis Prim 2021 71, 7(1):1–24 DOI: 10.1038/s41572-021-00252-7.

Hao HX, Xie Y, Zhang Y, Zhang O, Oster E, Avello M, Lei H, Mickanin C, Liu D, Ruffner H, Mao X, Ma Q, Zamponi R, Bouwmeester T, Finan PM, Kirschner MW, Porter JA, Serluca FC, Cong F. 2012. ZNRF3 promotes Wnt receptor turnover in an R-spondin-sensitive manner. Nat 2012 4857397, 485(7397):195–200 DOI: 10.1038/nature11019.

Hayward CS, Kelly RP, Collins P. 2000. The roles of gender, the menopause and hormone replacement on cardiovascular function. Cardiovasc Res, 46(1):28–49 DOI: 10.1016/S0008-6363(00)00005-5.

Heger K, Wickliffe KE, Ndoja A, Zhang J, Murthy A, Dugger DL, Maltzman A, De Sousa E Melo F, Hung J, Zeng Y, Verschueren E, Kirkpatrick DS, Vucic D, Lee WP, Roose-Girma M, Newman RJ, Warming S, Hsiao YC, Komuves LG, Webster JD, Newton K, Dixit VM. 2018. OTULIN limits cell death and inflammation by deubiquitinating LUBAC. Nature, 559(7712):120–124 DOI: 10.1038/S41586-018-0256-2.

Herrmann LJM, Heinze B, Fassnacht M, Willenberg HS, Quinkler M, Reisch N, Zink M, Allolio B, Hahner S. 2012. TP53 germline mutations in adult patients with adrenocortical carcinoma. J Clin Endocrinol Metab, 97(3) DOI: 10.1210/JC.2011-1982.

Hescot S, Amazit L, Lhomme M, Travers S, DuBow A, Battini S, Boulate G, Namer I, Lombes A, Kontush A, Imperiale A, Baudin E, Lombes M. 2017. Identifying mitotane-induced mitochondria-associated membranes dysfunctions: metabolomic and lipidomic approaches. Oncotarget, 8(66):109924–109940 DOI: 10.18632/ONCOTARGET.18968.

Hofmans S, Berghe T Vanden, Devisscher L, Hassannia B, Lyssens S, Joossens J, Van Der Veken P, Vandenabeele P, Augustyns K. 2016. Novel Ferroptosis Inhibitors with Improved Potency and ADME Properties. J Med Chem, 59(5):2041–2053 DOI: 10.1021/ACS.JMEDCHEM.5B01641.

Hoste EAJ, Kellum JA, Selby NM, Zarbock A, Palevsky PM, Bagshaw SM, Goldstein SL, Cerdá J, Chawla LS. 2018. Global epidemiology and outcomes of acute kidney injury. Nat Rev Nephrol, 14(10):607–625 DOI: 10.1038/S41581-018-0052-0.

Hrdinka M, Fiil BK, Zucca M, Leske D, Bagola K, Yabal M, Elliott PR, Damgaard RB, Komander D, Jost PJ, Gyrd-Hansen M. 2016. CYLD Limits Lys63- and Met1-Linked Ubiquitin at Receptor Complexes to Regulate Innate Immune Signaling. Cell Rep, 14(12):2846–2858 DOI: 10.1016/J.CELREP.2016.02.062.

Hu Z, Zhang H, Yi B, Yang S, Liu J, Hu J, Wang J, Cao K, Zhang W. 2020. VDR activation attenuate cisplatin induced AKI by inhibiting ferroptosis. Cell Death Dis, 11(1) DOI: 10.1038/S41419-020-2256-Z.

Huang L li, Liao X hui, Sun H, Jiang X, Liu Q, Zhang L. 2019. Augmenter of liver regeneration protects the kidney from ischaemia-reperfusion injury in ferroptosis. J Cell Mol Med, 23(6):4153–4164 DOI: 10.1111/JCMM.14302.

Husebye ES, Pearce SH, Krone NP, Kämpe O. 2021. Adrenal insufficiency. Lancet (London, England), 397(10274):613–629 DOI: 10.1016/S0140-6736(21)00136-7.

Ikeda F, Deribe YL, Skånland SS, Stieglitz B, Grabbe C, Franz-Wachtel M, Van Wijk SJL, Goswami P, Nagy V, Terzic J, Tokunaga F, Androulidaki A, Nakagawa T, Pasparakis M, Iwai K, Sundberg JP, Schaefer L, Rittinger K, MacEk B, Dikic I. 2011. SHARPIN forms a linear ubiquitin ligase complex regulating NF-κB activity and apoptosis. Nature, 471(7340):637–641 DOI: 10.1038/NATURE09814.

Ikeda M, Swide T, Vayl A, Lahm T, Anderson S, Hutchens MP. 2015. Estrogen administered after cardiac arrest and cardiopulmonary resuscitation ameliorates acute kidney injury in a sex- and age-specific manner. Crit Care, 19(1) DOI: 10.1186/S13054-015-1049-8.

Ingold I, Berndt C, Schmitt S, Doll S, Poschmann G, Buday K, Roveri A, Peng X, Porto Freitas F, Seibt T, Mehr L, Aichler M, Walch A, Lamp D, Jastroch M, Miyamoto S, Wurst W, Ursini F, Arnér ESJ, Fradejas-Villar N, Schweizer U, Zischka H, Friedmann Angeli JP, Conrad M. 2018. Selenium Utilization by GPX4 Is Required to Prevent Hydroperoxide-Induced Ferroptosis. Cell, 172(3):409-422.e21 DOI: 10.1016/J.CELL.2017.11.048.

Jhala NC, Jhala D, Eloubeidi MA, Chhieng DC, Crowe DR, Roberson J, Eltoum I. 2004. Endoscopic ultrasound-guided fine-needle aspiration biopsy of the adrenal glands: analysis of 24 patients. Cancer, 102(5):308–314 DOI: 10.1002/CNCR.20498.

Jiang L, Kon N, Li T, Wang S-J, Su T, Hibshoosh H, Baer R, Gu W. 2015. Ferroptosis as a p53-mediated activity during tumour suppression. Nat 2015 5207545, 520(7545):57–62 DOI: 10.1038/nature14344.

Jiang X, Stockwell BR, Conrad M. 2021. Ferroptosis: mechanisms, biology and role in disease. Nat Rev Mol Cell Biol 2021 224, 22(4):266–282 DOI: 10.1038/s41580-020-00324-8.

Kaiser WJ, Upton JW, Long AB, Livingston-Rosanoff D, Daley-Bauer LP, Hakem R, Caspary T, Mocarski ES. 2011. RIP3 mediates the embryonic lethality of caspase-8-deficient mice. Nature, 471(7338):368–373 DOI: 10.1038/NATURE09857.

Kaiser WJ, Upton JW, Mocarski ES. 2008. Receptor-interacting protein homotypic interaction

motif-dependent control of NF-kappa B activation via the DNA-dependent activator of IFN regulatory factors. J Immunol, 181(9):6427–6434 DOI: 10.4049/JIMMUNOL.181.9.6427.

Kaiser WJ, Upton JW, Mocarski ES. 2013. Viral modulation of programmed necrosis. Curr Opin Virol, 3(3):296–306 DOI: 10.1016/J.COVIRO.2013.05.019.

Kanczkowski W, Tymoszuk P, Ehrhart-Bornstein M, Wirth MP, Zacharowski K, Bornstein SR. 2010. Abrogation of TLR4 and CD14 expression and signaling in human adrenocortical tumors. J Clin Endocrinol Metab, 95(12):421–429 DOI: 10.1210/jc.2010-1100.

Kang TB, Yang SH, Toth B, Kovalenko A, Wallach D. 2013. Caspase-8 blocks kinase RIPK3-mediated activation of the NLRP3 inflammasome. Immunity, 38(1):27–40 DOI: 10.1016/J.IMMUNI.2012.09.015.

Katikaneni A, Jelcic M, Gerlach GF, Ma Y, Overholtzer M, Niethammer P. 2020. Lipid peroxidation regulates long-range wound detection through 5-lipoxygenase in zebrafish. Nat Cell Biol, 22(9):1049–1055 DOI: 10.1038/S41556-020-0564-2.

Kayagaki N, Stowe IB, Lee BL, O'Rourke K, Anderson K, Warming S, Cuellar T, Haley B, Roose-Girma M, Phung QT, Liu PS, Lill JR, Li H, Wu J, Kummerfeld S, Zhang J, Lee WP, Snipas SJ, Salvesen GS, Morris LX, Fitzgerald L, Zhang Y, Bertram EM, Goodnow CC, Dixit VM. 2015. Caspase-11 cleaves gasdermin D for non-canonical inflammasome signalling. Nature, 526(7575):666–671 DOI: 10.1038/NATURE15541.

Kenny EM, Fidan E, Yang Q, Anthonymuthu TS, New LA, Meyer EA, Wang H, Kochanek PM, Dixon CE, Kagan VE, Bayir H. 2019. Ferroptosis Contributes to Neuronal Death and Functional Outcome after Traumatic Brain Injury∗. Crit Care Med, 47(3):410–418 DOI: 10.1097/CCM.0000000000003555.

Keusekotten K, Elliott PR, Glockner L, Fiil BK, Damgaard RB, Kulathu Y, Wauer T, Hospenthal MK, Gyrd-Hansen M, Krappmann D, Hofmann K, Komander D. 2013. OTULIN antagonizes LUBAC signaling by specifically hydrolyzing Met1-linked polyubiquitin. Cell, 153(6):1312 DOI: 10.1016/J.CELL.2013.05.014.

Kim J, Kil IS, Seok YM, Yang ES, Kim DK, Lim DG, Park J-W, Bonventre J V., Park KM. 2006. Orchiectomy Attenuates Post-ischemic Oxidative Stress and Ischemia/Reperfusion Injury in Mice: A ROLE FOR MANGANESE SUPEROXIDE DISMUTASE *. J Biol Chem, 281(29):20349–20356 DOI: 10.1074/JBC.M512740200.

Kim SE, Zhang L, Ma K, Riegman M, Chen F, Ingold I, Conrad M, Turker MZ, Gao M, Jiang X, Monette S, Pauliah M, Gonen M, Zanzonico P, Quinn T, Wiesner U, Bradbury MS, Overholtzer M. 2016. Ultrasmall nanoparticles induce ferroptosis in nutrient-deprived cancer cells and suppress tumour growth. Nat Nanotechnol, 11(11):977–985 DOI: 10.1038/NNANO.2016.164.

De Kloet ER, Sarabdjitsingh RA. 2008. Everything Has Rhythm: Focus on Glucocorticoid Pulsatility. Endocrinology, 149(7):3241–3243 DOI: 10.1210/EN.2008-0471.

Koch CA, Pacak K, Chrousos GP. 2002. The Molecular Pathogenesis of Hereditary and Sporadic Adrenocortical and Adrenomedullary Tumors. J Clin Endocrinol Metab, 87(12):5367–5384 DOI: 10.1210/JC.2002-021069.

Krammer PH, Arnold R, Lavrik IN. 2007. Life and death in peripheral T cells. Nat Rev Immunol, 7(7):532–542 DOI: 10.1038/NRI2115.

Lalaoui N, Boyden SE, Oda H, Wood GM, Stone DL, Chau D, Liu L, Stoffels M, Kratina T, Lawlor KE, Zaal KJM, Hoffmann PM, Etemadi N, Shield-Artin K, Biben C, Tsai WL, Blake MD, Kuehn HS, Yang D, Anderton H, Silke N, Wachsmuth L, Zheng L, Moura NS, Beck DB, Gutierrez-Cruz G, Ombrello AK, Pinto-Patarroyo GP, Kueh AJ, Herold MJ, Hall C, Wang H, Chae JJ, Dmitrieva NI, McKenzie M, Light A, Barham BK, Jones A, Romeo TM, Zhou Q, Aksentijevich I, Mullikin JC, Gross AJ, Shum AK, Hawkins ED, Masters SL, Lenardo MJ, Boehm M, Rosenzweig SD, Pasparakis M, Voss AK, Gadina M, Kastner DL, Silke J. 2020. Mutations that prevent caspase cleavage of RIPK1 cause autoinflammatory disease. Nature, 577(7788):103–108 DOI: 10.1038/S41586-019-1828-5.

Lam AK yin. 2017. Update on Adrenal Tumours in 2017 World Health Organization (WHO) of Endocrine Tumours. Endocr Pathol, 28(3):213–227 DOI: 10.1007/S12022-017-9484-5.

Land WG, Agostinis P, Gasser S, Garg AD, Linkermann A. 2016. Transplantation and Damage-Associated Molecular Patterns (DAMPs). Am J Transplant, 16(12):3338–3361 DOI: 10.1111/AJT.13963.

Lau A, Rahn JJ, Chappellaz M, Chung H, Benediktsson H, Bihan D, Mässenhausen A von, Linkermann A, Jenne CN, Robbins SM, Senger DL, Lewis IA, Chun J, Muruve DA. 2022. Dipeptidase-1 governs renal inflammation during ischemia reperfusion injury. Sci Adv, 8(5):142 DOI: 10.1126/SCIADV.ABM0142.

Lawlor KE, Khan N, Mildenhall A, Gerlic M, Croker BA, D'Cruz AA, Hall C, Kaur Spall S, Anderton H, Masters SL, Rashidi M, Wicks IP, Alexander WS, Mitsuuchi Y, Benetatos CA, Condon SM, Wong WWL, Silke J, Vaux DL, Vince JE. 2015. RIPK3 promotes cell death and NLRP3 inflammasome activation in the absence of MLKL. Nat Commun, 6 DOI: 10.1038/NCOMMS7282.

Lehmann TP, Wrzesiński T, Jagodziński PP. 2013. The effect of mitotane on viability, steroidogenesis and gene expression in NCI-H295R adrenocortical cells. Mol Med Rep, 7(3):893–900 DOI: 10.3892/MMR.2012.1244.

Li D, Li C, Li L, Chen S, Wang L, Li Q, Wang X, Lei X, Shen Z. 2016. Natural Product Kongensin A is a Non-Canonical HSP90 Inhibitor that Blocks RIP3-dependent Necroptosis. Cell Chem Biol, 23(2):257–266 DOI: 10.1016/J.CHEMBIOL.2015.08.018.

Li D, Xu T, Cao Y, Wang H, Li L, Chen S, Wang X, Shen Z. 2015. A cytosolic heat shock protein 90 and cochaperone CDC37 complex is required for RIP3 activation during necroptosis. Proc Natl Acad Sci U S A, 112(16):5017–5022 DOI: 10.1073/PNAS.1505244112.

Li JY, Yao YM, Tian YP. 2021. Ferroptosis: A Trigger of Proinflammatory State Progression to Immunogenicity in Necroinflammatory Disease. Front Immunol, 12 DOI: 10.3389/FIMMU.2021.701163.

Li Y, Qian L, Yuan J. 2017. Small molecule probes for cellular death machines. Curr Opin Chem Biol, 39:74–82 DOI: 10.1016/J.CBPA.2017.05.007.

Lifton RP, Dluhy RG, Powers M, Rich GM, Cook S, Ulick S, Lalouel JM. 1992. A chimaeric 11

beta-hydroxylase/aldosterone synthase gene causes glucocorticoid-remediable aldosteronism and human hypertension. Nature, 355(6357):262–265 DOI: 10.1038/355262A0.

Lightman SL, Conway-Campbell BL. 2010. The crucial role of pulsatile activity of the HPA axis for continuous dynamic equilibration. Nat Rev Neurosci 2010 1110, 11(10):710–718 DOI: 10.1038/nrn2914.

Lin CY, Ström A, Vega VB, Kong SL, Yeo AL, Thomsen JS, Chan WC, Doray B, Bangarusamy DK, Ramasamy A, Vergara LA, Tang S, Chong A, Bajic VB, Miller LD, Gustafsson JA, Liu ET. 2004. Discovery of estrogen receptor alpha target genes and response elements in breast tumor cells. Genome Biol, 5(9) DOI: 10.1186/GB-2004-5-9-R66.

Lin J, Kumari S, Kim C, Van T-M, Wachsmuth L, Polykratis A, Pasparakis M. 2016. RIPK1 counteracts ZBP1-mediated necroptosis to inhibit inflammation. Nature, 540(7631):124–128 DOI: 10.1038/nature20558.

Linkermann A. 2016. Nonapoptotic cell death in acute kidney injury and transplantation. Kidney Int, 89(1):46–57 DOI: 10.1016/J.KINT.2015.10.008.

Linkermann A, Green DR. 2014. Necroptosis. N Engl J Med, 370(5):455–465 DOI: 10.1056/NEJMra1310050.

Linkermann A, Heller JO, Prókai Á, Weinberg JM, Zen F De, Himmerkus N, Szabó AJ, Bräsen JH, Kunzendorf U, Krautwald S. 2013. The RIP1-kinase inhibitor Necrostatin-1 prevents osmotic nephrosis and contrast-induced AKI in mice. J Am Soc Nephrol, 24(10):1545–1557 DOI: 10.1681/ASN.2012121169/-/DCSUPPLEMENTAL.

Linkermann A, Skouta R, Himmerkus N, Mulay SR, Dewitz C, De Zen F, Prokai A, Zuchtriegel G, Krombach F, Welz PS, Weinlich R, Berghe T Vanden, Vandenabeele P, Pasparakis M, Bleich M, Weinberg JM, Reichel CA, Bräsen JH, Kunzendorf U, Anders HJ, Stockwell BR, Green DR, Krautwald S. 2014. Synchronized renal tubular cell death involves ferroptosis. Proc Natl Acad Sci U S A, 111(47):16836–16841 DOI: 10.1073/PNAS.1415518111.

Llabani E, Hicklin RW, Lee HY, Motika SE, Crawford LA, Weerapana E, Hergenrother PJ. 2019a. Diverse compounds from pleuromutilin lead to a thioredoxin inhibitor and inducer of ferroptosis. Nat Chem, 11(6):521 DOI: 10.1038/S41557-019-0261-6.

Llabani E, Hicklin RW, Lee HY, Motika SE, Crawford LA, Weerapana E, Hergenrother PJ. 2019b. Diverse compounds from pleuromutilin lead to a thioredoxin inhibitor and inducer of ferroptosis. Nat Chem, 11(6):521 DOI: 10.1038/S41557-019-0261-6.

Lloyd RV, Osamura RY, Kloppel G, Rosai J. 2017. WHO Classification of Tumours of Endocrine Organs 4th edition. Lioyd RV, Osamura RY, Kloppel G RJ (ed) IARC.

Lyraki R, Schedl A. 2021. Adrenal cortex renewal in health and disease. Nat Rev Endocrinol, 17(7):421–434 DOI: 10.1038/s41574-021-00491-4.

Man SM, Hopkins LJ, Nugent E, Cox S, Glück IM, Tourlomousis P, Wright JA, Cicuta P, Monie TP, Bryant CE. 2014. Inflammasome activation causes dual recruitment of NLRC4 and NLRP3 to the same macromolecular complex. Proc Natl Acad Sci U S A, 111(20):7403–7408 DOI: 10.1073/PNAS.1402911111.

Mandal P, Berger SB, Pillay S, Moriwaki K, Huang C, Guo H, Lich JD, Finger J, Kasparcova V, Votta B, Ouellette M, King BW, Wisnoski D, Lakdawala AS, DeMartino MP, Casillas LN, Haile PA, Sehon CA, Marquis RW, Upton J, Daley-Bauer LP, Roback L, Ramia N, Dovey CM, Carette JE, Chan FKM, Bertin J, Gough PJ, Mocarski ES, Kaiser WJ. 2014. RIP3 induces apoptosis independent of pronecrotic kinase activity. Mol Cell, 56(4):481–495 DOI: 10.1016/J.MOLCEL.2014.10.021.

Mandal P, Feng Y, Lyons JD, Berger SB, Otani S, DeLaney A, Tharp GK, Maner-Smith K, Burd EM, Schaeffer M, Hoffman S, Capriotti C, Roback L, Young CB, Liang Z, Ortlund EA, DiPaolo NC, Bosinger S, Bertin J, Gough PJ, Brodsky IE, Coopersmith CM, Shayakhmetov DM, Mocarski ES. 2018. Caspase-8 Collaborates with Caspase-11 to Drive Tissue Damage and Execution of Endotoxic Shock. Immunity, 49(1):42-55.e6 DOI: 10.1016/J.IMMUNI.2018.06.011.

Maremonti F, Meyer C, Linkermann A. 2022. Mechanisms and Models of Kidney Tubular Necrosis and Nephron Loss. J Am Soc Nephrol:ASN.2021101293 DOI: 10.1681/ASN.2021101293.

Martin-Sanchez D, Ruiz-Andres O, Poveda J, Carrasco S, Cannata-Ortiz P, Sanchez-Niño MD, Ortega MR, Egido J, Linkermann A, Ortiz A, Sanz AB. 2017a. Ferroptosis, but Not Necroptosis, Is Important in Nephrotoxic Folic Acid–Induced AKI. J Am Soc Nephrol, 28(1):218–229 DOI: 10.1681/ASN.2015121376.

Martin-Sanchez D, Ruiz-Andres O, Poveda J, Carrasco S, Cannata-Ortiz P, Sanchez-Niño MD, Ruiz Ortega M, Egido J, Linkermann A, Ortiz A, Sanz AB. 2017b. Ferroptosis, but Not Necroptosis, Is Important in Nephrotoxic Folic Acid-Induced AKI. J Am Soc Nephrol, 28(1):218–229 DOI: 10.1681/ASN.2015121376.

Martin-Sanchez D, Ruiz-Andres O, Poveda J, Carrasco S, Cannata-Ortiz P, Sanchez-Niño MD, Ruiz Ortega M, Egido J, Linkermann A, Ortiz A, Sanz AB. 2017c. Ferroptosis, but Not Necroptosis, Is Important in Nephrotoxic Folic Acid-Induced AKI. J Am Soc Nephrol, 28(1):218–229 DOI: 10.1681/ASN.2015121376.

von Mässenhausen A, Tonnus W, Himmerkus N, Parmentier S, Saleh D, Rodriguez D, Ousingsawat J, Ang RL, Weinberg JM, Sanz AB, Ortiz A, Zierleyn A, Becker JU, Baratte B, Desban N, Bach S, Schiessl IM, Nogusa S, Balachandran S, Anders HJ, Ting AT, Bleich M, Degterev A, Kunzelmann K, Bornstein SR, Green DR, Hugo C, Linkermann A. 2018. Phenytoin inhibits necroptosis. Cell Death Dis 2018 93, 9(3):1–15 DOI: 10.1038/s41419-018-0394-3.

von Mässenhausen A, Zamora Gonzalez N, Maremonti F, Belavgeni A, Tonnus W, Meyer C, Beer K, Hannani M, Lau A, Peitzsch M, Hoppenz P, Locke S, Chavakis T, Kramann R, Muruve D, Hugo C, Bornstein S, Linkermann A. 2022. Dexamethasone Sensitizes to Ferroptosis by Glucocorticoid Receptor-induced Dipeptidase-1 expression and Glutathione Depletion. Sci Adv, 8(5).

McAteer JP, Huaco JA, Gow KW. 2013. Predictors of survival in pediatric adrenocortical carcinoma: a Surveillance, Epidemiology, and End Results (SEER) program study. J Pediatr Surg, 48(5):1025–1031 DOI: 10.1016/J.JPEDSURG.2013.02.017.

Merke DP, Chrousos GP, Eisenhofer G, Weise M, Keil MF, Rogol AD, Van Wyk JJ, Bornstein SR. 2000. Adrenomedullary dysplasia and hypofunction in patients with classic 21-hydroxylase deficiency. N Engl J Med, 343(19):1362–1368 DOI: 10.1056/NEJM200011093431903.

Miao N, Yin F, Xie H, Wang Y, Xu Y, Shen Y, Xu D, Yin J, Wang B, Zhou Z, Cheng Q, Chen P, Xue H, Zhou L, Liu J, Wang X, Zhang W, Lu L. 2019. The cleavage of gasdermin D by caspase-11 promotes tubular epithelial cell pyroptosis and urinary IL-18 excretion in acute kidney injury. Kidney Int, 96(5):1105–1120 DOI: 10.1016/J.KINT.2019.04.035.

Mishima E, Sato E, Ito J, Yamada KI, Suzuki C, Oikawa Y, Matsuhashi T, Kikuchi K, Toyohara T, Suzuki T, Ito S, Nakagawa K, Abe T. 2020. Drugs Repurposed as Antiferroptosis Agents Suppress Organ Damage, Including AKI, by Functioning as Lipid Peroxyl Radical Scavengers. J Am Soc Nephrol, 31(2):280–296 DOI: 10.1681/ASN.2019060570.

Miura T, Muraoka S, Ogiso T. 1996. Inhibition of lipid peroxidation by estradiol and 2-hydroxyestradiol. Steroids, 61(6):379–383 DOI: 10.1016/0039-128X(96)00044-X.

Mocarski ES, Upton JW, Kaiser WJ. 2011. Viral infection and the evolution of caspase 8-regulated apoptotic and necrotic death pathways. Nat Rev Immunol, 12(2):79–88 DOI: 10.1038/NRI3131.

Moquin DM, McQuade T, Chan FKM. 2013. CYLD deubiquitinates RIP1 in the TNFα-induced necrosome to facilitate kinase activation and programmed necrosis. PLoS One, 8(10) DOI: 10.1371/JOURNAL.PONE.0076841.

Muendlein HI, Jetton D, Connolly WM, Eidell KP, Magri Z, Smirnova I, Poltorak A. 2020. cFLIPL protects macrophages from LPS-induced pyroptosis via inhibition of complex II formation. Science, 367(6484):1379 DOI: 10.1126/SCIENCE.AAY3878.

Müller V, Szabó A, Viklicky O, Gaul I, Pörtl S, Philipp T, Heemann UW. 1999a. Sex hormones and gender-related differences: their influence on chronic renal allograft rejection. Kidney Int, 55(5):2011–2020 DOI: 10.1046/J.1523-1755.1999.00441.X.

Müller V, Szabó A, Viklicky O, Gaul I, Pörtl S, Philipp T, Heemann UW. 1999b. Sex hormones and gender-related differences: Their influence on chronic renal allograft rejection. Kidney Int, 55(5):2011–2020 DOI: 10.1046/J.1523-1755.1999.00441.X.

Murphy JM, Czabotar PE, Hildebrand JM, Lucet IS, Zhang JG, Alvarez-Diaz S, Lewis R, Lalaoui N, Metcalf D, Webb AI, Young SN, Varghese LN, Tannahill GM, Hatchell EC, Majewski IJ, Okamoto T, Dobson RCJ, Hilton DJ, Babon JJ, Nicola NA, Strasser A, Silke J, Alexander WS. 2013. The pseudokinase MLKL mediates necroptosis via a molecular switch mechanism. Immunity, 39(3):443–453 DOI: 10.1016/J.IMMUNI.2013.06.018.

Murphy JM, Lucet IS, Hildebrand JM, Tanzer MC, Young SN, Sharma P, Lessene G, Alexander WS, Babon JJ, Silke J, Czabotar PE. 2014. Insights into the evolution of divergent nucleotide-binding mechanisms among pseudokinases revealed by crystal structures of human and mouse MLKL. Biochem J, 457(3):369–377 DOI: 10.1042/BJ20131270.

Nagata S. 1996. Fas-mediated apoptosis. Adv Exp Med Biol, 406:119–124 DOI: 10.1007/978-1-4899-0274-0_12.

Newton K, Wickliffe KE, Dugger DL, Maltzman A, Roose-Girma M, Dohse M, Kőműves L, Webster JD, Dixit VM. 2019a. Cleavage of RIPK1 by caspase-8 is crucial for limiting apoptosis and necroptosis. Nature, 574(7778):428–431 DOI: 10.1038/S41586-019-1548-X.

Newton K, Wickliffe KE, Maltzman A, Dugger DL, Reja R, Zhang Y, Roose-Girma M, Modrusan Z, Sagolla MS, Webster JD, Dixit VM. 2019b. Activity of caspase-8 determines plasticity between cell death pathways. Nature, 575(7784):679–682 DOI: 10.1038/S41586-019-1752-8.

Ng L, Libertino JM. 2003. Adrenocortical carcinoma: Diagnosis, evaluation and treatment. J Urol, 169(1):5–11 DOI: 10.1016/S0022-5347(05)64023-2.

Nyman D, Wahlberg P. 1970. Necrotic phaeochromocytoma with gastric haemorrhage, shock, and uncommonly high catecholamine excretion. Acta Med Scand, 187(5):381–383 DOI: 10.1111/J.0954-6820.1970.TB02959.X.

Oberst A, Dillon CP, Weinlich R, McCormick LL, Fitzgerald P, Pop C, Hakem R, Salvesen GS, Green DR. 2011. Catalytic activity of the caspase-8-FLIP(L) complex inhibits RIPK3-dependent necrosis. Nature, 471(7338):363–368 DOI: 10.1038/NATURE09852.

Onizawa M, Oshima S, Schulze-Topphoff U, Oses-Prieto JA, Lu T, Tavares R, Prodhomme T, Duong B, Whang MI, Advincula R, Agelidis A, Barrera J, Wu H, Burlingame A, Malynn BA, Zamvil SS, Ma A. 2015. The ubiquitin-modifying enzyme A20 restricts ubiquitination of the kinase RIPK3 and protects cells from necroptosis. Nat Immunol, 16(6):618–627 DOI: 10.1038/NI.3172.

Orning P, Weng D, Starheim K, Ratner D, Best Z, Lee B, Brooks A, Xia S, Wu H, Kelliher MA, Berger SB, Gough PJ, Bertin J, Proulx MM, Goguen JD, Kayagaki N, Fitzgerald KA, Lien E. 2018. Pathogen blockade of TAK1 triggers caspase-8-dependent cleavage of gasdermin D and cell death. Science, 362(6418):1064–1069 DOI: 10.1126/SCIENCE.AAU2818.

Ousingsawat J, Cabrita I, Wanitchakool P, Sirianant L, Krautwald S, Linkermann A, Schreiber R, Kunzelmann K. 2016. Ca2+ signals, cell membrane disintegration, and activation of TMEM16F during necroptosis. Cell Mol Life Sci 2016 741, 74(1):173–181 DOI: 10.1007/S00018-016-2338-3.

Paragliola RM, Corsello A, Locantore P, Papi G, Pontecorvi A, Corsello SM. 2020. Medical Approaches in Adrenocortical Carcinoma. Biomedicines, 8(12):1–18 DOI: 10.3390/BIOMEDICINES8120551.

Paragliola RM, Torino F, Papi G, Locantore P, Pontecorvi A, Corsello SM. 2018. Role of Mitotane in Adrenocortical Carcinoma – Review and State of the art. Eur Endocrinol, 14(2):62 DOI: 10.17925/EE.2018.14.2.62.

Park KM, Kim JI, Ahn Y, Bonventre AJ, Bonventre J V. 2004. Testosterone is responsible for enhanced susceptibility of males to ischemic renal injury. J Biol Chem, 279(50):52282–52292 DOI: 10.1074/JBC.M407629200.

Pascoe L, Curnow KM, Slutsker L, Connell JMC, Speiser PW, New MI, White PC. 1992. Glucocorticoid-suppressible hyperaldosteronism results from hybrid genes created by unequal crossovers between CYP11B1 and CYP11B2. Proc Natl Acad Sci U S A,

89(17):8327–8331 DOI: 10.1073/PNAS.89.17.8327.

Peltzer N, Darding M, Montinaro A, Draber P, Draberova H, Kupka S, Rieser E, Fisher A, Hutchinson C, Taraborrelli L, Hartwig T, Lafont E, Haas TL, Shimizu Y, Böiers C, Sarr A, Rickard J, Alvarez-Diaz S, Ashworth MT, Beal A, Enver T, Bertin J, Kaiser W, Strasser A, Silke J, Bouillet P, Walczak H. 2018. LUBAC is essential for embryogenesis by preventing cell death and enabling haematopoiesis. Nature, 557(7703):112–117 DOI: 10.1038/S41586-018-0064-8.

Peng Y, Fang Z, Liu M, Wang Z, Li L, Ming S, Lu C, Dong H, Zhang W, Wang Q, Shen R, Xie F, Zhang W, Yang C, Gao X, Sun Y. 2019. Testosterone induces renal tubular epithelial cell death through the HIF-1α/BNIP3 pathway. J Transl Med, 17(1) DOI: 10.1186/S12967-019-1821-7.

Pereira SS, Monteiro MP, Antonini SR, Pignatelli D. 2019. Apoptosis regulation in adrenocortical carcinoma. Endocr Connect, 8(5):R91 DOI: 10.1530/EC-19-0114.

Peter Guengerich F. 2019. Cytochrome P450 research and The Journal of Biological Chemistry. J Biol Chem, 294(5):1671 DOI: 10.1074/JBC.TM118.004144.

Philip NH, Dillon CP, Snyder AG, Fitzgerald P, Wynosky-Dolfi MA, Zwack EE, Hu B, Fitzgerald L, Mauldin EA, Copenhaver AM, Shin S, Wei L, Parker M, Zhang J, Oberst A, Green DR, Brodsky IE. 2014. Caspase-8 mediates caspase-1 processing and innate immune defense in response to bacterial blockade of NF-κB and MAPK signaling. Proc Natl Acad Sci U S A, 111(20):7385–7390 DOI: 10.1073/PNAS.1403252111.

Rainey W, Saner K, Schimmer B. 2004. Adrenocortical cell lines. Mol Cell Endocrinol, 228(1–2):23–38 DOI: 10.1016/J.MCE.2003.12.020.

Ranjit S, Henriksen K, Dvornikov A, Delsante M, Rosenberg A, Levi M, Gratton E. 2020. Phasor approach to autofluorescence lifetime imaging FLIM can be a quantitative biomarker of chronic renal parenchymal injury. Kidney Int, 98(5):1341–1346 DOI: 10.1016/J.KINT.2020.02.019.

Raymond VM, Else T, Everett JN, Long JM, Gruber SB, Hammer GD. 2013. Prevalence of germline TP53 mutations in a prospective series of unselected patients with adrenocortical carcinoma. J Clin Endocrinol Metab, 98(1) DOI: 10.1210/JC.2012-2198.

Rebsamen M, Heinz LX, Meylan E, Michallet MC, Schroder K, Hofmann K, Vazquez J, Benedict CA, Tschopp J. 2009. DAI/ZBP1 recruits RIP1 and RIP3 through RIP homotypic interaction motifs to activate NF-κB. EMBO Rep, 10(8):916 DOI: 10.1038/EMBOR.2009.109.

Reibetanz J, Jurowich C, Erdogan I, Nies C, Rayes N, Dralle H, Behrend M, Allolio B, Fassnacht M. 2012. Impact of lymphadenectomy on the oncologic outcome of patients with adrenocortical carcinoma. Ann Surg, 255(2):363–369 DOI: 10.1097/SLA.0B013E3182367AC3.

Reimer K., Jennings R. 1971. Alterations in renal cortex following ischemic injury. I. PAH uptake by slices of cortex after ischemia or autolysis - PubMed. Lab Investig a J Tech methods Pathol, 25(2):176–184 [accessed: 02/02/2022] URL: https://pubmed.ncbi.nlm.nih.gov/5559308/.

Reppert SM, Weaver DR. 2002. Coordination of circadian timing in mammals. Nat 2002 4186901, 418(6901):935–941 DOI: 10.1038/nature00965.

Riegman M, Bradbury MS, Overholtzer M. 2019. Population Dynamics in Cell Death: Mechanisms of Propagation. Trends in cancer, 5(9):558 DOI: 10.1016/J.TRECAN.2019.07.008.

Riegman M, Sagie L, Galed C, Levin T, Steinberg N, Dixon SJ, Wiesner U, Bradbury MS, Niethammer P, Zaritsky A, Overholtzer M. 2020a. Ferroptosis occurs through an osmotic mechanism and propagates independently of cell rupture. Nat Cell Biol, 22(9):1042–1048 DOI: 10.1038/S41556-020-0565-1.

Riegman M, Sagie L, Galed C, Levin T, Steinberg N, Dixon SJ, Wiesner U, Bradbury MS, Niethammer P, Zaritsky A, Overholtzer M. 2020b. Ferroptosis occurs through an osmotic mechanism and propagates independently of cell rupture. Nat Cell Biol 2020 229, 22(9):1042–1048 DOI: 10.1038/s41556-020-0565-1.

Rodriguez DA, Weinlich R, Brown S, Guy C, Fitzgerald P, Dillon CP, Oberst A, Quarato G, Low J, Cripps JG, Chen T, Green DR. 2016. Characterization of RIPK3-mediated phosphorylation of the activation loop of MLKL during necroptosis. Cell Death Differ, 23(1):76–88 DOI: 10.1038/CDD.2015.70.

Rogers C, Erkes DA, Nardone A, Aplin AE, Fernandes-Alnemri T, Alnemri ES. 2019. Gasdermin pores permeabilize mitochondria to augment caspase-3 activation during apoptosis and inflammasome activation. Nat Commun, 10(1) DOI: 10.1038/S41467-019-09397-2.

Romagnani P, Remuzzi G, Glassock R, Levin A, Jager KJ, Tonelli M, Massy Z, Wanner C, Anders HJ. 2017. Chronic kidney disease. Nat Rev Dis Prim, 3 DOI: 10.1038/NRDP.2017.88.

Ruan J, Xia S, Liu X, Lieberman J, Wu H. 2018. Cryo-EM structure of the gasdermin A3 membrane pore. Nature, 557(7703):62–67 DOI: 10.1038/S41586-018-0058-6.

Rühl S, Shkarina K, Demarco B, Heilig R, Santos JC, Broz P. 2018. ESCRT-dependent membrane repair negatively regulates pyroptosis downstream of GSDMD activation. Science, 362(6417):956–960 DOI: 10.1126/SCIENCE.AAR7607.

Ruiz-Ortega M, Rayego-Mateos S, Lamas S, Ortiz A, Rodrigues-Diez RR. 2020. Targeting the progression of chronic kidney disease. Nat Rev Nephrol, 16(5):269–288 DOI: 10.1038/S41581-019-0248-Y.

Russell G, Lightman S. 2019. The human stress response. Nat Rev Endocrinol 2019 159, 15(9):525–534 DOI: 10.1038/s41574-019-0228-0.

Sarabdjitsingh RA, Isenia S, Polman A, Mijalkovic J, Lachize S, Datson N, De Kloet ER, Meijer OC. 2010. Disrupted Corticosterone Pulsatile Patterns Attenuate Responsiveness to Glucocorticoid Signaling in Rat Brain. Endocrinology, 151(3):1177–1186 DOI: 10.1210/EN.2009-1119.

Sarhan J, Liu BC, Muendlein HI, Li P, Nilson R, Tang AY, Rongvaux A, Bunnell SC, Shao F, Green DR, Poltorak A. 2018a. Caspase-8 induces cleavage of gasdermin D to elicit pyroptosis during Yersinia infection. Proc Natl Acad Sci U S A, 115(46):E10888–E10897 DOI: 10.1073/PNAS.1809548115/-/DCSUPPLEMENTAL.

Sarhan M, Land WG, Tonnus W, Hugo CP, Linkermann A. 2018b. Origin and Consequences of Necroinflammation. Physiol Rev, 98(2):727–780 DOI: 10.1152/physrev.00041.2016.

Sbiera S, Leich E, Liebisch G, Sbiera I, Schirbel A, Wiemer L, Matysik S, Eckhardt C, Gardill F, Gehl A, Kendl S, Weigand I, Bala M, Ronchi CL, Deutschbein T, Schmitz G, Rosenwald A, Allolio B, Fassnacht M, Kroiss M. 2015. Mitotane inhibits sterol-o-Acyl transferase 1 triggering lipid-mediated endoplasmic reticulum stress and apoptosis in adrenocortical carcinoma cells. Endocrinology, 156(11):3895–3908 DOI: 10.1210/en.2015-1367.

Scholz H, Boivin FJ, Schmidt-Ott KM, Bachmann S, Eckardt KU, Scholl UI, Persson PB. 2021. Kidney physiology and susceptibility to acute kidney injury: implications for renoprotection. Nat Rev Nephrol 2021 175, 17(5):335–349 DOI: 10.1038/s41581-021-00394-7.

Schteingart D, Doherty G, Gauger P, Giordano T, Hammer G, Korobkin M, Worden F. 2005. Management of patients with adrenal cancer: recommendations of an international consensus conference. Endocr Relat Cancer, 12(3):667–680 DOI: 10.1677/ERC.1.01029.

Scindia Y, Dey P, Thirunagari A, Liping H, Rosin DL, Floris M, Okusa MD, Swaminathan S. 2015. Hepcidin Mitigates Renal Ischemia-Reperfusion Injury by Modulating Systemic Iron Homeostasis. J Am Soc Nephrol, 26(11):2800–2814 DOI: 10.1681/ASN.2014101037.

Scriba LD, Bornstein SR, Santambrogio A, Mueller G, Huebner A, Hauer J, Schedl A, Wielockx B, Eisenhofer G, Andoniadou CL, Steenblock C. 2020. Cancer Stem Cells in Pheochromocytoma and Paraganglioma. Front Endocrinol (Lausanne), 11:79 DOI: 10.3389/FENDO.2020.00079.

Shi J, Zhao Y, Wang K, Shi X, Wang Y, Huang H, Zhuang Y, Cai T, Wang F, Shao F. 2015. Cleavage of GSDMD by inflammatory caspases determines pyroptotic cell death. Nature, 526(7575):660–665 DOI: 10.1038/NATURE15514.

Shimada K, Skouta R, Kaplan A, Yang WS, Hayano M, Dixon SJ, Brown LM, Valenzuela CA, Wolpaw AJ, Stockwell BR. 2016. Global survey of cell death mechanisms reveals metabolic regulation of ferroptosis. Nat Chem Biol 2016 127, 12(7):497–503 DOI: 10.1038/nchembio.2079.

Short IA, Padfield PL. 1976. Malignant phaeochromocytoma with severe constipation and myocardial necrosis. Br Med J, 2(6039):793–794 DOI: 10.1136/BMJ.2.6039.793-A.

Sies H, Belousov V V., Chandel NS, Davies MJ, Jones DP, Mann GE, Murphy MP, Yamamoto M, Winterbourn C. 2022. Defining roles of specific reactive oxygen species (ROS) in cell biology and physiology. Nat Rev Mol Cell Biol 2022:1–17 DOI: 10.1038/s41580-022-00456-z.

Sies H, Jones DP. 2020. Reactive oxygen species (ROS) as pleiotropic physiological signalling agents. Nat Rev Mol Cell Biol 2020 217, 21(7):363–383 DOI: 10.1038/s41580-020-0230-3.

Silva Barbosa AC, Zhou D, Xie Y, Choi YJ, Tung HC, Chen X, Xu M, Gibbs RB, Poloyac SM, Liu S, Yu Y, Luo J, Liu Y, Xie W. 2020. Inhibition of Estrogen Sulfotransferase (SULT1E1/EST) Ameliorates Ischemic Acute Kidney Injury in Mice. J Am Soc Nephrol, 31(7):1496–1508 DOI: 10.1681/ASN.2019080767.

Singh AP, Singh N, Bedi PMS. 2017. Estradiol mitigates ischemia reperfusion-induced acute renal

failure through NMDA receptor antagonism in rats. Mol Cell Biochem 2017 4341, 434(1):33–40 DOI: 10.1007/S11010-017-3034-9.

Skouta R, Dixon S, Wang J, Dunn D, Orman M, Shimada K, Rosenberg P, Lo D, Weinberg J, Linkermann A, Stockwell B. 2014. Ferrostatins inhibit oxidative lipid damage and cell death in diverse disease models. J Am Chem Soc, 136(12):4551–4556 DOI: 10.1021/JA411006A.

Sogabe K, Roeser NF, Venkatachalam MA, Weinberg JM. 1996. Differential cytoprotection by glycine against oxidant damage to proximal tubule cells. Kidney Int, 50(3):845–854 DOI: 10.1038/KI.1996.384.

Souers AJ, Leverson JD, Boghaert ER, Ackler SL, Catron ND, Chen J, Dayton BD, Ding H, Enschede SH, Fairbrother WJ, Huang DCS, Hymowitz SG, Jin S, Khaw SL, Kovar PJ, Lam LT, Lee J, Maecker HL, Marsh KC, Mason KD, Mitten MJ, Nimmer PM, Oleksijew A, Park CH, Park CM, Phillips DC, Roberts AW, Sampath D, Seymour JF, Smith ML, Sullivan GM, Tahir SK, Tse C, Wendt MD, Xiao Y, Xue JC, Zhang H, Humerickhouse RA, Rosenberg SH, Elmore SW. 2013. ABT-199, a potent and selective BCL-2 inhibitor, achieves antitumor activity while sparing platelets. Nat Med, 19(2):202–208 DOI: 10.1038/NM.3048.

Squadrito F, Altavilla D, Squadrito G, Campo GM, Arlotta M, Arcoraci V, Minutoli L, Serrano' M, Saitta A, Caputi AP. 1997. 17β-oestradiol reduces cardiac leukocyte accumulation in myocardial ischaemia reperfusion injury in rat. Eur J Pharmacol, 335(2–3):185–192 DOI: 10.1016/S0014-2999(97)01201-6.

Stockwell BR, Friedmann Angeli JP, Bayir H, Bush AI, Conrad M, Dixon SJ, Fulda S, Gascón S, Hatzios SK, Kagan VE, Noel K, Jiang X, Linkermann A, Murphy ME, Overholtzer M, Oyagi A, Pagnussat GC, Park J, Ran Q, Rosenfeld CS, Salnikow K, Tang D, Torti FM, Torti S V., Toyokuni S, Woerpel KA, Zhang DD. 2017a. Ferroptosis: A Regulated Cell Death Nexus Linking Metabolism, Redox Biology, and Disease. Cell, 171(2):273–285 DOI: 10.1016/J.CELL.2017.09.021.

Stockwell BR, Friedmann Angeli JP, Bayir H, Bush AI, Conrad M, Dixon SJ, Fulda S, Gascón S, Hatzios SK, Kagan VE, Noel K, Jiang X, Linkermann A, Murphy ME, Overholtzer M, Oyagi A, Pagnussat GC, Park J, Ran Q, Rosenfeld CS, Salnikow K, Tang D, Torti FM, Torti S V., Toyokuni S, Woerpel KA, Zhang DD. 2017b. Ferroptosis: A Regulated Cell Death Nexus Linking Metabolism, Redox Biology, and Disease. Cell, 171(2):273–285 DOI: 10.1016/j.cell.2017.09.021.

Su L, Jiang X, Yang C, Zhang J, Chen B, Li Y, Yao S, Xie Q, Gomez H, Murugan R, Peng Z. 2019. Pannexin 1 mediates ferroptosis that contributes to renal ischemia/reperfusion injury. J Biol Chem, 294(50):19395–19404 DOI: 10.1074/JBC.RA119.010949.

Sun L, Wang H, Wang Z, He S, Chen S, Liao D, Wang L, Yan J, Liu W, Lei X, Wang X. 2012. Mixed lineage kinase domain-like protein mediates necrosis signaling downstream of RIP3 kinase. Cell, 148(1–2):213–227 DOI: 10.1016/J.CELL.2011.11.031.

Taabazuing CY, Okondo MC, Bachovchin DA. 2017. Pyroptosis and Apoptosis Pathways Engage in Bidirectional Crosstalk in Monocytes and Macrophages. Cell Chem Biol, 24(4):507-514.e4 DOI: 10.1016/J.CHEMBIOL.2017.03.009.

Tait S, Oberst A, Quarato G, Milasta S, Haller M, Wang R, Karvela M, Ichim G, Yatim N, Albert

M, Kidd G, Wakefield R, Frase S, Krautwald S, Linkermann A, Green D. 2013. Widespread mitochondrial depletion via mitophagy does not compromise necroptosis. Cell Rep, 5(4):878–885 DOI: 10.1016/J.CELREP.2013.10.034.

Takahashi N, Duprez L, Grootjans S, Cauwels A, Nerinckx W, DuHadaway JB, Goossens V, Roelandt R, Van Hauwermeiren F, Libert C, Declercq W, Callewaert N, Prendergast GC, Degterev A, Yuan J, Vandenabeele P. 2012. Necrostatin-1 analogues: critical issues on the specificity, activity and in vivo use in experimental disease models. Cell Death Dis 2012 311, 3(11):e437–e437 DOI: 10.1038/cddis.2012.176.

Tan ME, Li J, Xu HE, Melcher K, Yong EL. 2014. Androgen receptor: structure, role in prostate cancer and drug discovery. Acta Pharmacol Sin 2015 361, 36(1):3–23 DOI: 10.1038/aps.2014.18.

Tanaka R, Yazawa M, Morikawa Y, Tsutsui H, Ohkita M, Yukimura T, Matsumura Y. 2017. Sex differences in ischaemia/reperfusion-induced acute kidney injury depends on the degradation of noradrenaline by monoamine oxidase. Clin Exp Pharmacol Physiol, 44(3):371–377 DOI: 10.1111/1440-1681.12713.

Tang C, Cai J, Yin XM, Weinberg JM, Venkatachalam MA, Dong Z. 2021. Mitochondrial quality control in kidney injury and repair. Nat Rev Nephrol, 17(5):299–318 DOI: 10.1038/S41581-020-00369-0.

Tang D, Kepp O, Kroemer G. 2020. Ferroptosis becomes immunogenic: implications for anticancer treatments. Oncoimmunology, 10(1) DOI: 10.1080/2162402X.2020.1862949.

Taylor AM, Shih J, Ha G, Gao GF, Zhang X, Berger AC, Schumacher SE, Wang C, Hu H, Liu J, Lazar AJ, Caesar-Johnson SJ, Demchok JA, Felau I, Kasapi M, Ferguson ML, Hutter CM, Sofia HJ, Tarnuzzer R, Wang Z, Yang L, Zenklusen JC, Zhang J (Julia), Chudamani S, Liu J, Lolla L, Naresh R, Pihl T, Sun Q, Wan Y, Wu Y, Cho J, DeFreitas T, Frazer S, Gehlenborg N, Getz G, Heiman DI, Kim J, Lawrence MS, Lin P, Meier S, Noble MS, Saksena G, Voet D, Zhang H, Bernard B, Chambwe N, Dhankani V, Knijnenburg T, Kramer R, Leinonen K, Liu Y, Miller M, Reynolds S, Shmulevich I, Thorsson V, Zhang W, Akbani R, Broom BM, Hegde AM, Ju Z, Kanchi RS, Korkut A, Li J, Liang H, Ling S, Liu W, Lu Y, Mills GB, Ng KS, Rao A, Ryan M, Wang J, Weinstein JN, Zhang J, Abeshouse A, Armenia J, Chakravarty D, Chatila WK, de Bruijn I, Gao J, Gross BE, Heins ZJ, Kundra R, La K, Ladanyi M, Luna A, Nissan MG, Ochoa A, Phillips SM, Reznik E, Sanchez-Vega F, Sander C, Schultz N, Sheridan R, Sumer SO, Sun Y, Taylor BS, Wang J, Zhang H, Anur P, Peto M, Spellman P, Benz C, Stuart JM, Wong CK, Yau C, Hayes DN, Parker JS, Wilkerson MD, Ally A, Balasundaram M, Bowlby R, Brooks D, Carlsen R, Chuah E, Dhalla N, Holt R, Jones SJM, Kasaian K, Lee D, Ma Y, Marra MA, Mayo M, Moore RA, Mungall AJ, Mungall K, Robertson AG, Sadeghi S, Schein JE, Sipahimalani P, Tam A, Thiessen N, Tse K, Wong T, Berger AC, Beroukhim R, Cherniack AD, Cibulskis C, Gabriel SB, Ha G, Meyerson M, Schumacher SE, Shih J, Kucherlapati MH, Kucherlapati RS, Baylin S, Cope L, Danilova L, Bootwalla MS, Lai PH, Maglinte DT, Van Den Berg DJ, Weisenberger DJ, Auman JT, Balu S, Bodenheimer T, Fan C, Hoadley KA, Hoyle AP, Jefferys SR, Jones CD, Meng S, Mieczkowski PA, Mose LE, Perou AH, Perou CM, Roach J, Shi Y, Simons J V., Skelly T, Soloway MG, Tan D, Veluvolu U, Fan H, Hinoue T, Laird PW, Shen H, Zhou W, Bellair M, Chang K, Covington K, Creighton CJ, Dinh H, Doddapaneni HV, Donehower LA,

Drummond J, Gibbs RA, Glenn R, Hale W, Han Y, Hu J, Korchina V, Lee S, Lewis L, Li W, Liu X, Morgan M, Morton D, Muzny D, Santibanez J, Sheth M, Shinbrot E, Wang L, Wang M, Wheeler DA, Xi L, Zhao F, Hess J, Appelbaum EL, Bailey M, Cordes MG, Ding L, Fronick CC, Fulton LA, Fulton RS, Kandoth C, Mardis ER, McLellan MD, Miller CA, Schmidt HK, Wilson RK, Crain D, Curley E, Gardner J, Lau K, Mallery D, Morris S, Paulauskis J, Penny R, Shelton C, Shelton T, Sherman M, Thompson E, Yena P, Bowen J, Gastier-Foster JM, Gerken M, Leraas KM, Lichtenberg TM, Ramirez NC, Wise L, Zmuda E, Corcoran N, Costello T, Hovens C, Carvalho AL, de Carvalho AC, Fregnani JH, Longatto-Filho A, Reis RM, Scapulatempo-Neto C, Silveira HCS, Vidal DO, Burnette A, Eschbacher J, Hermes B, Noss A, Singh R, Anderson ML, Castro PD, Ittmann M, Huntsman D, Kohl B, Le X, Thorp R, Andry C, Duffy ER, Lyadov V, Paklina O, Setdikova G, Shabunin A, Tavobilov M, McPherson C, Warnick R, Berkowitz R, Cramer D, Feltmate C, Horowitz N, Kibel A, Muto M, Raut CP, Malykh A, Barnholtz-Sloan JS, Barrett W, Devine K, Fulop J, Ostrom QT, Shimmel K, Wolinsky Y, Sloan AE, De Rose A, Giuliante F, Goodman M, Karlan BY, Hagedorn CH, Eckman J, Harr J, Myers J, Tucker K, Zach LA, Deyarmin B, Hu H, Kvecher L, Larson C, Mural RJ, Somiari S, Vicha A, Zelinka T, Bennett J, Iacocca M, Rabeno B, Swanson P, Latour M, Lacombe L, Têtu B, Bergeron A, McGraw M, Staugaitis SM, Chabot J, Hibshoosh H, Sepulveda A, Su T, Wang T, Potapova O, Voronina O, Desjardins L, Mariani O, Roman-Roman S, Sastre X, Stern MH, Cheng F, Signoretti S, Berchuck A, Bigner D, Lipp E, Marks J, McCall S, McLendon R, Secord A, Sharp A, Behera M, Brat DJ, Chen A, Delman K, Force S, Khuri F, Magliocca K, Maithel S, Olson JJ, Owonikoko T, Pickens A, Ramalingam S, Shin DM, Sica G, Van Meir EG, Zhang H, Eijckenboom W, Gillis A, Korpershoek E, Looijenga L, Oosterhuis W, Stoop H, van Kessel KE, Zwarthoff EC, Calatozzolo C, Cuppini L, Cuzzubbo S, DiMeco F, Finocchiaro G, Mattei L, Perin A, Pollo B, Chen C, Houck J, Lohavanichbutr P, Hartmann A, Stoehr C, Stoehr R, Taubert H, Wach S, Wullich B, Kycler W, Murawa D, Wiznerowicz M, Chung K, Edenfield WJ, Martin J, Baudin E, Bubley G, Bueno R, De Rienzo A, Richards WG, Kalkanis S, Mikkelsen T, Noushmehr H, Scarpace L, Girard N, Aymerich M, Campo E, Giné E, Guillermo AL, Van Bang N, Hanh PT, Phu BD, Tang Y, Colman H, Evason K, Dottino PR, Martignetti JA, Gabra H, Juhl H, Akeredolu T, Stepa S, Hoon D, Ahn K, Kang KJ, Beuschlein F, Breggia A, Birrer M, Bell D, Borad M, Bryce AH, Castle E, Chandan V, Cheville J, Copland JA, Farnell M, Flotte T, Giama N, Ho T, Kendrick M, Kocher JP, Kopp K, Moser C, Nagorney D, O'Brien D, O'Neill BP, Patel T, Petersen G, Que F, Rivera M, Roberts L, Smallridge R, Smyrk T, Stanton M, Thompson RH, Torbenson M, Yang JD, Zhang L, Brimo F, Ajani JA, Angulo Gonzalez AM, Behrens C, Bondaruk J, Broaddus R, Czerniak B, Esmaeli B, Fujimoto J, Gershenwald J, Guo C, Logothetis C, Meric-Bernstam F, Moran C, Ramondetta L, Rice D, Sood A, Tamboli P, Thompson T, Troncoso P, Tsao A, Wistuba I, Carter C, Haydu L, Hersey P, Jakrot V, Kakavand H, Kefford R, Lee K, Long G, Mann G, Quinn M, Saw R, Scolyer R, Shannon K, Spillane A, Stretch J, Synott M, Thompson J, Wilmott J, Al-Ahmadie H, Chan TA, Ghossein R, Gopalan A, Levine DA, Reuter V, Singer S, Singh B, Tien NV, Broudy T, Mirsaidi C, Nair P, Drwiega P, Miller J, Smith J, Zaren H, Park JW, Hung NP, Kebebew E, Linehan WM, Metwalli AR, Pacak K, Pinto PA, Schiffman M, Schmidt LS, Vocke CD, Wentzensen N, Worrell R, Yang H, Moncrieff M, Goparaju C, Melamed J, Pass H, Botnariuc N, Caraman I, Cernat M, Chemencedji I, Clipca A, Doruc S, Gorincioi G, Mura S, Pirtac M, Stancul I, Tcaciuc D, Albert M, Alexopoulou I, Arnaout A, Bartlett J, Engel J, Gilbert S, Parfitt J, Sekhon H, Thomas G, Rassl DM, Rintoul RC, Bifulco

C, Tamakawa R, Urba W, Hayward N, Timmers H, Antenucci A, Facciolo F, Grazi G, Marino M, Merola R, de Krijger R, Gimenez-Roqueplo AP, Piché A, Chevalier S, McKercher G, Birsoy K, Barnett G, Brewer C, Farver C, Naska T, Pennell NA, Raymond D, Schilero C, Smolenski K, Williams F, Morrison C, Borgia JA, Liptay MJ, Pool M, Seder CW, Junker K, Omberg L, Dinkin M, Manikhas G, Alvaro D, Bragazzi MC, Cardinale V, Carpino G, Gaudio E, Chesla D, Cottingham S, Dubina M, Moiseenko F, Dhanasekaran R, Becker KF, Janssen KP, Slotta-Huspenina J, Abdel-Rahman MH, Aziz D, Bell S, Cebulla CM, Davis A, Duell R, Elder JB, Hilty J, Kumar B, Lang J, Lehman NL, Mandt R, Nguyen P, Pilarski R, Rai K, Schoenfield L, Senecal K, Wakely P, Hansen P, Lechan R, Powers J, Tischler A, Grizzle WE, Sexton KC, Kastl A, Henderson J, Porten S, Waldmann J, Fassnacht M, Asa SL, Schadendorf D, Couce M, Graefen M, Huland H, Sauter G, Schlomm T, Simon R, Tennstedt P, Olabode O, Nelson M, Bathe O, Carroll PR, Chan JM, Disaia P, Glenn P, Kelley RK, Landen CN, Phillips J, Prados M, Simko J, Smith-McCune K, VandenBerg S, Roggin K, Fehrenbach A, Kendler A, Sifri S, Steele R, Jimeno A, Carey F, Forgie I, Mannelli M, Carney M, Hernandez B, Campos B, Herold-Mende C, Jungk C, Unterberg A, von Deimling A, Bossler A, Galbraith J, Jacobus L, Knudson M, Knutson T, Ma D, Milhem M, Sigmund R, Godwin AK, Madan R, Rosenthal HG, Adebamowo C, Adebamowo SN, Boussioutas A, Beer D, Giordano T, Mes-Masson AM, Saad F, Bocklage T, Landrum L, Mannel R, Moore K, Moxley K, Postier R, Walker J, Zuna R, Feldman M, Valdivieso F, Dhir R, Luketich J, Mora Pinero EM, Quintero-Aguilo M, Carlotti CG, Dos Santos JS, Kemp R, Sankarankuty A, Tirapelli D, Catto J, Agnew K, Swisher E, Creaney J, Robinson B, Shelley CS, Godwin EM, Kendall S, Shipman C, Bradford C, Carey T, Haddad A, Moyer J, Peterson L, Prince M, Rozek L, Wolf G, Bowman R, Fong KM, Yang I, Korst R, Rathmell WK, Fantacone-Campbell JL, Hooke JA, Kovatich AJ, Shriver CD, DiPersio J, Drake B, Govindan R, Heath S, Ley T, Van Tine B, Westervelt P, Rubin MA, Lee J Il, Aredes ND, Mariamidze A, Cherniack AD, Beroukhim R, Meyerson M. 2018. Genomic and Functional Approaches to Understanding Cancer Aneuploidy. Cancer Cell, 33(4):676-689.e3 DOI: 10.1016/J.CCELL.2018.03.007.

Tissier F, Cavard C, Groussin L, Perlemoine K, Fumey G, Hagneré AM, René-Corail F, Jullian E, Gicquel C, Bertagna X, Vacher-Lavenu MC, Perret C, Bertherat J. 2005. Mutations of beta-catenin in adrenocortical tumors: activation of the Wnt signaling pathway is a frequent event in both benign and malignant adrenocortical tumors. Cancer Res, 65(17):7622–7627 DOI: 10.1158/0008-5472.CAN-05-0593.

Tonnus W, Belavgeni A, Beuschlein F, Eisenhofer G, Fassnacht M, Kroiss M, Krone N, Reincke M, Bornstein S, Linkermann A. 2021a. The role of regulated necrosis in endocrine diseases. Nat Rev Endocrinol, 17(8):497–510 DOI: 10.1038/S41574-021-00499-W.

Tonnus W, Belavgeni A, Beuschlein F, Eisenhofer G, Fassnacht M, Kroiss M, Krone NP, Reincke M, Bornstein SR, Linkermann A. 2021b. The role of regulated necrosis in endocrine diseases. Nat Rev Endocrinol, 17(8):497–510 DOI: 10.1038/s41574-021-00499-w.

Tonnus W, Gembardt F, Latk M, Parmentier S, Hugo C, Bornstein SR, Linkermann A. 2018. The clinical relevance of necroinflammation—highlighting the importance of acute kidney injury and the adrenal glands. Cell Death Differ, 26:68–82 DOI: 10.1038/s41418-018-0193-5.

Tonnus W, Meyer C, Paliege A, Belavgeni A, von Mässenhausen A, Bornstein SR, Hugo C, Becker JU, Linkermann A. 2019. The pathological features of regulated necrosis. J Pathol, 247(5):697–707 DOI: 10.1002/path.5248.

Tonnus W, Meyer C, Steinebach C, Belavgeni A, von Mässenhausen A, Gonzalez NZ, Maremonti F, Gembardt F, Himmerkus N, Latk M, Locke S, Marschner J, Li W, Short S, Doll S, Ingold I, Proneth B, Daniel C, Kabgani N, Kramann R, Motika S, Hergenrother PJ, Bornstein SR, Hugo C, Becker JU, Amann K, Anders HJ, Kreisel D, Pratt D, Gütschow M, Conrad M, Linkermann A. 2021c. Dysfunction of the key ferroptosis-surveilling systems hypersensitizes mice to tubular necrosis during acute kidney injury. Nat Commun, 12(1) DOI: 10.1038/S41467-021-24712-6.

Tsarpali V, Belavgeni A, Dailianis S. 2015. Investigation of toxic effects of imidazolium ionic liquids, [bmim][BF4] and [omim][BF4], on marine mussel Mytilus galloprovincialis with or without the presence of conventional solvents, such as acetone. Aquat Toxicol, 164:72–80 DOI: 10.1016/J.AQUATOX.2015.04.021.

Tuo Q, Lei P, Jackman KA, Li X, Xiong H, Li X, Liuyang Z, Roisman L, Zhang S, Ayton S, Wang Q, Crouch PJ, Ganio K, Wang X, Pei L, Adlard PA, Lu Y, Cappai R, Wang J, Liu R, Bush AI. 2017. Tau-mediated iron export prevents ferroptotic damage after ischemic stroke. Mol Psychiatry 2017 2211, 22(11):1520–1530 DOI: 10.1038/mp.2017.171.

Turubanova VD, Mishchenko TA, Balalaeva I V., Efimova I, Peskova NN, Klapshina LG, Lermontova SA, Bachert C, Krysko O, Vedunova M V., Krysko D V. 2021. Novel porphyrazine-based photodynamic anti-cancer therapy induces immunogenic cell death. Sci Rep, 11(1) DOI: 10.1038/S41598-021-86354-4.

Upton JW, Kaiser WJ, Mocarski ES. 2012. DAI/ZBP1/DLM-1 complexes with RIP3 to mediate virus-induced programmed necrosis that is targeted by murine cytomegalovirus vIRA. Cell Host Microbe, 11(3):290–297 DOI: 10.1016/J.CHOM.2012.01.016.

Vanlangenakker N, Vanden Berghe T, Bogaert P, Laukens B, Zobel K, Deshayes K, Vucic D, Fulda S, Vandenabeele P, Bertrand MJM. 2011. cIAP1 and TAK1 protect cells from TNF-induced necrosis by preventing RIP1/RIP3-dependent reactive oxygen species production. Cell Death Differ, 18(4):656–665 DOI: 10.1038/CDD.2010.138.

de Vasconcelos NM, Van Opdenbosch N, Lamkanfi M. 2016. Inflammasomes as polyvalent cell death platforms. Cell Mol Life Sci, 73(11–12):2335–2347 DOI: 10.1007/S00018-016-2204-3.

Venkatachalam MA, Weinberg JM, Kriz W, Bidani AK. 2015. Failed Tubule Recovery, AKI-CKD Transition, and Kidney Disease Progression. J Am Soc Nephrol, 26(8):1765–1776 DOI: 10.1681/ASN.2015010006.

Vidal V, Sacco S, Rocha AS, Da Silva F, Panzolini C, Dumontet T, Doan TMP, Shan J, Rak-Raszewska A, Bird T, Vainio S, Martinez A, Schedl A. 2016. The adrenal capsule is a signaling center controlling cell renewal and zonation through Rspo3. Genes Dev, 30(12):1389–1394 DOI: 10.1101/GAD.277756.116.

Vince JE, Wong WWL, Gentle I, Lawlor KE, Allam R, O'Reilly L, Mason K, Gross O, Ma S, Guarda G, Anderton H, Castillo R, Häcker G, Silke J, Tschopp J. 2012. Inhibitor of apoptosis proteins limit RIP3 kinase-dependent interleukin-1 activation. Immunity, 36(2):215–227 DOI: 10.1016/J.IMMUNI.2012.01.012.

Wachenfeld C, Beuschlein F, Zwermann O, Mora P, Fassnacht M, Allolio B, Reincke M. 2001.

Discerning malignancy in adrenocortical tumors: are molecular markers useful? Eur J Endocrinol, 145(3):335–341 DOI: 10.1530/EJE.0.1450335.

Walczak EM, Kuick R, Finco I, Bohin N, Hrycaj SM, Wellik DM, Hammer GD. 2014. Wnt Signaling Inhibits Adrenal Steroidogenesis by Cell-Autonomous and Non–Cell-Autonomous Mechanisms. Mol Endocrinol, 28(9):1471 DOI: 10.1210/ME.2014-1060.

Wallace MA. 1998. Anatomy and physiology of the kidney. AORN J, 68(5):799–800 DOI: 10.1016/S0001-2092(06)62377-6.

Wang H, Sun L, Su L, Rizo J, Liu L, Wang LF, Wang FS, Wang X. 2014. Mixed lineage kinase domain-like protein MLKL causes necrotic membrane disruption upon phosphorylation by RIP3. Mol Cell, 54(1):133–146 DOI: 10.1016/J.MOLCEL.2014.03.003.

Wang T, Rainey W. 2012. Human adrenocortical carcinoma cell lines. Mol Cell Endocrinol, 351(1):58–65 DOI: 10.1016/J.MCE.2011.08.041.

Wang Y, Gao W, Shi X, Ding J, Liu W, He H, Wang K, Shao F. 2017. Chemotherapy drugs induce pyroptosis through caspase-3 cleavage of a gasdermin. Nature, 547(7661):99–103 DOI: 10.1038/NATURE22393.

Wartz IE, O'Rourke KM, Zhou H, Eby M, Aravind L, Seshagiri S, Wu P, Wiesmann C, Baker R, Boone DL, Ma A, Koonin E V., Dixit VM. 2004. De-ubiquitination and ubiquitin ligase domains of A20 downregulate NF-kappaB signalling. Nature, 430(7000):694–699 DOI: 10.1038/NATURE02794.

Wasserman JD, Novokmet A, Eichler-Jonsson C, Ribeiro RC, Rodriguez-Galindo C, Zambetti GP, Malkin D. 2015. Prevalence and functional consequence of TP53 mutations in pediatric adrenocortical carcinoma: a children's oncology group study. J Clin Oncol, 33(6):602–609 DOI: 10.1200/JCO.2013.52.6863.

Weigand I, Schreiner J, Röhrig F, Sun N, Landwehr L, Urlaub H, Kendl S, Kiseljak-Vassiliades K, Wierman M, Angeli J, Walch A, Sbiera S, Fassnacht M, Kroiss M. 2020. Active steroid hormone synthesis renders adrenocortical cells highly susceptible to type II ferroptosis induction. Cell Death Dis, 11(3):192–204 DOI: 10.1038/S41419-020-2385-4.

Weinberg JM, Bienholz A, Venkatachalam MA. 2016. The role of glycine in regulated cell death. Cell Mol Life Sci, 73(11–12):2285–2308 DOI: 10.1007/s00018-016-2201-6.

Weinberg JM, Roeser NF, Davis JA, Venkatachalam MA. 1997. Glycine-protected, hypoxic, proximal tubules develop severely compromised energetic function. Kidney Int I/o!, 52:140–151 DOI: 10.1038/ki.1997.313.

Weiss LM. 1984. Comparative histologic study of 43 metastasizing and nonmetastasizing adrenocortical tumors. Am J Surg Pathol, 8(3):163–169 DOI: 10.1097/00000478-198403000-00001.

Weksberg R, Shuman C, Beckwith JB. 2010. Beckwith-Wiedemann syndrome. Eur J Hum Genet, 18(1):8–14 DOI: 10.1038/EJHG.2009.106.

Widmaier EP-, Raff H, Strang KT, Shoepe TC. 2019. Vander's human physiology - The mechanisms of body function-McGraw-Hill Education.

Windle RJ, Wood SA, Kershaw YM, Lightman SL, Ingram CD, Harbuz MS. 2001. Increased corticosterone pulse frequency during adjuvant-induced arthritis and its relationship to alterations in stress responsiveness. J Neuroendocrinol, 13(10):905–911 DOI: 10.1046/J.1365-2826.2001.00715.X.

Wong WWL, Gentle IE, Nachbur U, Anderton H, Vaux DL, Silke J. 2010. RIPK1 is not essential for TNFR1-induced activation of NF-kappaB. Cell Death Differ, 17(3):482–487 DOI: 10.1038/CDD.2009.178.

Yan B, Ai Y, Sun Q, Ma Y, Cao Y, Wang J, Zhang Z, Wang X. 2021. Membrane Damage during Ferroptosis Is Caused by Oxidation of Phospholipids Catalyzed by the Oxidoreductases POR and CYB5R1. Mol Cell, 81(2):355-369.e10 DOI: 10.1016/J.MOLCEL.2020.11.024.

Yan Y, Ouyang J, Wang C, Wu Z, Ma X, Li H, Xu H, Hu Z, Li J, Wang B, Shi T, Gong D, Ni D, Zhang X. 2010. Aortic cell apoptosis in rat primary aldosteronism model. J Huazhong Univ Sci Technolog Med Sci, 30(3):385–390 DOI: 10.1007/S11596-010-0362-3.

Yang WS, Kim KJ, Gaschler MM, Patel M, Shchepinov MS, Stockwell BR. 2016. Peroxidation of polyunsaturated fatty acids by lipoxygenases drives ferroptosis. Proc Natl Acad Sci U S A, 113(34):E4966–E4975 DOI: 10.1073/PNAS.1603244113.

Yang WS, SriRamaratnam R, Welsch ME, Shimada K, Skouta R, Viswanathan VS, Cheah JH, Clemons PA, Shamji AF, Clish CB, Brown LM, Girotti AW, Cornish VW, Schreiber SL, Stockwell BR. 2014. Regulation of Ferroptotic Cancer Cell Death by GPX4. Cell, 156(1):317–331 DOI: 10.1016/J.CELL.2013.12.010.

Yang WS, Stockwell BR. 2008. Synthetic Lethal Screening Identifies Compounds Activating Iron-Dependent, Nonapoptotic Cell Death in Oncogenic-RAS-Harboring Cancer Cells. Chem Biol, 15(3):234–245 DOI: 10.1016/J.CHEMBIOL.2008.02.010.

Yang Y, Tetti M, Vohra T, Adolf C, Seissler J, Hristov M, Belavgeni A, Bidlingmaier M, Linkermann A, Mulatero P, Beuschlein F, Reincke M, Williams TA. 2021. BEX1 Is Differentially Expressed in Aldosterone-Producing Adenomas and Protects Human Adrenocortical Cells From Ferroptosis. Hypertens (Dallas, Tex 1979), 77(5):1647–1658 DOI: 10.1161/HYPERTENSIONAHA.120.16774.

Yin H, Xu L, Porter NA. 2011. Free Radical Lipid Peroxidation: Mechanisms and Analysis. Chem Rev, 111(10):5944–5972 DOI: 10.1021/CR200084Z.

Yoon S, Kovalenko A, Bogdanov K, Wallach D. 2017. MLKL, the Protein that Mediates Necroptosis, Also Regulates Endosomal Trafficking and Extracellular Vesicle Generation. Immunity, 47(1):51-65.e7 DOI: 10.1016/J.IMMUNI.2017.06.001.

Zager RA, Foerder CA. 1992. Effects of inorganic iron and myoglobin on in vitro proximal tubular lipid peroxidation and cytotoxicity. J Clin Invest, 89(3):989–995 DOI: 10.1172/JCI115682.

Zargarian S, Shlomovitz I, Erlich Z, Hourizadeh A, Ofir-Birin Y, Croker BA, Regev-Rudzki N, Edry-Botzer L, Gerlic M. 2017. Phosphatidylserine externalization, “necroptotic bodies” release, and phagocytosis during necroptosis. PLoS Biol, 15(6) DOI: 10.1371/JOURNAL.PBIO.2002711.

Zarjou A, Bolisetty S, Joseph R, Traylor A, Apostolov EO, Arosio P, Balla J, Verlander J, Darshan

D, Kuhn LC, Agarwal A. 2013. Proximal tubule H-ferritin mediates iron trafficking in acute kidney injury. J Clin Invest, 123(10):4423–4434 DOI: 10.1172/JCI67867.

Zebisch M, Xu Y, Krastev C, Macdonald BT, Chen M, Gilbert RJC, He X, Jones EY. 2013. Structural and molecular basis of ZNRF3/RNF43 transmembrane ubiquitin ligase inhibition by the Wnt agonist R-spondin. Nat Commun 2013 41, 4(1):1–12 DOI: 10.1038/ncomms3787.

Zennaro MC, Boulkroun S, Fernandes-Rosa FL. 2020. Pathogenesis and treatment of primary aldosteronism. Nat Rev Endocrinol 2020 1610, 16(10):578–589 DOI: 10.1038/s41574-020-0382-4.

Zhang Y, Tan H, Daniels JD, Zandkarimi F, Liu H, Brown LM, Uchida K, O'Connor OA, Stockwell BR. 2019. Imidazole Ketone Erastin Induces Ferroptosis and Slows Tumor Growth in a Mouse Lymphoma Model. Cell Chem Biol, 26(5):623-633.e9 DOI: 10.1016/J.CHEMBIOL.2019.01.008.

Zhao H, Ning J, Lemaire A, Koumpa FS, Sun JJ, Fung A, Gu J, Yi B, Lu K, Ma D. 2015. Necroptosis and parthanatos are involved in remote lung injury after receiving ischemic renal allografts in rats. Kidney Int, 87(4):738–748 DOI: 10.1038/KI.2014.388.

Zheng S, Cherniack AD, Dewal N, Moffitt RA, Danilova L, Murray BA, Lerario AM, Else T, Knijnenburg TA, Ciriello G, Kim S, Assie G, Morozova O, Akbani R, Shih J, Hoadley KA, Choueiri TK, Waldmann J, Mete O, Robertson AG, Wu H-T, Raphael BJ, Shao L, Meyerson M, Demeure MJ, Beuschlein F, Gill AJ, Sidhu SB, Almeida MQ, Fragoso MCBV, Cope LM, Kebebew E, Habra MA, Whitsett TG, Bussey KJ, Rainey WE, Asa SL, Bertherat J, Fassnacht M, Wheeler DA, Zheng S, Verhaak RGW, Giordano TJ, Hammer GD, Cherniack AD, Dewal N, Moffitt RA, Danilova L, Murray BA, Lerario AM, Else T, Knijnenburg TA, Ciriello G, Kim S, Assié G, Morozova O, Akbani R, Shih J, Hoadley KA, Choueiri TK, Waldmann J, Mete O, Robertson AG, Wu H-T, Raphael BJ, Meyerson M, Demeure MJ, Beuschlein F, Gill AJ, Sidhu SB, Almeida M, Fragoso MCB, Cope LM, Kebebew E, Habra MA, Whitsett TG, Bussey KJ, Rainey WE, Asa SL, Bertherat J, Fassnacht M, Wheeler DA, Benz C, Ally A, Balasundaram M, Bowlby R, Brooks D, Butterfield YSN, Carlsen R, Dhalla N, Guin R, Holt RA, Jones SJM, Kasaian K, Lee D, Li HI, Lim L, Ma Y, Marra MA, Mayo M, Moore RA, Mungall AJ, Mungall K, Sadeghi S, Schein JE, Sipahimalani P, Tam A, Thiessen N, Park PJ, Kroiss M, Gao J, Sander C, Schultz N, Jones CD, Kucherlapati R, Mieczkowski PA, Parker JS, Perou CM, Tan D, Veluvolu U, Wilkerson MD, Hayes DN, Ladanyi M, Quinkler M, Auman JT, Latronico AC, Mendonca BB, Sibony M, Sanborn Z, Bellair M, Buhay C, Covington K, Dahdouli M, Dinh H, Doddapaneni H, Downs B, Drummond J, Gibbs R, Hale W, Han Y, Hawes A, Hu J, Kakkar N, Kalra D, Khan Z, Kovar C, Lee S, Lewis L, Morgan M, Morton D, Muzny D, Santibanez J, Xi L, Dousset B, Groussin L, Libé R, Chin L, Reynolds S, Shmulevich I, Chudamani S, Liu J, Lolla L, Wu Y, Yeh JJ, Balu S, Bodenheimer T, Hoyle AP, Jefferys SR, Meng S, Mose LE, Shi Y, Simons J V., Soloway MG, Wu J, Zhang W, Shaw KRM, Demchok JA, Felau I, Sheth M, Tarnuzzer R, Wang Z, Yang L, Zenklusen JC, Zhang J (Julia), Davidsen T, Crawford C, Hutter CM, Sofia HJ, Roach J, Bshara W, Gaudioso C, Morrison C, Soon P, Alonso S, Baboud J, Pihl T, Raman R, Sun Q, Wan Y, Naresh R, Arachchi H, Beroukhim R, Carter SL, Cho J, Frazer S, Gabriel SB, Getz G, Heiman DI, Kim J, Lawrence MS, Lin P, Noble MS, Saksena G, Schumacher SE, Sougnez C, Voet D, Zhang H, Bowen J, Coppens S, Gastier-Foster JM, Gerken M, Helsel C, Leraas KM, Lichtenberg TM, Ramirez NC, Wise L, Zmuda E, Baylin S, Herman JG, LoBello J, Watanabe A, Haussler

D, Radenbaugh A, Rao A, Zhu J, Bartsch DK, Sbiera S, Allolio B, Deutschbein T, Ronchi C, Raymond VM, Vinco M, Shao L, Amble L, Bootwalla MS, Lai PH, Berg DJ Van Den, Weisenberger DJ, Robinson B, Ju Z, Kim H, Ling S, Liu W, Lu Y, Mills GB, Sircar K, Wang Q, Yoshihara K, Laird PW, Fan Y, Wang W, Shinbrot E, Reincke M, Weinstein JN, Meier S, Defreitas T, Hammer GD, Giordano TJ, Verhaak RGW. 2016. Comprehensive Pan-Genomic Characterization of Adrenocortical Carcinoma. Cancer Cell, 29(5):723–736 DOI: 10.1016/J.CCELL.2016.04.002.

Zhou W, Yuan J. 2014. Necroptosis in health and diseases. Semin Cell Dev Biol, 35:14–23 DOI: 10.1016/J.SEMCDB.2014.07.013.

Zhu BT, Conney AH. 1998. Functional role of estrogen metabolism in target cells: review and perspectives. Carcinogenesis, 19(1):1–27 DOI: 10.1093/CARCIN/19.1.1.

Ziegler CG, Ullrich M, Schally A V., Bergmann R, Pietzsch J, Gebauer L, Gondek K, Qin N, Pacak K, Ehrhart-Bornstein M, Eisenhofer G, Bornstein SR. 2013. Anti-tumor effects of peptide analogs targeting neuropeptide hormone receptors on mouse pheochromocytoma cells. Mol Cell Endocrinol, 371(1–2):189–194 DOI: 10.1016/J.MCE.2012.12.011.

Anlage 1

Erklärungen zur Eröffnung des Promotionsverfahrens

1. Hiermit versichere ich, dass ich die vorliegende Arbeit ohne unzulässige Hilfe Dritter und ohne Benutzung anderer als der angegebenen Hilfsmittel angefertigt habe; die aus fremden Quellen direkt oder indirekt übernommenen Gedanken sind als solche kenntlich gemacht.
2. Bei der Auswahl und Auswertung des Materials sowie bei der Herstellung des Manuskripts habe ich Unterstützungsleistungen von folgenden Personen erhalten:
3. Weitere Personen waren an der geistigen Herstellung der vorliegenden Arbeit nicht beteiligt. Insbesondere habe ich nicht die Hilfe eines kommerziellen Promotionsberaters in Anspruch genommen. Dritte haben von mir weder unmittelbar noch mittelbar geldwerte Leistungen für Arbeiten erhalten, die im Zusammenhang mit dem Inhalt der vorgelegten Dissertation stehen.
4. Die Arbeit wurde bisher weder im Inland noch im Ausland in gleicher oder ähnlicher Form einer anderen Prüfungsbehörde vorgelegt.
5. Die Inhalte dieser Dissertation wurden in folgender Form veröffentlicht:
6. Ich bestätige, dass es keine zurückliegenden erfolglosen Promotionsverfahren gab.
7. Ich bestätige, dass ich die Promotionsordnung der Medizinischen Fakultät der Technischen Universität Dresden anerkenne.
8. Ich habe die Zitierrichtlinien für Dissertationen an der Medizinischen Fakultät der Technischen Universität Dresden zur Kenntnis genommen und befolgt.
9. Ich bin mit den "Richtlinien zur Sicherung guter wissenschaftlicher Praxis, zur Vermeidung wissenschaftlichen Fehlverhaltens und für den Umgang mit Verstößen" der Technischen Universität Dresden einverstanden.

Ort, Datum

Unterschrift des Doktoranden

Anlage 2

Erklärung über die Einhaltung gesetzlicher Bestimmungen

Hiermit bestätige ich die Einhaltung der folgenden aktuellen gesetzlichen Vorgaben im Rahmen meiner Dissertation

☐ das zustimmende Votum der Ethikkommission bei Klinischen Studien, epidemiologischen Untersuchungen mit Personenbezug oder Sachverhalten, die das Medizinproduktegesetz betreffen

☐ die Einhaltung der Bestimmungen des Tierschutzgesetzes
Aktenzeichen der Genehmigungsbehörde zum Vorhaben/zur Mitwirkung: TVV 57/2017

☐ die Einhaltung des Gentechnikgesetzes/Projektnummer: Az. 56-8811.71/160

☐ die Einhaltung von Datenschutzbestimmungen der Medizinischen Fakultät und des Universitätsklinikums Carl Gustav Carus.

Ort, Datum

Unterschrift des Doktoranden